DEPARTMENT OF COMMERCE
SINCLAIR WEEKS, Secretary

WEATHER BUREAU
F. W. REICHELDERFER, Chief

MONTHLY WEATHER REVIEW

JAMES E. CASKEY, JR., Editor

Volume 86
Number 6

JUNE 1958

Closed August 15, 1958
Issued September 15, 1958

A METHOD FOR FORECASTING THE MAXIMUM SURGE AT BOSTON DUE TO EXTRATROPICAL STORMS

ANTHONY E. TANCRETO

Weather Bureau Office, Boston, Mass.

[Manuscript received October 18, 1957; revised April 28, 1958]

ABSTRACT

An empirical relationship between computed significant wave height and height of extratropical storm surge at Boston is found. The relationship is expressed as a linear regression equation for forecasting surge height from significant wave height as computed from the Bretschneider graph.

1. INTRODUCTION

Abnormal elevations of the sea surface along coastal regions may accompany both tropical and extratropical storms. The rise of the sea surface induced by meteorological factors is frequently referred to as the storm surge, while the normal rise and fall is called the predicted or normal tide. The predicted tide is based both on astronomical theory and on a series of observations which include a climatic factor. No satisfactory method of completely separating these effects is now available. However, the contribution of the climatic term is usually small and has no practical importance in the forecast problem [1]. For this type of investigation the term storm surge is defined as the departure of the observed tide from the predicted tide.

The most devastating surges along the coast of the United States have been generated by hurricanes. Severe extratropical storms have, however, induced surges which are comparable in magnitude with those accompanying some of the less intense hurricanes. The available tide data indicate that many sections of coastal United States are particularly vulnerable to storm surges associated with extratropical storms, and that maximum surge heights along the east coast of New England have been a direct result of these storms [2]. The intense storm of November 29–30, 1945, produced a surge of 5.3 feet at Boston and caused damage estimated at about $1,000,000. Had this storm struck at spring tide, rather than at neap tide, coastal damage due to inundation and heavy seas would have far exceeded this figure.[1]

The purpose of this paper is to present a technique which would adequately predict the height of the surges accompanying extratropical storms. As shown by Harris [3] and Reid and Wilson [4], the magnitude and lateral extent of the storm surge associated with tropical storms along the open coast are dependent mainly upon the wind field, pressure reduction, size and speed of the storm, configuration of the coastline, and bottom topography near the coast. Local effects, such as convergence and divergence in bays, seiching, and local set-up, will further affect the storm surge. Since each of the above meteorological parameters may individually induce an abnormality in the elevation of the sea surface, and since the other factors tend only to modify this abnormality, one may logically conclude that the extratropical storm surge also will be dependent upon all the factors listed above, although, in all probability, the order of their importance may not be

[1] Form 1014, U. S. Weather Bureau, Boston, Mass., Nov. 29, 1945.

474509—58——1

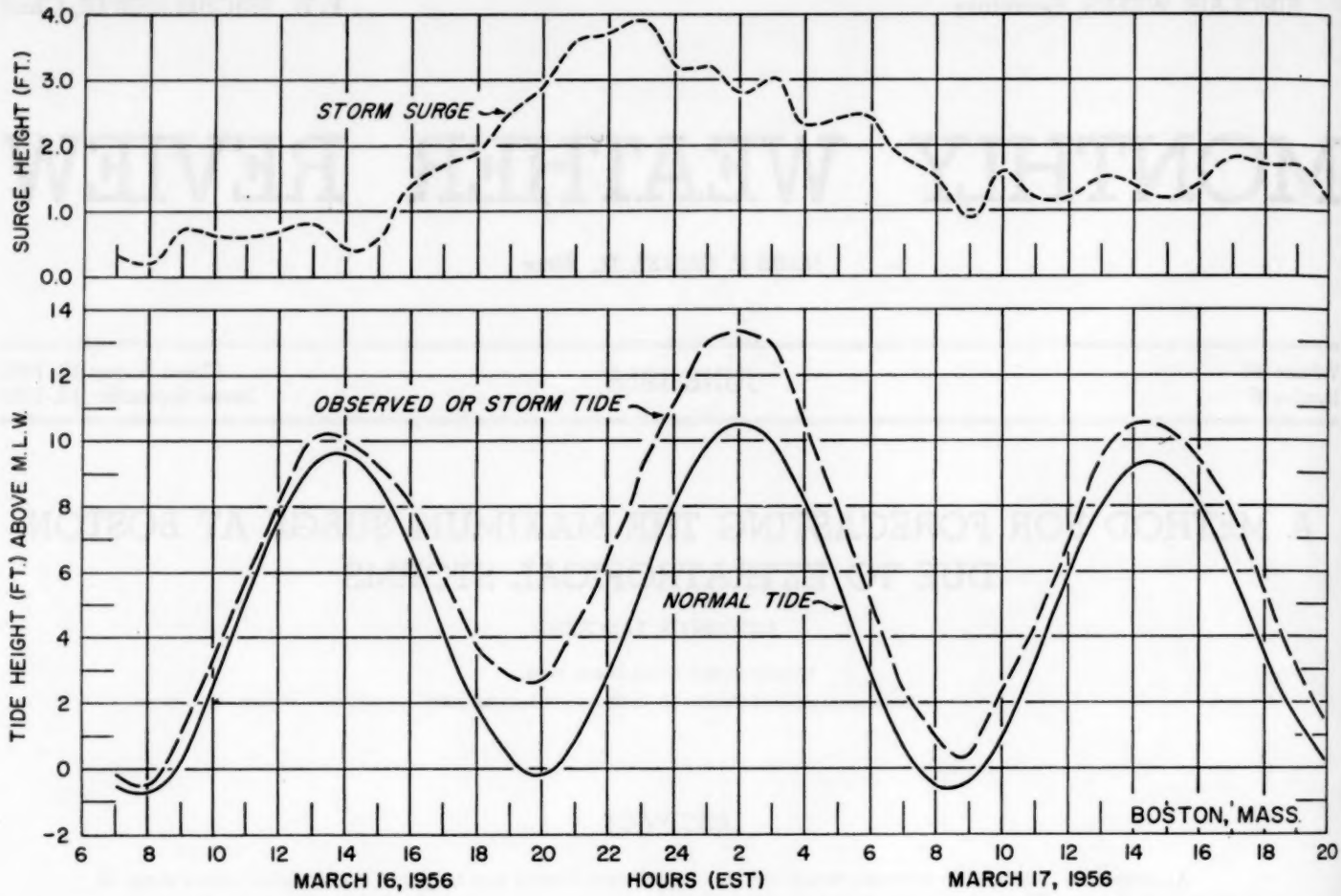

FIGURE 1.—The lower curves illustrate the periodicity and range of the normal and storm tide for the storm of March 16–17, 1956. The upper curve represents the resultant storm surge on an expanded vertical scale.

the same. To eliminate the variation in local effects, coastal configuration, and bottom topography, the study was restricted to one location.

Figure 1 illustrates an actual case at Boston of the periodicity and magnitude of the predicted and actual tides, and the resultant storm surge. Note that the range in the predicted tide at Boston on this date was about 10.5 feet (the mean range is 9.5 feet), more than twice that of the storm surge. The large tidal range further complicates the flood prediction problem by demanding very accurate timing of the storm surge. Had the storm surge occurred a few hours earlier, coastal flooding would have been negligible.

2. DATA

Research on the problem of storm surges is hampered by the lack of quantitative data in the proper form. Only the departures of the actual tide from the normal tide at times of high and low water are readily obtainable from tidal records of the U. S. Coast and Geodetic Survey. Where the mean tidal range is large, these data seldom indicate the maximum surge heights. To obtain the required data, the hourly values of the normal tide must be computed for each day in which a storm surge may have occurred. This computation is slow and tedious without the aid of a tide prediction machine. Hourly predictions of the tide, as well as the hourly observed tide heights, were obtained from the U. S. Coast and Geodetic Survey for storm periods in 1953, 1954, 1955, and for eight additional severe storms of other years, a total of 45 cases. These data were used in the study, along with the 6-hourly surface weather maps on file at the U. S. Weather Bureau, East Boston, Mass.

3. SYNOPTIC INVESTIGATION

The sea level weather maps associated with storm surges in excess of 2 feet were examined for possible stratification by weather types, and for characteristic features. No marked separation by types was possible. In most cases, 12 hours prior to the occurrence of the maximum surge at Boston, a storm was centered near or off the middle Atlantic coast, and a strong east-west or southeast-northwest ridge was located not too far north of New England. For example, see figure 2.

The charts did clearly show in all cases strong winds with an easterly component along and off the southern New England coast. In addition, the fetch (the stretch

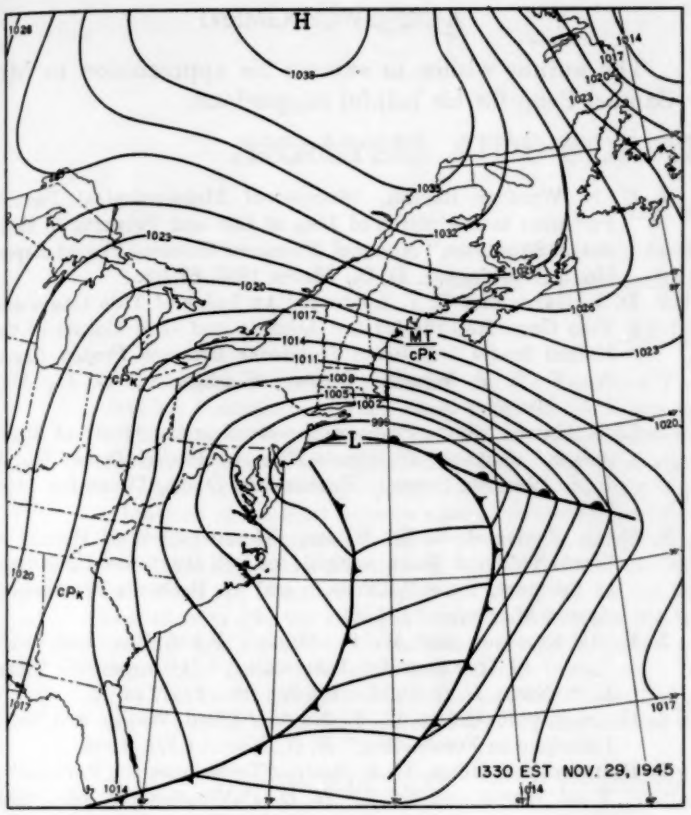

FIGURE 2.—Sectional sea level map, 1330 EST, November 29, 1945.

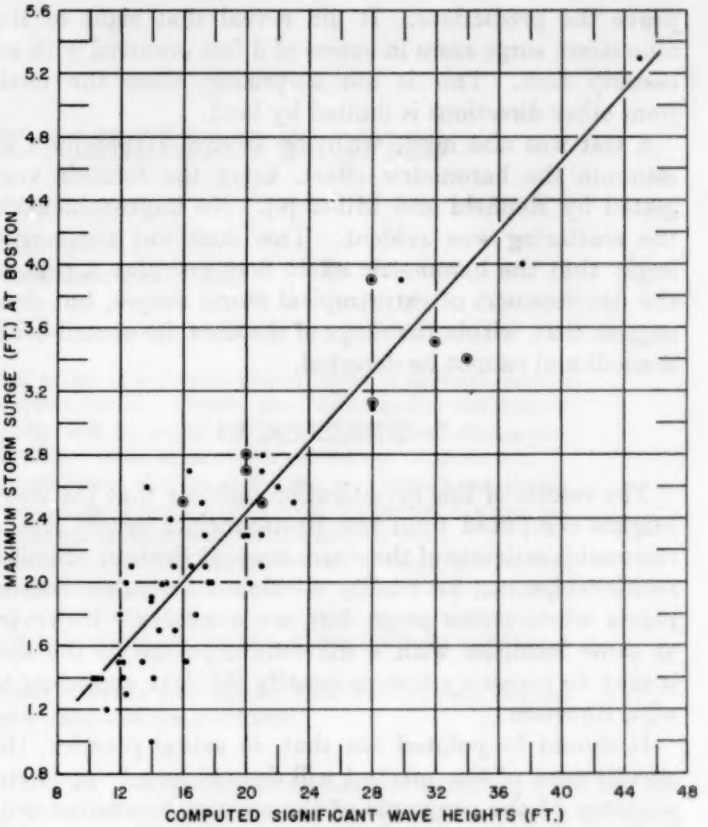

FIGURE 3.—The maximum storm surge at Boston as a function of the computed offshore wave heights. The dependent data are plotted as dots and the independent as encircled dots.

of water over which a wind of nearly constant direction is blowing) off the Massachusetts coast was relatively large. Since the total energy imparted by a given wind over a given fetch may be limited by the interval of time the wind is blowing, the duration time must also be considered as a factor affecting the height of the storm surge. Thus it appears that the extratropical surge may be related to certain synoptic features, namely: wind force, wind duration, and fetch.

Sverdrup and Munk [5], in studying the transfer of energy from wind to wave, derived equations which relate wave height to wind velocity, wind duration, and fetch. Then, with the aid of empirical data, they developed graphs [6 and 7] for forecasting the height of significant wind waves and swell. If one considers that the significant wave heights [2] at the end of the fetch are indicative of the energy imparted to the water over the fetch, and that they are, further, an indication or index of the intensity of the storm for that area, it seems reasonable to suspect there should be some relationship between the height of the waves and the magnitude of the storm surge.

4. RELATING SIGNIFICANT WAVE HEIGHT TO STORM SURGE HEIGHT

The significant wave heights were computed by 6-hourly periods, using the so-called Bretschneider-Revised Sverdrup-Munk Method [8]. For the sake of objectivity these values were not modified, although it is generally acknowledged that the method tends to overforecast wave heights for the higher wind values.

The relationship between the height of the storm surge and the computed wave heights offshore at the time of maximum surge at Boston is shown in figure 3. Considering only those cases represented by the dots, the regression equation obtained by the method of least squares is

$$S_h = .24 + .11\ H,$$

where S_h is the height of the surge and H is the significant wave height, both measured in feet. The correlation coefficient is 0.88.

It is apparent from this figure that there are few data to support the curve above the 3-foot level. Fortunately, immediately prior to the completion of this paper, eight additional cases developed. These are the encircled points in figure 3. It is clear that these cases lend support to the derived relationship. Of particular significance is the confirmation of the curve in the region of sparse data.

In an attempt to improve the prediction equation, the data were stratified into two classes determined by the predominant wind flow over the fetch, namely, east and northeast. This stratification did not significantly im-

[2] The significant wave height is defined as the average of the heights of the one-third highest waves observed at a given time.

prove the predictions. It did reveal that eight of the nine storm surge cases in excess of 3 feet occurred with an easterly flow. This is not surprising, since the fetch from other directions is limited by land.

A test was also made with the 1954 and 1955 data to estimate the barometric effect, using the formula suggested by Redfield and Miller [9]. No improvement in the scattering was evident. This does not necessarily imply that the barometric effect does not play a part in the development of extratropical storm surges, but does suggest that, within the range of the data, its contribution is small and cannot be detected.

5. CONCLUSIONS

The results of this investigation indicate that the wave heights computed from the Bretschneider graph give a reasonable estimate of the storm surge at Boston. Similar relationships can be readily developed for other coastal points where storm surge data are available. However, at some localities with a different exposure to the sea, it may be necessary first to stratify the data according to wind direction.

It should be pointed out that, in actual practice, the effectiveness of this method will depend largely upon the accuracy of the prognosis of the surface circulation patterns from which the significant wave heights are computed. On several occasions during the winter of 1957–58, this technique was applied on an operational basis. When the surface prognostic chart was reasonably accurate, the predictions made from figure 3 were very satisfactory.

ACKNOWLEDGMENT

The author wishes to express his appreciation to Mr. Samuel Penn for his helpful suggestions.

REFERENCES

1. U. S. Weather Bureau, "Survey of Meteorological Factors Pertinent to Reduction of Loss of Life and Property in Hurricane Situations," *National Hurricane Research Project Report* No. 5, Washington, D. C., March 1957, 87 pp.
2. D. L. Harris and C. V. Lindsay, "An Index of Tide Gages and Tide Gage Records for the Atlantic and Gulf Coasts of the United States," *National Hurricane Research Project Report* No. 7, U. S. Weather Bureau, Washington, D. C., May 1957, 104 pp.
3. D. L. Harris, "Some Problems Involved in the Study of Storm Surges," *National Hurricane Research Project Report* No. 4, U. S. Weather Bureau, Washington, D. C., December 1956, 30 pp.
4. R. O. Reid and B. W. Wilson, "Compendium of Results of Storm Tide and Wave Analysis for Full Hurricane Conditions at Freeport, Texas," Texas A. and M. Research Foundation, *A. and M. Project 91*, 1954.
5. H. U. Sverdrup and W. H. Munk, "Wind, Sea, and Swell: Theory of Relations for Forecasting," Hydrographic Office, U. S. Navy, *H. O. Publication* No. 601, 1947, 44 pp.
6. Hydrographic Office, U. S. Navy, "Wind Waves and Swell Principles in Forecasting," *H. O. Misc.* 11,275, 1944.
7. Hydrographic Office, U. S. Navy, "Techniques for Forecasting Wind Waves and Swell," *H. O. Publication* No. 604, 1951, 37 pp.
8. C. L. Bretschneider, "Revised Wave Forecasting Curves and Procedure," *U. S. Navy Technical Report* No. 155–47, University of California, 1951, 28 pp.
9. A. C. Redfield and A. R. Miller, "Memorandum on Water Levels Accompanying Atlantic Coast Hurricanes," Woods Hole Oceanographic Institution, Reference No. 55–28, June 1955, 14 pp.

ANALYSIS AIDS FOR THE AMERICAN TROPICS

L. F. HUBERT

U. S. Weather Bureau, Washington, D. C.

[Manuscript received February 12, 1958; revised April 14, 1958]

ABSTRACT

Analysis of upper-level charts for the American Tropics, which is a largely oceanic area, is difficult because data are inadequate and are likely to remain so in the foreseeable future. Despite this handicap and the unsatisfactory character of the map, the 500-mb. analyses are routinely used for many different tropical forecasting procedures. Some aids are suggested for improving the analyses that are made to meet this continuing requirement.

Since the lower troposphere is somewhat barotropic, pressure-height changes at 700 mb. and 500 mb. are largely a function of sea level pressure change so that a careful surface analysis along with a good differential analysis can yield great improvement in upper-air analysis compared to a straightforward analysis of upper-air data.

Maps of normal thicknesses, 1000–700 mb., 700–500 mb., and 1000–500 mb., based on all constant pressure data from the American Tropics are presented for the hurricane season. Statistics relative to these fields of thickness such as 24-hour changes, correlation between the upper and lower strata, and typical anomaly patterns, are included and discussed. In addition, several indicators of anomaly which are useful in higher latitudes were investigated and found to be of limited value in this area.

Finally it is concluded that tropical maps must be re-analyzed as late data become available and that analyses must be made under the control of thermal and time-continuity restraints discussed here.

1. INTRODUCTION

Perhaps the greatest single obstacle to research and forecast development in the Tropics is the deficiency of observations and the consequent uncertainty in our description of the atmosphere. It is patently absurd to expect improvement in forecasting some *future* state of the atmosphere until it is possible to obtain a reasonably accurate knowledge of its *initial* state.

Because our tropical region is largely oceanic, the problem of adequate observations will not be solved in the foreseeable future, but some improvement in analysis can be realized by a careful and unremitting use of all climatology and knowledge available to us.

The fundamental question of utility of pressure contour analysis in the Tropics is outside the scope of this paper. There is little doubt however, that pressure analysis by itself in low latitudes is inadequate, for it is but a blurred and distorted reflection of the field of motion, and the 500-mb. surface is particularly unsatisfactory in many situations. Despite their shortcomings, 500-mb. data are used routinely as input for numerical weather predictions and for hurricane motion computations, so there is an immediate demand for the best possible 500-mb. analysis. In addition there are other methods of analyzing tropical data under study (e. g., [1]) which must ultimately take account of the pressure gradient because the pressure field represents an important force that cannot be neglected.

The primary purpose of this paper is to present monthly mean thicknesses for the American Tropics during the hurricane season, and in addition some upper-air synoptic climatology is included which will help in the use of mean thicknesses in preparation of 700- and 500-mb. analyses.

The statistics are by no means exhaustive nor are they based on the maximum number of samples, with the exception of the thicknesses, but it was felt that a report even of this limited scope should be circulated because up to this time no such material has been available.[1] Too, the value—indeed the necessity—of differential analysis in the Tropics needs to be emphasized. Wherever the density of surface reports is greater than that of the upper-air network, vertical extrapolation is worthwhile. Not to consider *every single* surface report while analyzing the 700-mb. and 500-mb. maps is to ignore expensive observations that are as important as radiosonde observations. In practice a convenient procedure is to consider every surface report in constructing a 1000-mb. chart and extrapolate to the desired pressure-height in regions of no upper-air data.

2. DATA USED

The charts of mean thicknesses (700 mb.–1000 mb. is referred to as ΔH_1, 500 mb.–700 mb. as ΔH_2, and 500 mb.–1000 mb. as ΔH_3 in the following pages), figures 6 through 15, are based on all available constant pressure data of the American Tropics. Table 1 shows the stations and period of record used. The statistics are not based on upper-air analyses because over this area there is an unknown amount of human error and bias.

The thicknesses at the Islands of Sal and Funchal are shown, when available, as insets to figures 6–15, but because such a large expanse of data-free ocean exists between those stations and our network, it was impossible to extend a reliable analysis eastward.

The thicknesses shown in parentheses are considered to be of a lower order of accuracy than the remaining ones,

[1] Similar normals have been published [2, 3] but the emphasis has been on the mid-latitudes so they are of limited utility for tropical analysis.

TABLE 1.—*Radiosonde records used in computation of mean thicknesses*

Location	Number of observations*				
	July	August	September	October	November
	0300 GMT				
Antigua, B.W.I.	48	24	27	42	40
Balboa, C. Z.	241	257	271	255	271
Bermuda	282	289	262	279	264
Brownsville, Tex.	278	262	266	277	266
Burrwood, La.	278	262	266	277	266
Charleston, S. C.	279	278	268	279	270
Funchal, Madeira Islands					
Georgetown, British Guiana	13	26	36	40	33
Hatteras, N. C.	278	276	270	277	269
Havana, Cuba	233	244	244	242	263
Maracay, Venezuela	4 yr.	3 yr.	4 yr.	3 yr.	4 yr.
Merida, Yucatan	9 yr.	8 yr.	7 yr.	8 yr.	8 yr.
Miami, Fla.	276	277	267	274	269
St. Lucia, B. W. I.		2	16	31	29
Sal Island (22.9° N., 16.7° W.)	8 yr.	7 yr.	8 yr.	7 yr.	8 yr.
San Juan, P. R.	277	271	266	274	266
Ship E (35° N., 48° W.)	243	233	240	269	270
Swan Island	253	268	261	247	235
Trinidad, B. W. I.	132	152	151	159	129
Vera Cruz, Mexico	9 yr.	8 yr.	6 yr.	7 yr.	7 yr.
	1500 GMT				
Antigua, B. W. I.	37	26	37	46	43
Balboa, C. Z.	227	260	271	254	269
Bermuda	274	287	259	282	278
Brownsville, Tex.	276	276	266	278	268
Burrwood, La.	271	263	263	276	267
Charleston, S. C.	279	279	270	279	269
Funchal, Madeira Islands	6 yr.	6 yr.	6 yr.	6 yr.	5 yr.
Georgetown, British Guiana	16	25	32	40	46
Hatteras, N. C.	278	277	270	276	269
Havana, Cuba	226	246	248	242	266
Maracay, Venezuela	4 yr.	3 yr.	4 yr.	3 yr.	4 yr.
Merida, Yucatan					
Miami, Fla.	279	279	266	276	270
St. Lucia, B. W. I.	12	29	30	31	29
Sal Island (22.9° N., 16.7° W.)					
San Juan, P. R.	273	277	267	277	266
Ship E (35° N., 48° W.)	240	233	241	270	268
Swan Island	259	270	264	240	229
Trinidad, B. W. I.	123	184	179	171	134
Vera Cruz, Mexico	5 yr.	5 yr.	5 yr.	5 yr.	5 yr.

*"9 yr." indicates 9 monthly means for that month were averaged.

either because of a short period of record or because they were adjusted to correct for a systematic error that appeared when the means were analyzed for homogeneity. For example, the thicknesses at Miami, Fla., and Merida, Yucatan were adjusted to correct for systematic errors that have since been corrected.

Since the nighttime soundings have little radiation error, the 0300 GMT maps of ΔH_1 and ΔH_2 were analyzed first; then maps of 12-hour changes were prepared in order to obtain smooth and reasonable change patterns.[2] This procedure indicated the data which apparently had systematic daytime errors and the 1500 GMT thicknesses were adjusted. The ΔH_3 charts were then constructed by addition of ΔH_1 and ΔH_2.

Figures 6–15 inevitably include a certain amount of subjectivity. For example, the large area east of the Windward Islands is completely innocent of data just where general considerations indicate the greatest thicknesses occur. The actual maximum values are of course unknown but in each case they were estimated from the frequency distribution of thicknesses at San Juan, modified where necessary by the constraint of a reasonable space gradient. This involves the assumption that distribution in time is quite similar to distribution in space; i. e., if a large number of observations of a given thickness appeared at San Juan during a given month, those values were assumed to have existed elsewhere in space during the same month when some other thickness was observed at San Juan. Since the oceanic High is frequently displaced westward over San Juan it was assumed the large thicknesses were advected from the east. For example, figure 6A shows a large area of ΔH_1 of 3050 meters and a small maximum of 3055 meters. During that month the frequency distribution at San Juan had a mean of 3046 meters, but 31 percent of the thicknesses were in the class interval 3048 to 3055 meters and another 16 percent were greater than 3055 meters, and a "reasonable" gradient of thickness was not inconsistent with a maximum value of 3055 meters.

3. EXTRAPOLATION OF PRESSURE HEIGHTS

Differential analysis is not new, for it has been used for more than a decade [4, 5, 6]. The material that is new, however, is the climatology upon which the tropical analyst must base his differential analysis; information which previously resided only in the minds of a few experienced tropical analysts.

The suggested use of these mean maps is to add onto the 1000 mb. heights the appropriate thickness at a network of grid points, plus or minus local adjustments to those means; i. e., local anomalies where they can be estimated. The validity of vertical extrapolation is clear when we consider the tropical atmosphere over oceans. The horizontal temperature gradient is normally small so if the atmosphere were entirely barotropic the day-to-day height variation of upper pressure surfaces would be controlled to a high degree by the sea level pressure. Most of the lower tropical atmosphere is in fact nearly barotropic for the 700-mb. and 500-mb. heights are highly correlated with the 1000-mb. height. It follows that a straightforward addition of normal thicknesses to a *good* 1000-mb. analysis wherever there are no upper-air data, would produce an upper-air map that is superior to an analysis made solely from upper-air observations. Such a procedure is not recommended, however, for it neglects significant features that can be added by a skillful analyst whose task it is to determine the pattern of anomalies. It was a search for anomaly indicators that comprised a large part of this study.

Extrapolation for purposes of synoptic description in the Tropics is more difficult than at higher latitudes for two reasons. First, because the gradients are small, upper-air analysis must delineate relatively small changes in time and space. Second, the semidiurnal pressure wave and the diurnal temperature wave are large and in practice these real complications are compounded by communications, instrumental, and human errors. The effect of large day-to-night changes is to decrease the value of normals based on combined 0300–1500 GMT soundings. The first requirement, then, is separate

[2] The 12-hour change charts are not included here because they are of limited usefulness with the new observation times. Upper-air diurnal changes to be published soon by R. C. Gentry indicate that the line of zero change that lies along our east coast for the 0300–1500 changes will be shifted eastward for 0000–1200 GMT times.

normals. A second requirement—detection of errors—can be met by the careful application of time continuity. Many errors can be eliminated by maintaining a surveillance of the reported changes in light of the changes to be expected in a tropical atmosphere.

4. INADEQUATE ANOMALY INDICATORS

Many avenues were explored in an effort to find some practical means of estimating thickness anomalies both from the surface parameters and from circulation features. Since other investigators may want to avoid covering the same ground, those avenues which did not yield usable results will be mentioned, but without documentation. It should be borne in mind that all the following pertains to the tropical atmosphere below 500 mb. in the American Tropics during the hurricane season.

Airmass considerations, so important at higher latitudes [4] were of small value because, except at the boundaries of our region, e. g., north of 20° N. and in the Gulf of Mexico, almost no detectable airmass differences exist. Even when fronts are found at the surface, the cool air is quite shallow so that frontal analysis is seldom any clue to thickness anomaly. This does not preclude the use of frontal analysis in the rare occasions when it is clear that a deep cool airmass has invaded the Tropics.

Weather and cloud distribution is frequently used in tropical analysis as an indication of stability and subsidence warming or of a moist adiabatic lapse rate. Only insignificant correlations were found between thickness and weather distribution, but this is understandable for the following reasons. Perhaps the most important is that weather distribution analysis is strongly influenced by the complete and regular reports from island stations where local terrain effects produce weather not representative of large areas. This particular phase of the study cannot be considered complete until it is repeated with weather distribution charts based on ship reports, but a similar study for higher latitudes has not been encouraging [7]. In oceanic Highs there are compensating effects which will always produce a great variety of anomalies of *both signs* with fair weather. On one hand, the atmosphere has subsided various unknown amounts so that the degree of warming is uncertain, but at the same time the layer between, say 1000 mb. and 700 mb. is at a greater elevation, thus is cooled as the 1000-mb. surface rises because the temperature at sea surface and the lapse rate from surface to 1000 mb. remain nearly constant.

Surface temperature and pressure are very poor indicators of thickness anomaly. Insofar as temperature is concerned, the lowest values are usually associated with showers so that any given report may show the temperature of precipitation-cooled air that is unrepresentative. The effect of pressure is indeterminate as well, in part for the reason just mentioned in connection with the high pressure cells.

Circulation features such as troughs and ridges or curvature of the flow are associated with only a small part of the anomalies and, in general, do not assist in estimating their magnitude. In the absence of any other information, a safe rule is to assign a small negative anomaly to the immediate region of a moving trough in the easterlies. Ridges do not appear to carry with them significant anomalies. Furthermore, less than half of all large anomalies are associated with circulation features detectable from the conventional analysis so that if one assigned anomalies strictly on the basis of circulation, he would indicate zero anomaly in about 60 percent of the cases where large anomalies actually exist and small anomalies of the correct sign would be estimated correctly no better than expected by chance.

Horizontal interpolation has been used successfully in oceanic analysis at higher latitudes [7] and these considerations are of some value in the Tropics, but not to the same degree. The manner in which this is applied is discussed below.

Estimating 700-mb. or 500-mb. temperatures as a step in estimating the various thicknesses cannot be done any more accurately than estimating the anomaly directly. If reliable aircraft or short-run raobs are available, however, good estimates of ΔH_3 can be obtained and this is discussed below.

Estimating ΔH_2 anomalies from those that exist in ΔH_1 is a valid procedure if there are more data for the 700-mb. analysis than for the 500-mb. analysis. Where no additional data exist at 700 mb., however, no accrual of accuracy can result because no clues to ΔH_2 anomalies were found on the 700-mb. analysis that were not also evident at the surface. It is evident from the larger standard deviations of ΔH_3 that the 500-mb. analysis will always be more uncertain than the 700-mb. analysis. (See discussion of vertical distribution of anomalies in section 5.)

5. STATISTICAL ANALYSIS AIDS

The only systems that carry with them definite anomalies are strong troughs, tropical storms, and hurricanes. Obviously, in a typical situation, this leaves something over 90 percent of the tropical region with no dependable clues to thickness anomalies insofar as circulation or weather indications are concerned. The analyst must therefore turn to time continuity and horizontal extrapolation from regions of upper-air data. Statistical evidence upon which to base the latter is not entirely satisfactory because the results are based on anomalies at widely separated stations. Time continuity statistics, since they depend upon local changes only, are much more dependable and are recommended as the main tool. Since time continuity is presently the best analysis aid, it is vital that careful re-analysis of upper-air and surface maps be made routinely as subsequent data [3] become available, for it is clear that if maps during the past 24 hours are not revised to obtain the most accurate pattern possible there is very little point to time extrapolation.

[3] "Subsequent data" includes weather events right up to the re-analysis time as well as late ship and upper-air reports, both on and off map time.

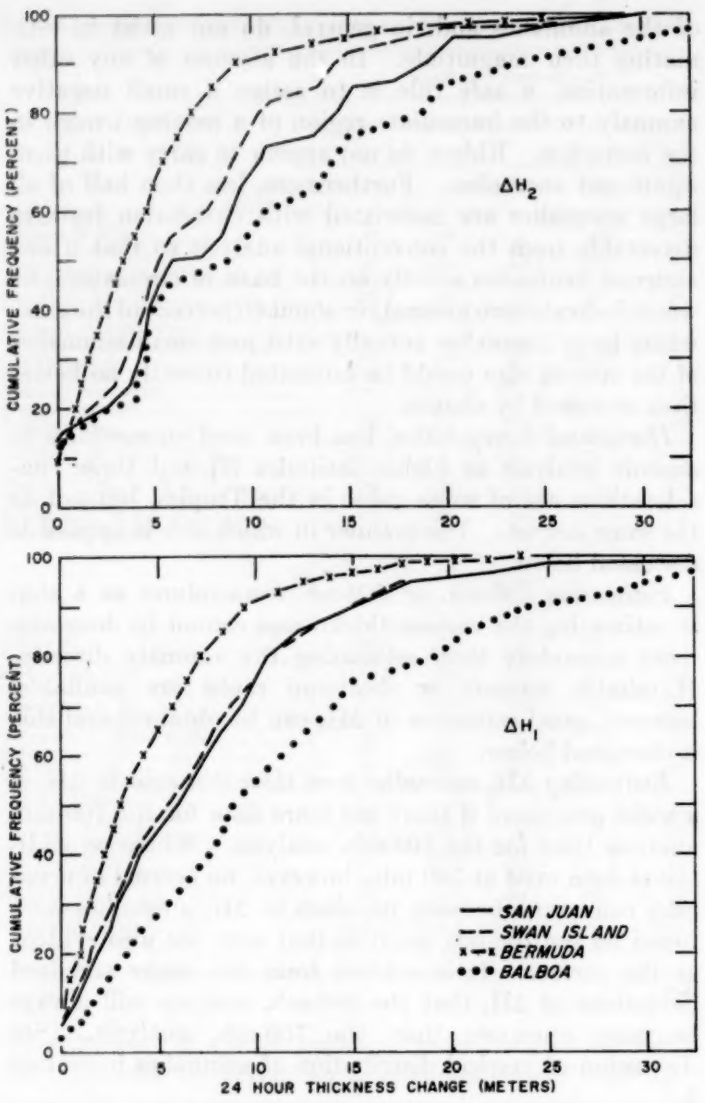

FIGURE 1.—Cumulative frequency of 24-hour thickness changes for the layers 1000–700 mb. (ΔH_1) and 700–500 mb. (ΔH_2), July through November.

Time continuity of thickness anomalies is a valuable analysis aid if it is applied with the help of pertinent climatology of the area. Following are some of the statistics that the analyst must incorporate into every map.

Figure 1 shows cumulative frequencies of 24-hour thickness changes for ΔH_1 and ΔH_2, showing that over most of the American Tropics 90 percent of the 24-hour changes are 15 meters or less in the lower stratum and 90 percent are 20 meters or less in the upper layer. During this season some of the larger changes are produced by traveling waves that pass a given point every 4 to 5 days (see San Juan, fig. 2) so that on the average, perhaps 5 to 10 percent of the changes are produced by these waves. Some of the wave-induced changes in ΔH_1 must be greater than 15 meters, so it follows that a large part of the area not under the immediate influence of a wave must show changes less than 15 meters; on a typical map this represents most of the analysis area. This statistic therefore represents a definite restraint the analyst is obliged to impose. For example, in regions where there is no reason to suspect a disturbance, changes much greater than 15 meters must be viewed with suspicion and every effort made to revise the map to eliminate the large changes.

The tendency for the thickness (or anomaly) to be similar on two successive days is also shown by autocorrelation (lag) coefficients.[4] Figure 2 shows this statistic for ΔH_1 for five stations. The 4- to 5-day periodicity prominent at Trinidad and San Juan is understandably absent at Bermuda where the circulation is dominated by an anticyclone, but the absence of any lag correlation at the Canal Zone is more difficult to interpret. No doubt circulation changes bring intermittent invasions of continental air from South America or cool air from the eastern Pacific. Some of the erratic changes (thus the low lag correlation) must be due to low quality soundings because few of the larger anomalies appear on two successive days, but a certain amount of this effect must be real because at Swan Island the 24-hour lag coefficient is also low. Whatever the cause, it is apparent that 24-hour time continuity is of little value in this area. Even here some analysis stability can be obtained by using longer-term tendencies. Large areas frequently are above or below normal for several successive weeks, so a running mean of thickness anomaly will often provide an indication of the anomaly that is better than using the normal value (zero anomaly). This is illustrated by figure 3. Notice the period during which the running mean is completely above or below normal.

The statistics discussed above, being averages, characterized the central tendency and suppress the extremes. On almost every map the analyst finds areas of large anomalies that are not documented by data one day later and a useful statistic is the amount these large anomalies are likely to decrease in 24 hours at that locality. Figure 4 shows the 24-hour change of anomaly toward zero as a function of the anomaly magnitude. When the analyst is faced with the problem of estimating a thickness anomaly 24 hours after a large, reliable value appeared, in the absence of other information the best estimate may be based on the graph for the appropriate area. Because these graphs were constructed from all large anomalies during the period involved, a certain proportion are changes due to traveling disturbances. Therefore, the 24-hour changes indicated do not apply strictly to either wave or to non-wave anomalies, but the influence of synoptic systems is believed small. It must be borne in mind that this statistic refers to the anomaly change at a fixed point and that large anomalies associated with traveling disturbances frequently do not decrease in any given 24-hour period, so the 24-hour decrease is a measure of the advective decrease.

Horizontal extrapolation is useful in a qualitative manner only, for thicknesses are influenced strongly by vertical motions not detectable from routine analysis. Further-

[4] These were computed for full days only and the coefficient for 1-day, 2-day, etc. connected with a smooth curve. This fact, along with a different period of record, accounts for a 4-day periodicity at Trinidad but a 5-day period at San Juan.

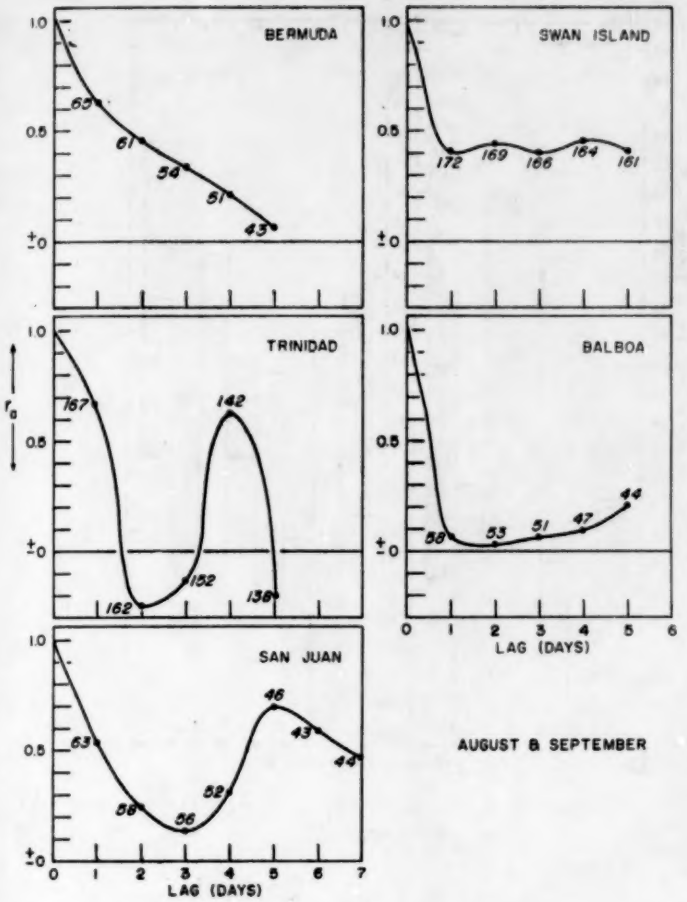

FIGURE 2.—Lag correlation coefficients for layer 1000–700 mb. for months of August and September. Number of cases is shown at each point.

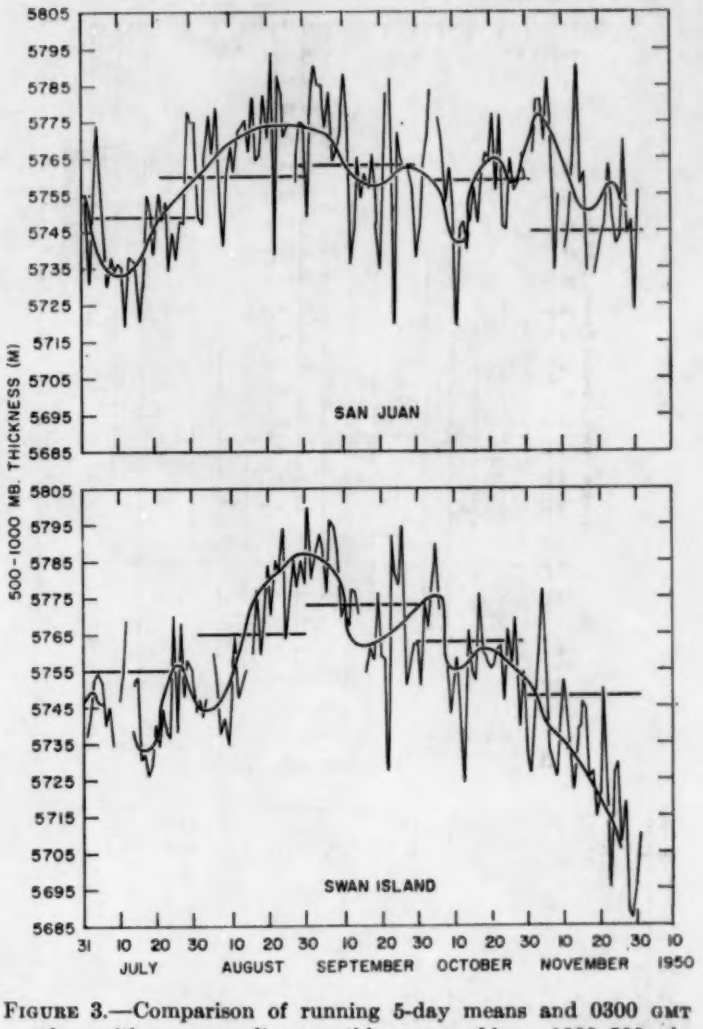

FIGURE 3.—Comparison of running 5-day means and 0300 GMT values with corresponding monthly means of layer 1000–500 mb. (ΔH_3), hurricane season 1950.

more, the areas of anomaly associated with synoptic systems are quite small. For example, *waves in the easterlies* frequently have negative anomalies of 10 to 20 meters in ΔH_1 and in ΔH_2 about 100 n.mi. up- and downstream from the trough line. (Troughs in the westerlies are usually colder and have larger anomaly areas.)

Tropical storms usually have associated with them negative anomalies greater than 15 meters since they are associated with strong troughs, but the anomaly areas rarely extend over the entire region of cyclonically curved contours.

The mature hurricane always carries a positive anomaly in ΔH_2 and ΔH_3, but the area is typically perhaps less than 3° of latitude from the center [8]. On the other hand, the area of positive anomaly in the 700–1000-mb. layer is so small that it is not apparent from data unless the storm is very near an upper-air station, and even 50 to 100 miles from the eye negative ΔH_1 anomalies are observed.[5]

Areal distribution of anomalies apparently is homogeneous enough to permit qualitative extrapolation. Inspection of several months of anomaly charts (plotted from station data—not analyses) showed that a single zero line frequently appears in the tropical region, or at most, a central zone of one sign is flanked on either side by areas of the opposite sign. This is analogous to an airmass characteristic with large continuous areas slightly cooler than normal or slightly above normal. Although the boundaries of these zones are not marked by fronts or shearlines, this feature permits one to extrapolate at least the sign of the anomaly over relatively large areas.

Vertical distribution of anomalies also shows some regularity, but the relation of ΔH_1 to ΔH_2 changes from place to place, as one might expect in view of the different circulation regimes. Figure 5 shows linear correlation coefficients between the strata for each of the five hurricane months. It is significant that the correlations are lowest through the central portion of the analysis area, just where the waves attain their greatest amplitude, reflecting perhaps the fact that in the non-disturbed areas the temperatures fluctuate as a single "airmass", while in the waves variable vertical motions affect the layers in a more complex manner. The analyst therefore should estimate anomalies to be quite similar in both

[5] This is evident from a mean hurricane sounding [9] which is typical of radial distances of 1° to 2.5° of latitude, when it is compared to the mean tropical sounding for the same area and months [10] as follows:
Anomalies: $\Delta H_1 = -3$m.; $\Delta H_2 = +21$m.; $\Delta H_3 = +18$m.

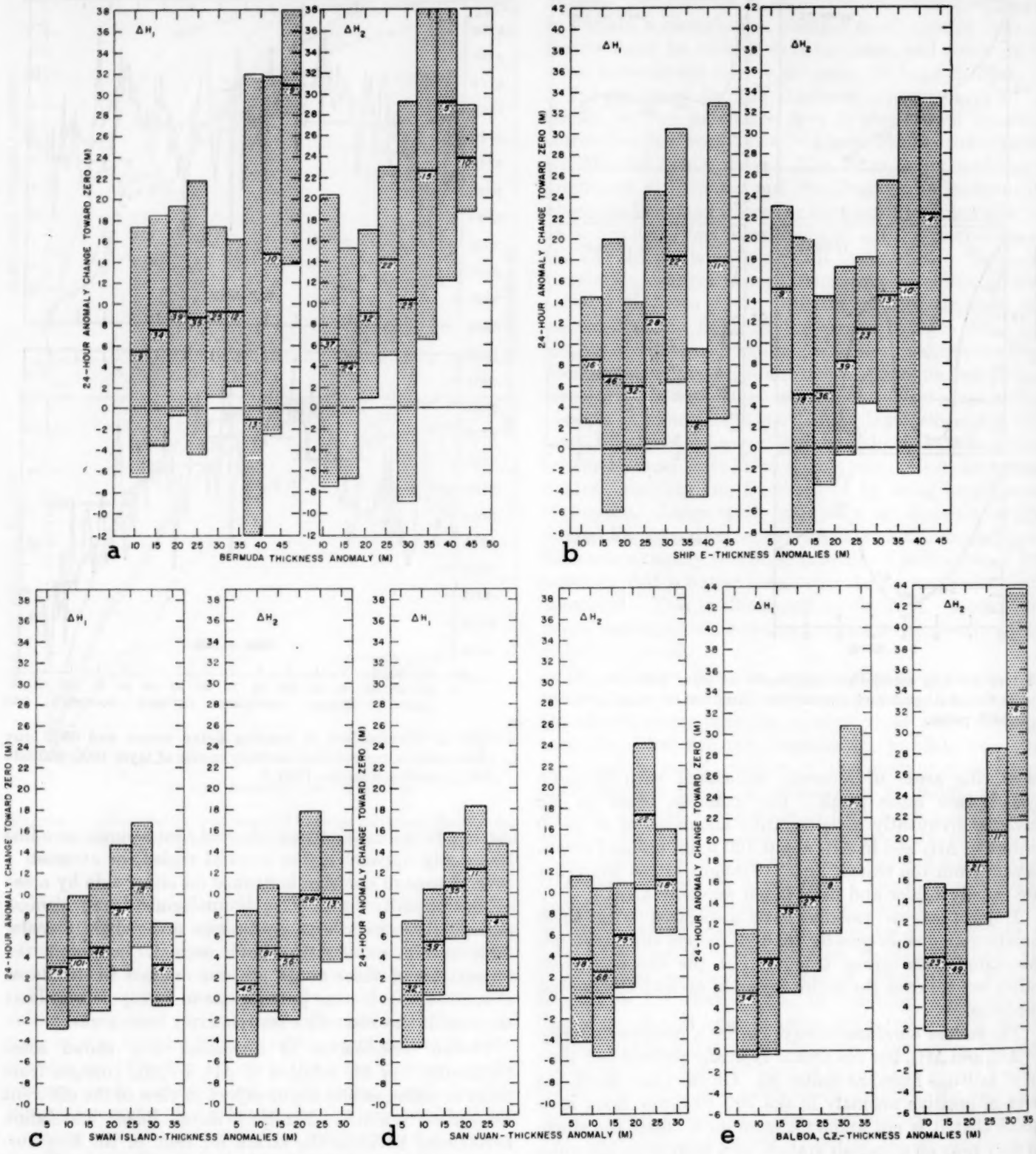

FIGURE 4.—Twenty-four-hour "return to normal" of thickness as a function of anomaly magnitude in the layers 1000–700 mb. (ΔH_1) and 700–500 mb. (ΔH_2), July through November. Horizontal lines indicate values of mean 24-hour change and size of class intervals used, with number of cases in each class shown. Shaded bar indicates range of the probable error.

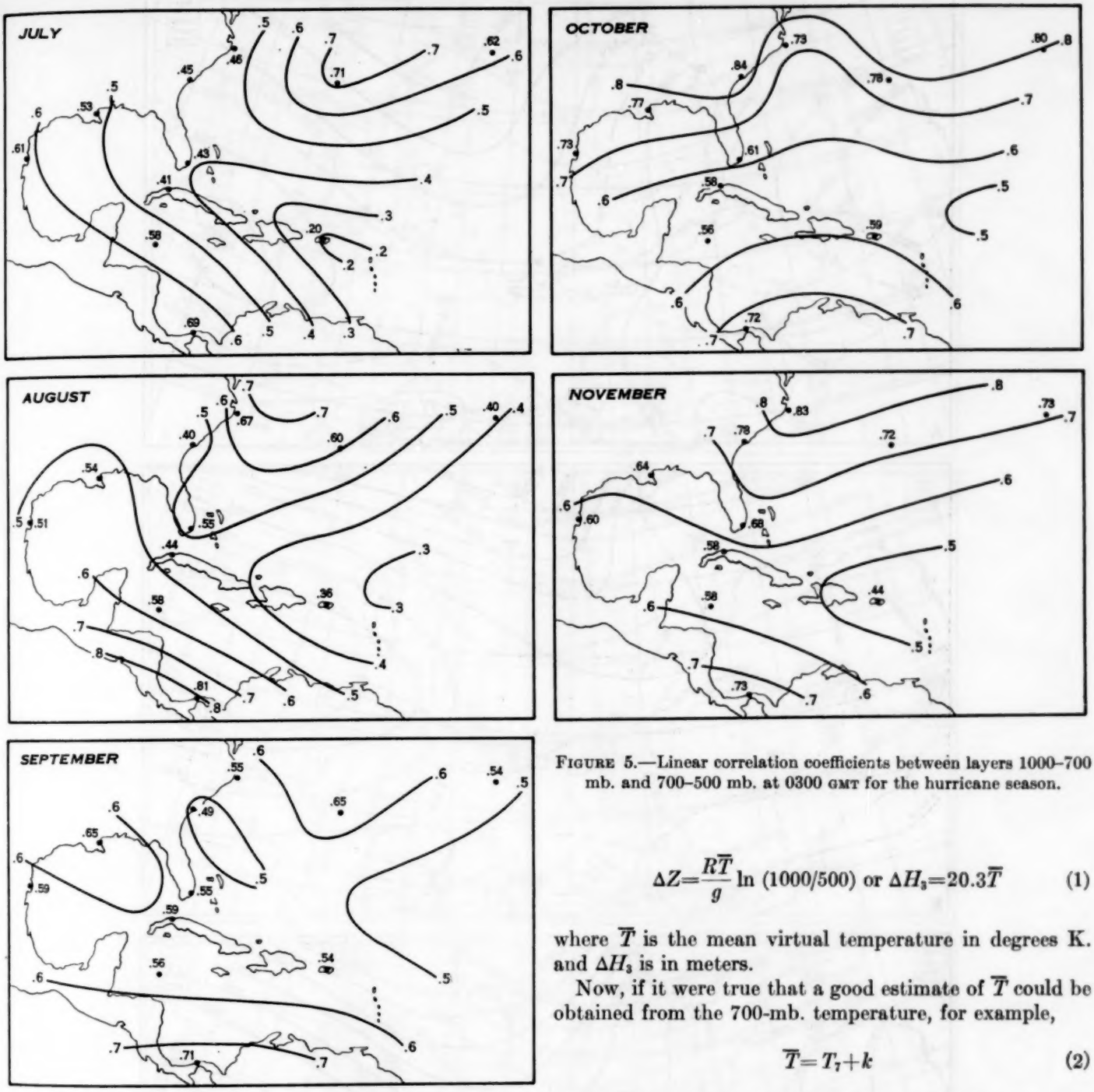

FIGURE 5.—Linear correlation coefficients between layers 1000–700 mb. and 700–500 mb. at 0300 GMT for the hurricane season.

layers in the northern and southern zones, but should not attempt to place this restriction on the patterns of the central part, especially in disturbed areas.

Temperature at 700 mb. is correlated with thickness, thus with anomaly in the various layers discussed here. It is of interest to notice, however, that it is not a simple relation, such for example that a degree of temperature increase at 700 mb. corresponds to a degree of increase in the mean virtual temperature in the layer 1000–500 mb., as illustrated by the following:

The hydrostatic equation can be written

$$\Delta Z=\frac{R\overline{T}}{g}\ln(1000/500) \text{ or } \Delta H_3=20.3\overline{T} \qquad (1)$$

where $\overline{T}$ is the mean virtual temperature in degrees K. and ΔH_3 is in meters.

Now, if it were true that a good estimate of $\overline{T}$ could be obtained from the 700-mb. temperature, for example,

$$\overline{T}=T_7+k \qquad (2)$$

where $\overline{T}_7$ is the 700-mb. temperature and k is a constant depending upon the average stability and moisture content of the layer involved, then

$$\Delta H_3=20.3\ k+20.3\ T_7 \qquad (3)$$

The linear regression lines of T_7 on ΔH_3 for Balboa, C. Z. and for Ship E have slopes of 15 and 13, respectively, as compared to 20.3 of equation (3). Therefore the relation between mean virtual temperature and the 700-mb. temperature expressed in equation (2) is not sufficiently good for this purpose; so it is necessary to use empirically derived regression lines from point to point

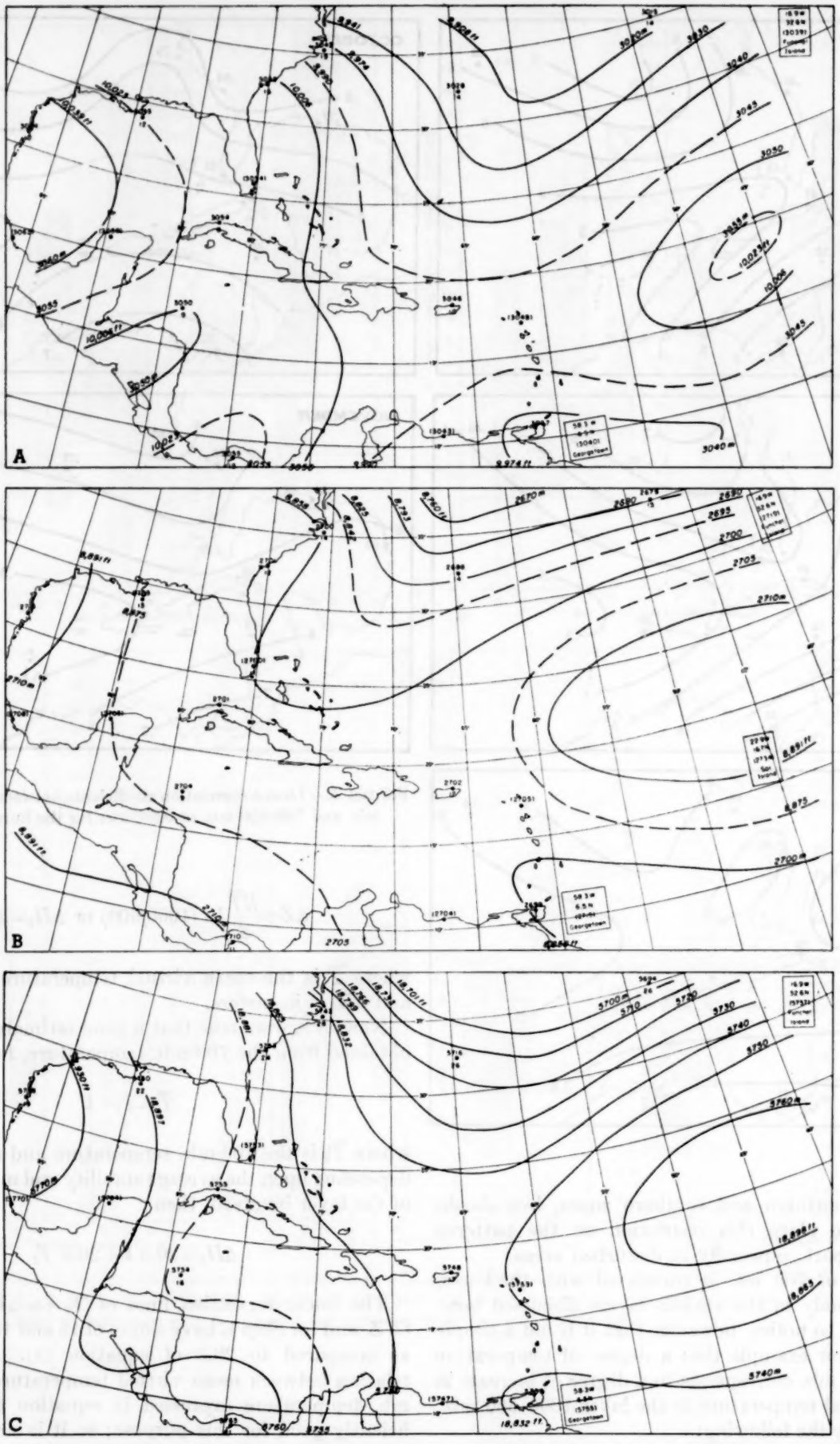

FIGURE 6.—Mean thickness and standard deviation of thickness (meters) for 0300 GMT, for July. (A) 1000–700 mb. (ΔH_1), (B) 700–500 mb. (ΔH_2), and (C) 1000–500 mb. (ΔH_3).

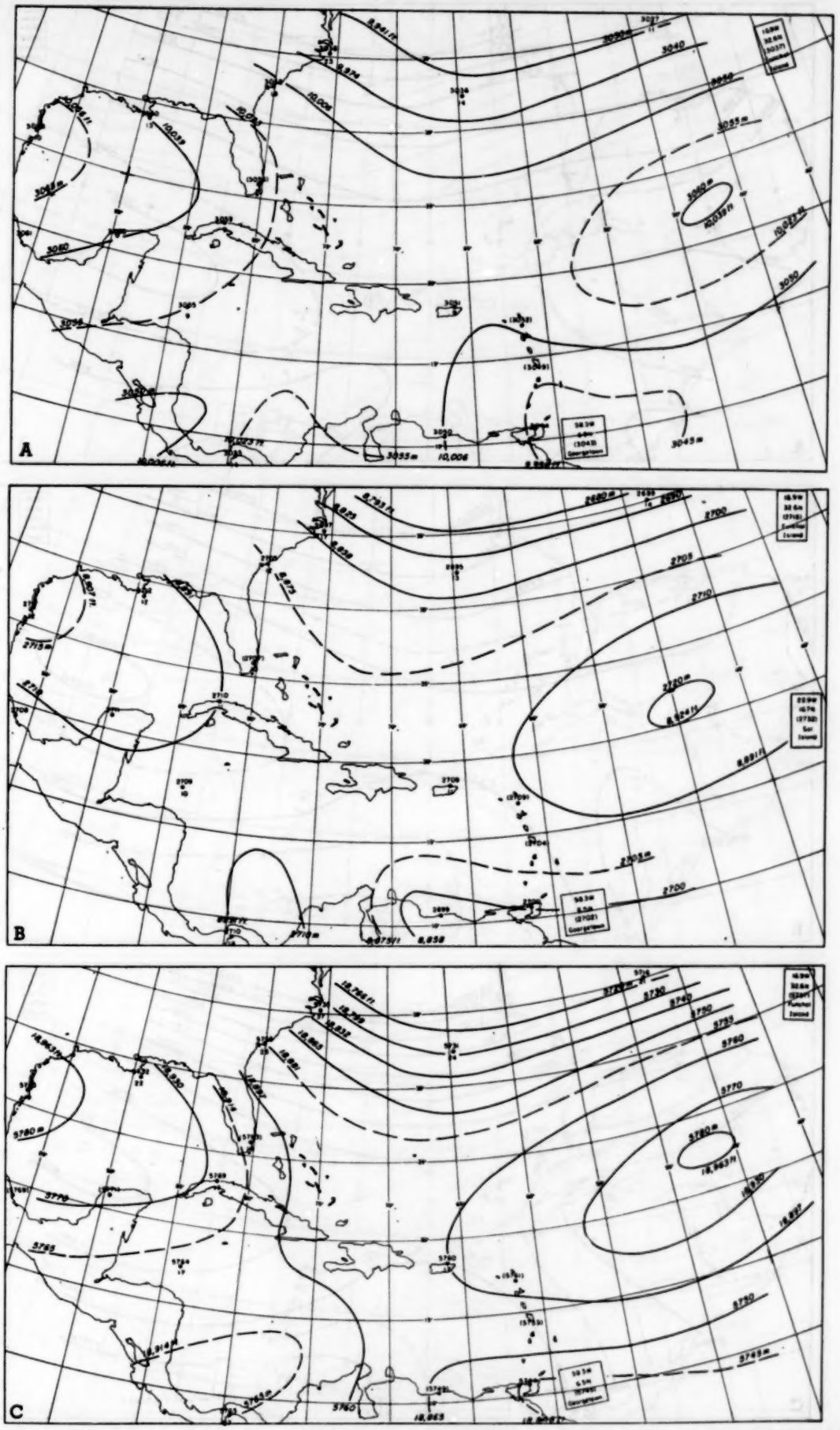

FIGURE 7.—Mean thickness and standard deviation of thickness (meters) for 0300 GMT, for August. (A) 1000–700 mb. (ΔH_1), (B) 700–500 mb. (ΔH_2), and (C) 1000–500 mb. (ΔH_3).

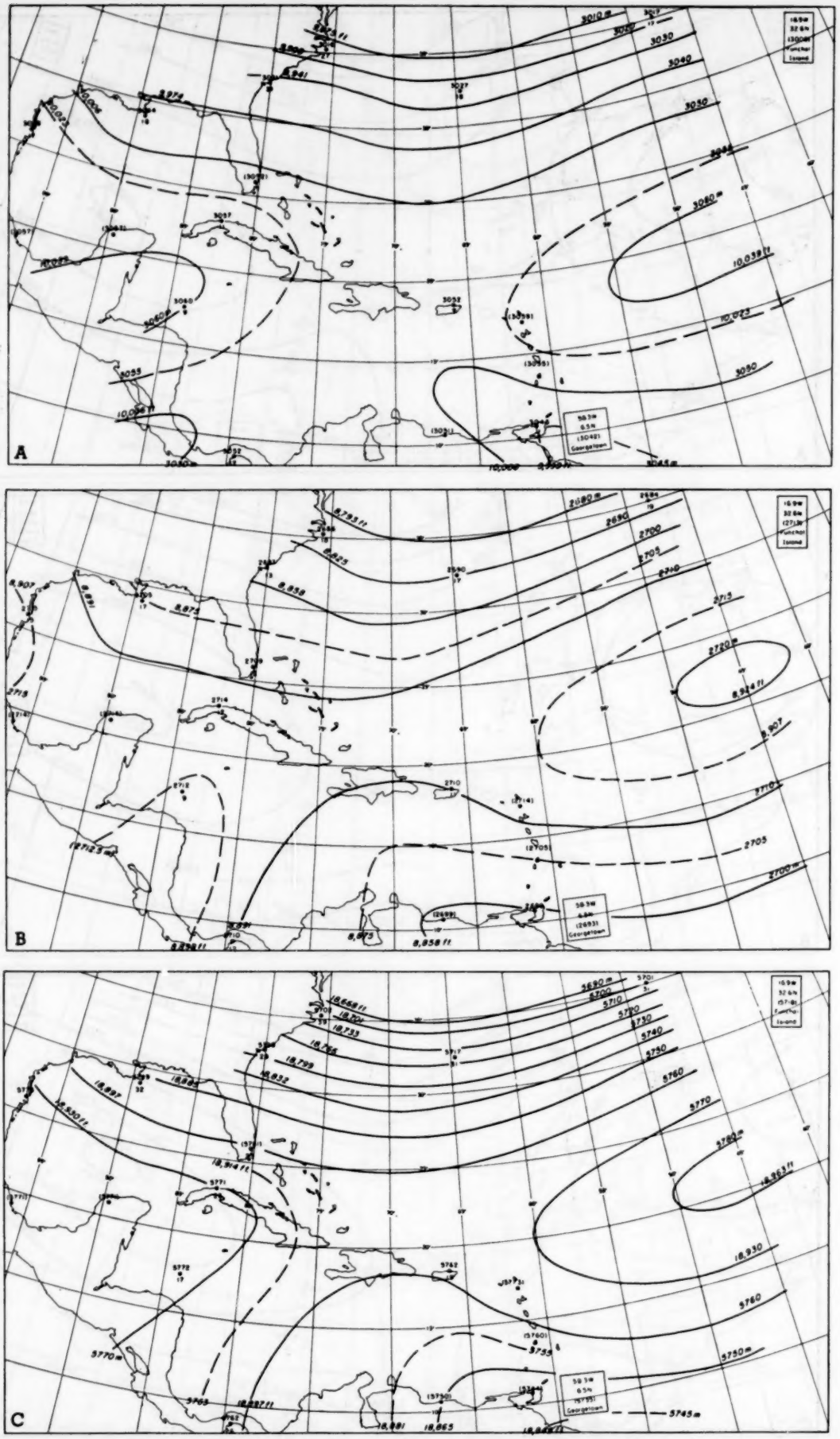

FIGURE 8.—Mean thickness and standard deviation of thickness (meters) for 0300 GMT for September. (A) 1000–700 mb. (ΔH_1), (B) 700–500 mb. (ΔH_2), and (C) 1000–500 mb. (ΔH_3).

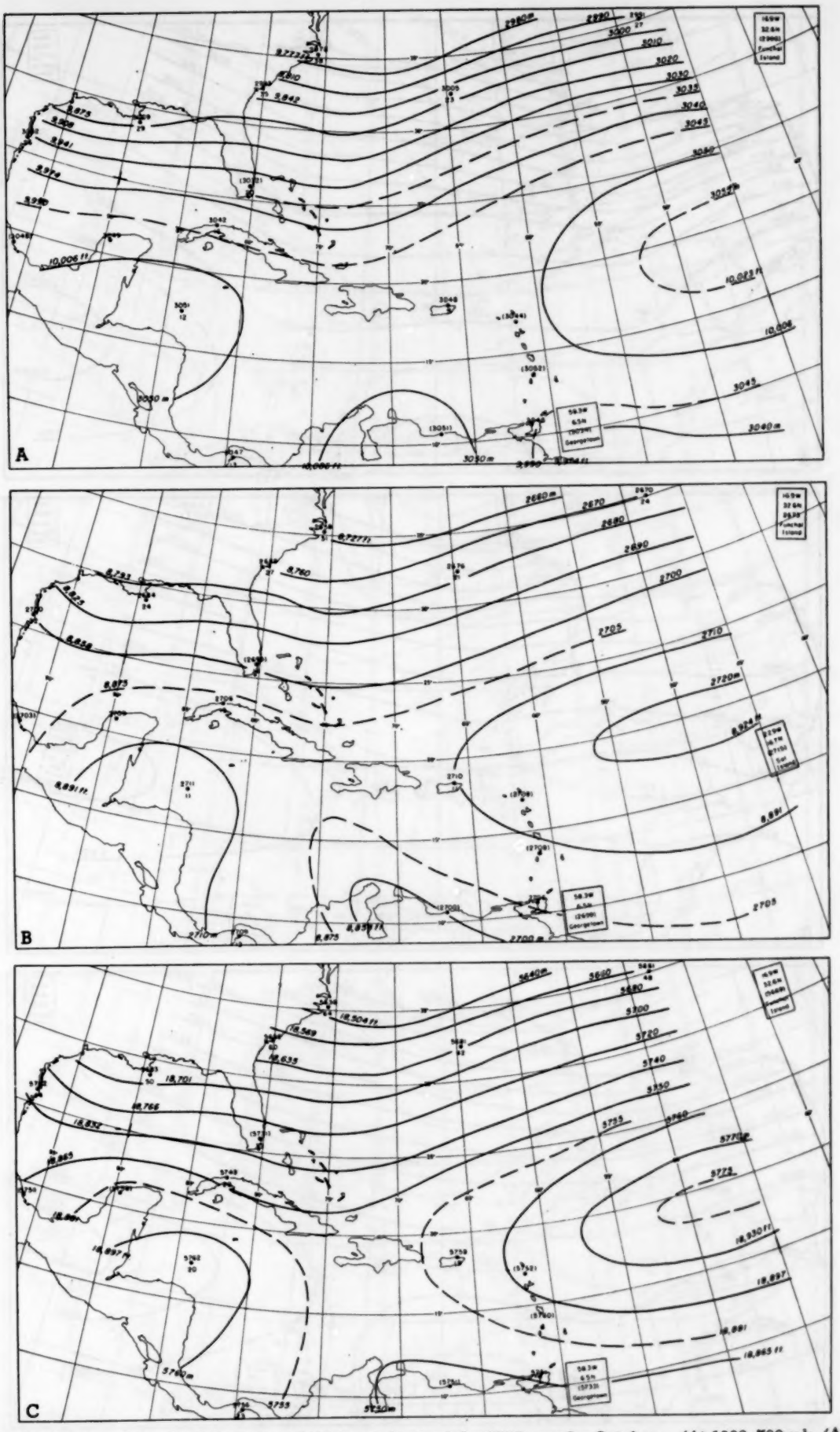

FIGURE 9.—Mean thickness and standard deviation of thickness (meters) for 0300 GMT for October. (A) 1000–700 mb. (ΔH_1), (B) 700–500 mb. (ΔH_2), and (C) 1000–500 mb. (ΔH_3).

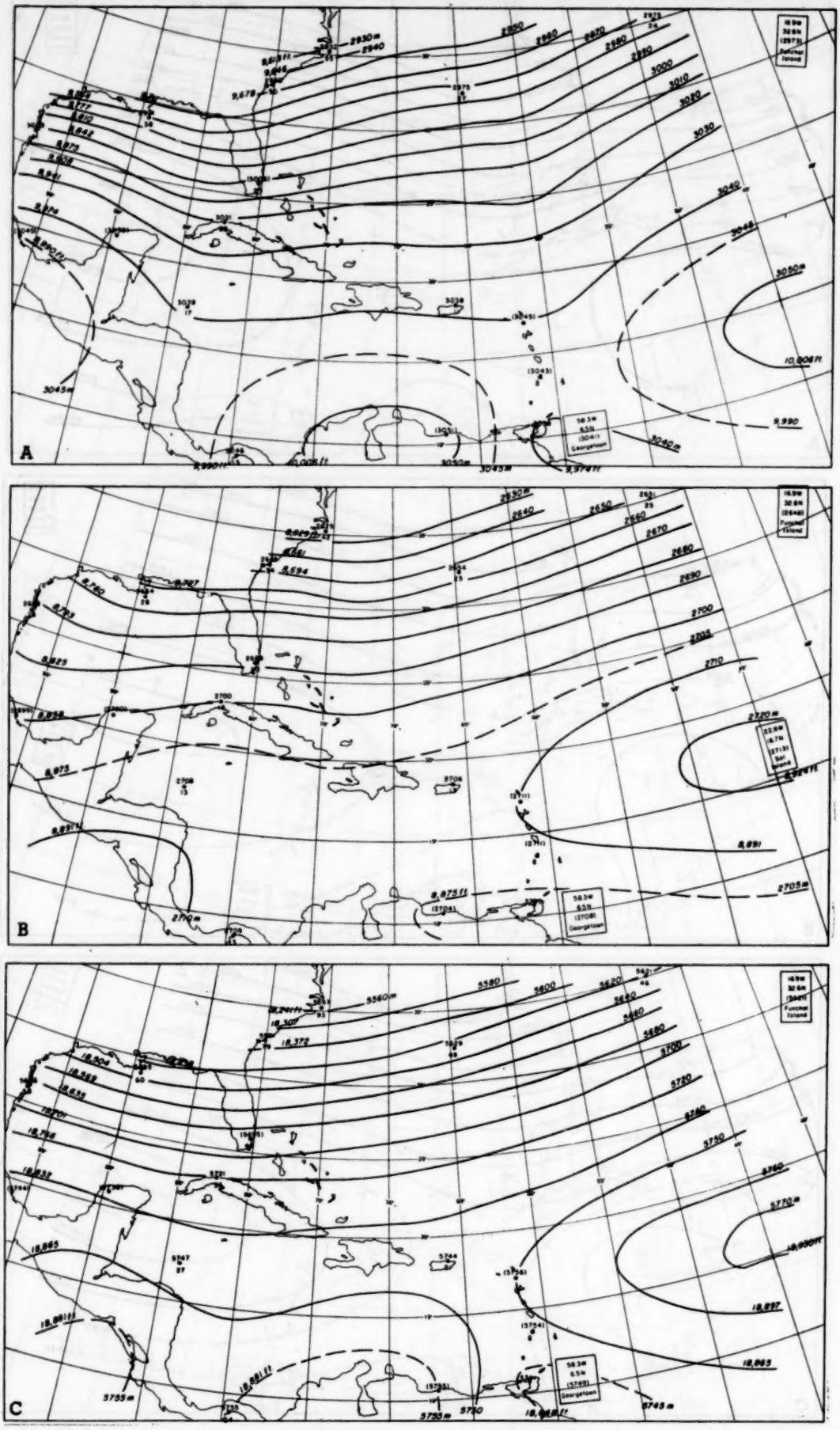

FIGURE 10.—Mean thickness and standard deviation of thickness (meters) for 0300 GMT for November. (A) 1000–700 mb. (ΔH_1), (B) 700–500 mb. (ΔH_2), and (C) 1000–500 mb. (ΔH_3).

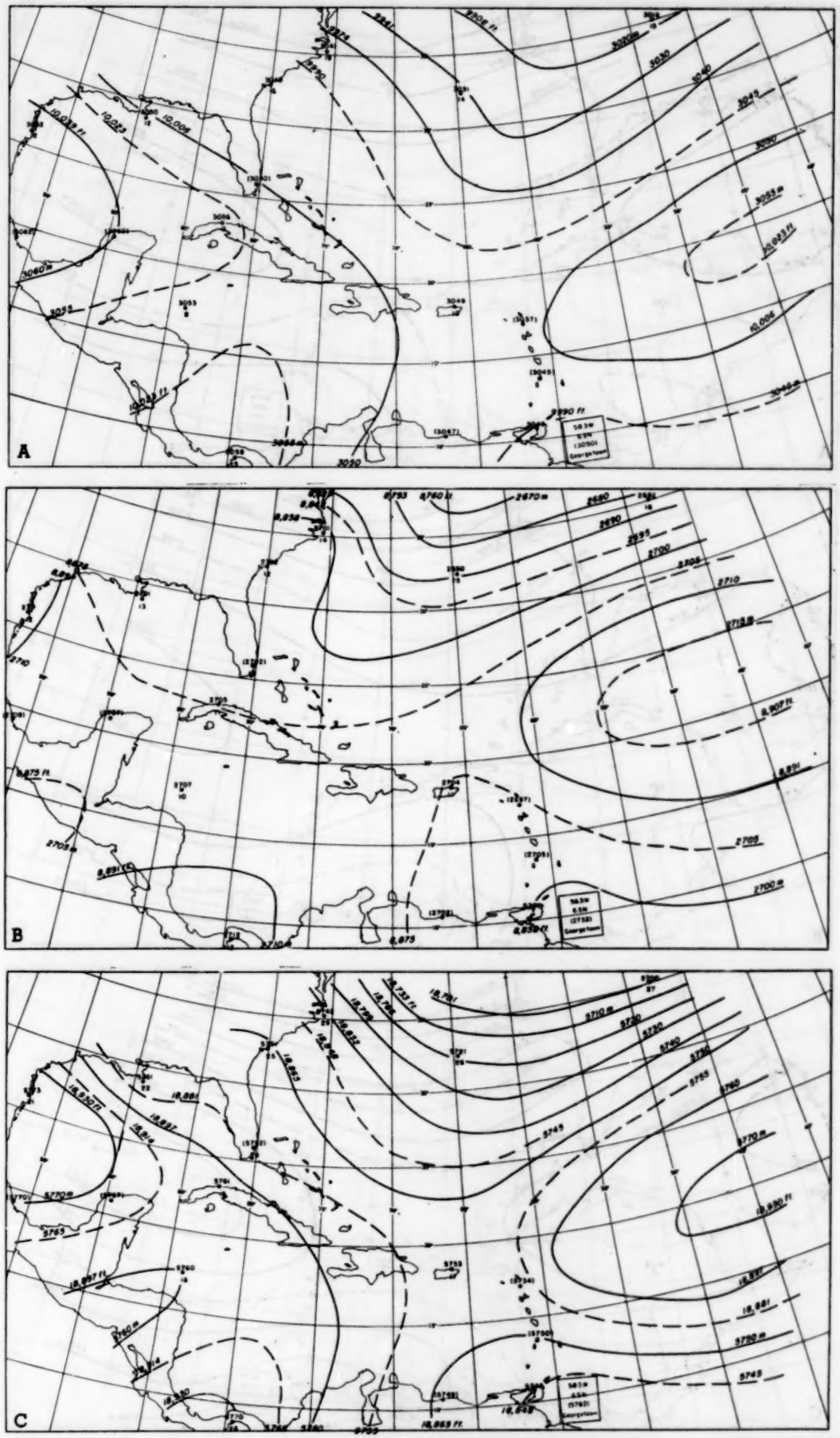

FIGURE 11.—Mean thickness and standard deviation of thickness (meters) for 1500 GMT for July. (A) 1000–700 mb. (ΔH_1), (B) 700–500 mb. (ΔH_2), and (C) 1000–500 mb. (ΔH_3).

474509—58——2

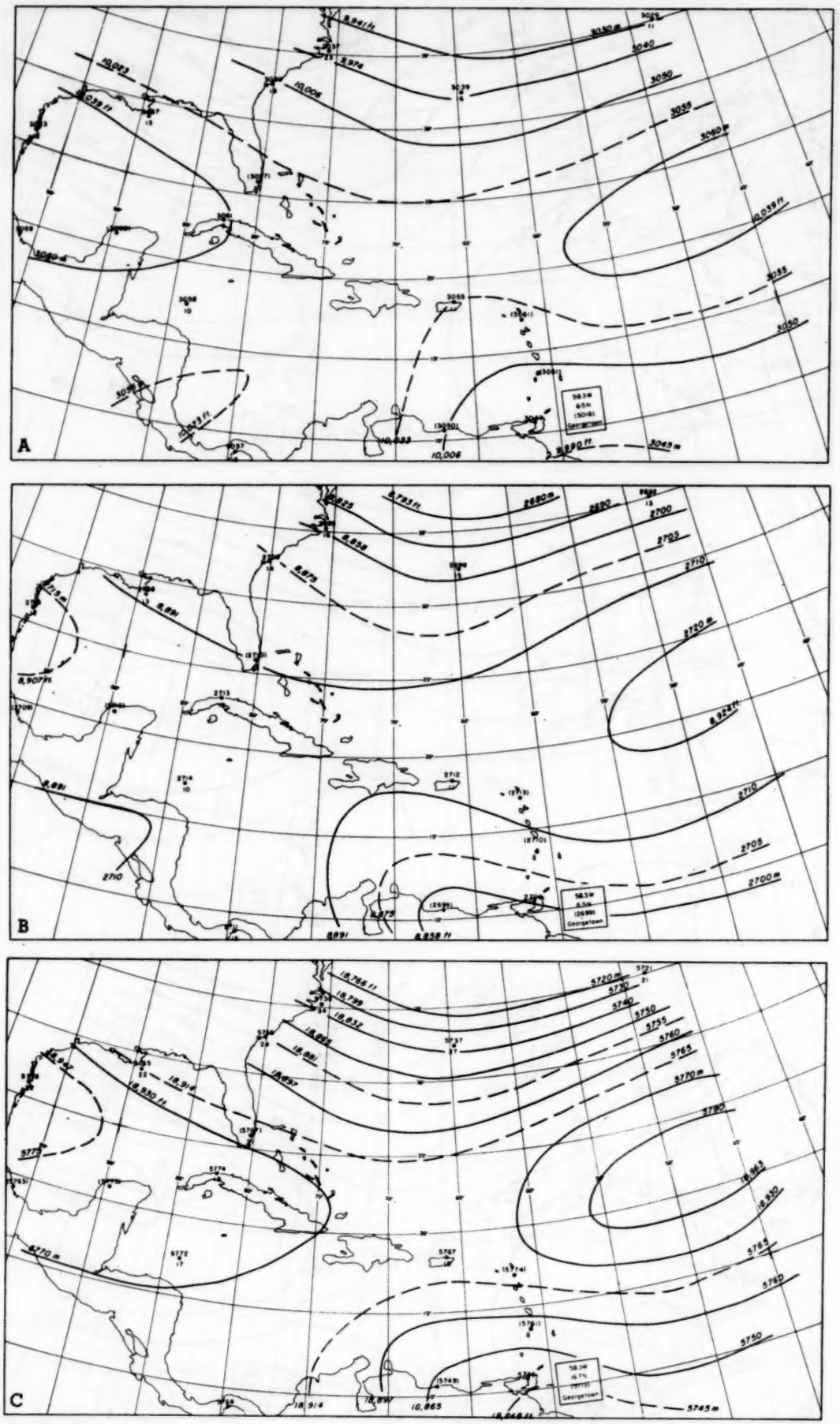

FIGURE 12.—Mean thickness and standard deviation of thickness (meters) for 1500 GMT for August. (A) 1000–700 mb. (ΔH_1), (B) 700–500 mb. (ΔH_2), and (C) 1000–500 mb. (ΔH_3).

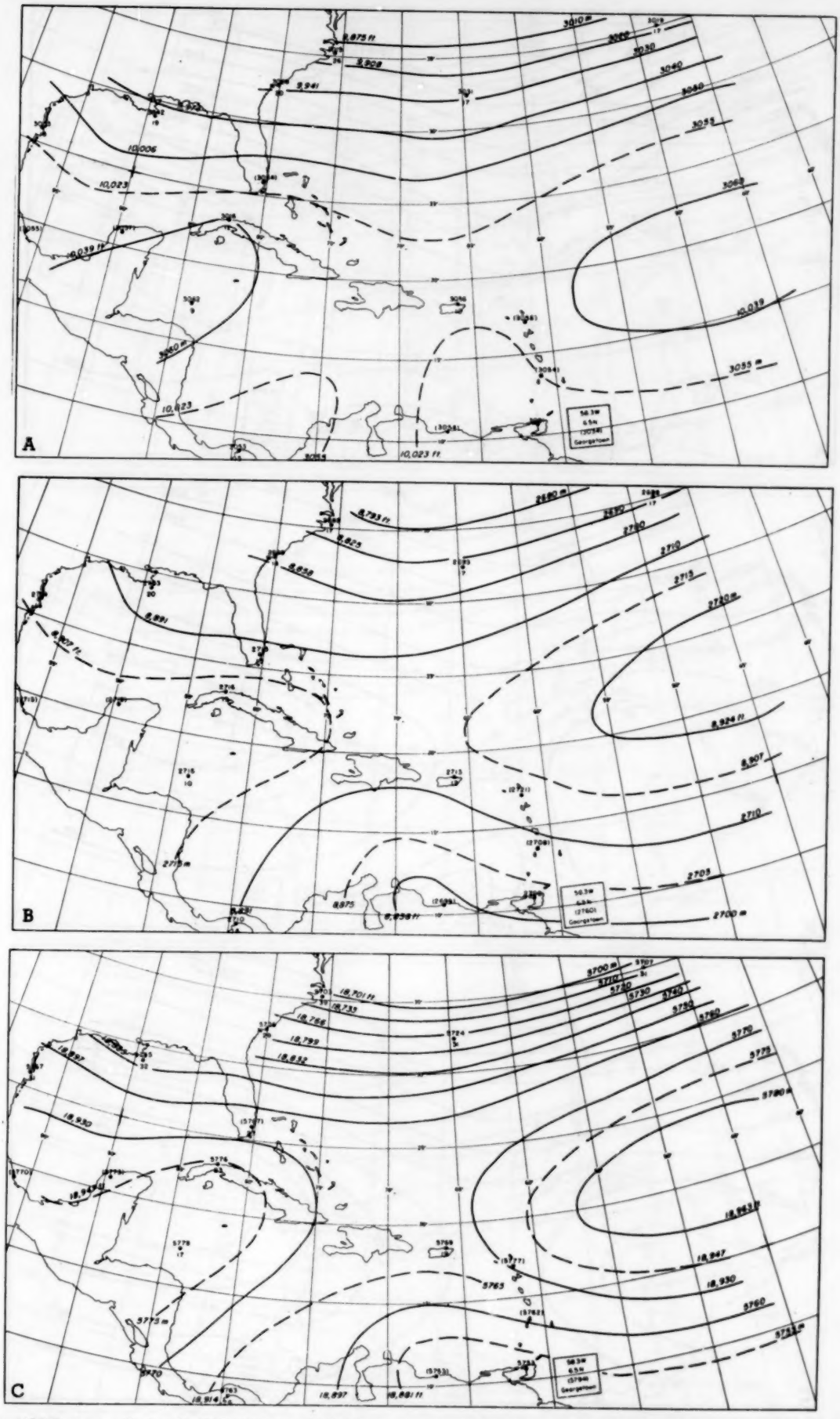

FIGURE 13.—Mean thickness and standard deviation of thickness (meters) for 1500 GMT for September. (A) 1000–700 mb. (ΔH_1), (B) 700–500 mb. (ΔH_2), and (C) 1000–500 mb. (ΔH_3).

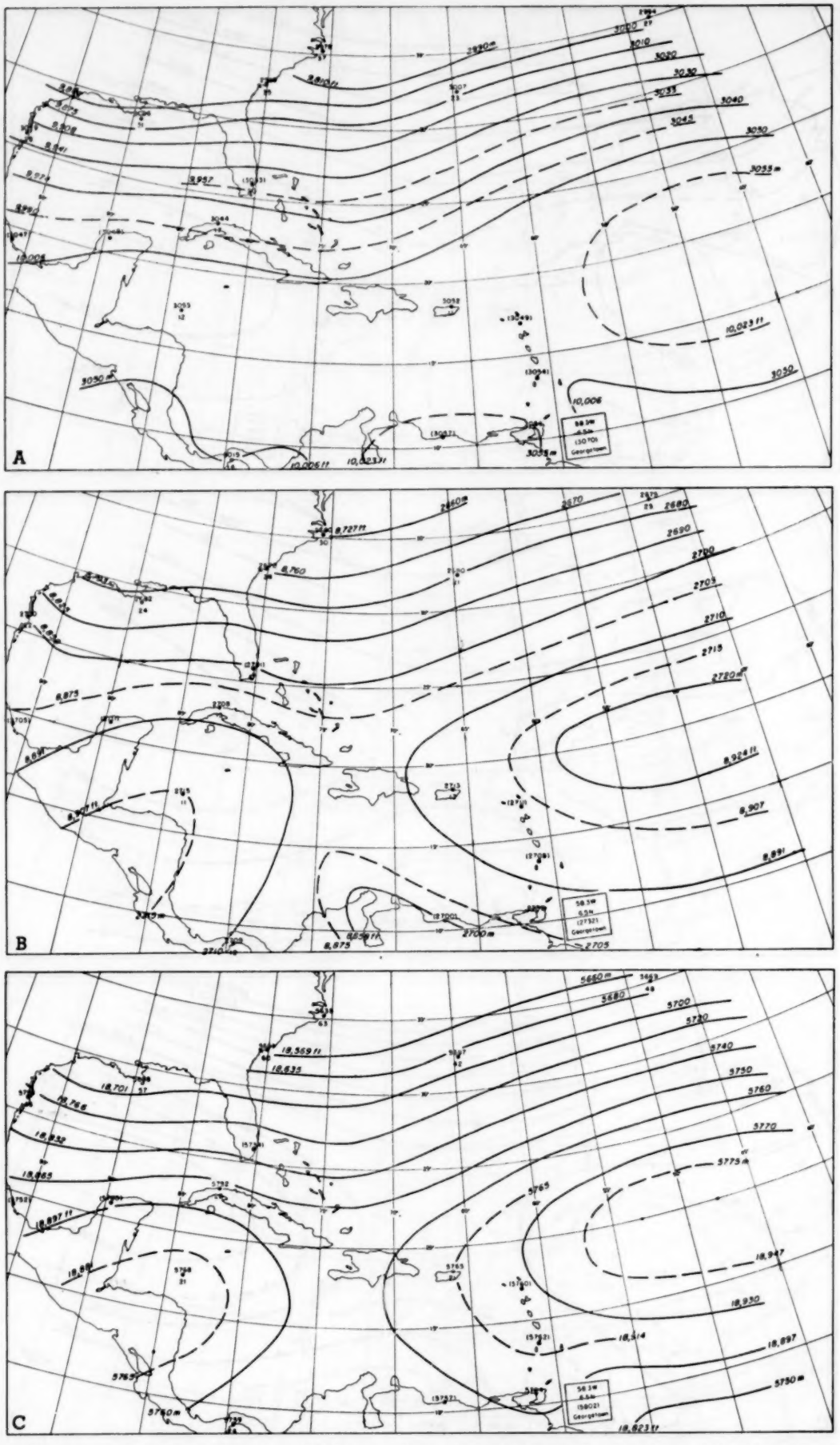

FIGURE 14.—Mean thickness and standard deviation of thickness (meters) for 1500 GMT for October. (A) 1000–700 mb. (ΔH_1), (B) 700–500 mb. (ΔH_2), and (C) 1000–500 mb. (ΔH_3).

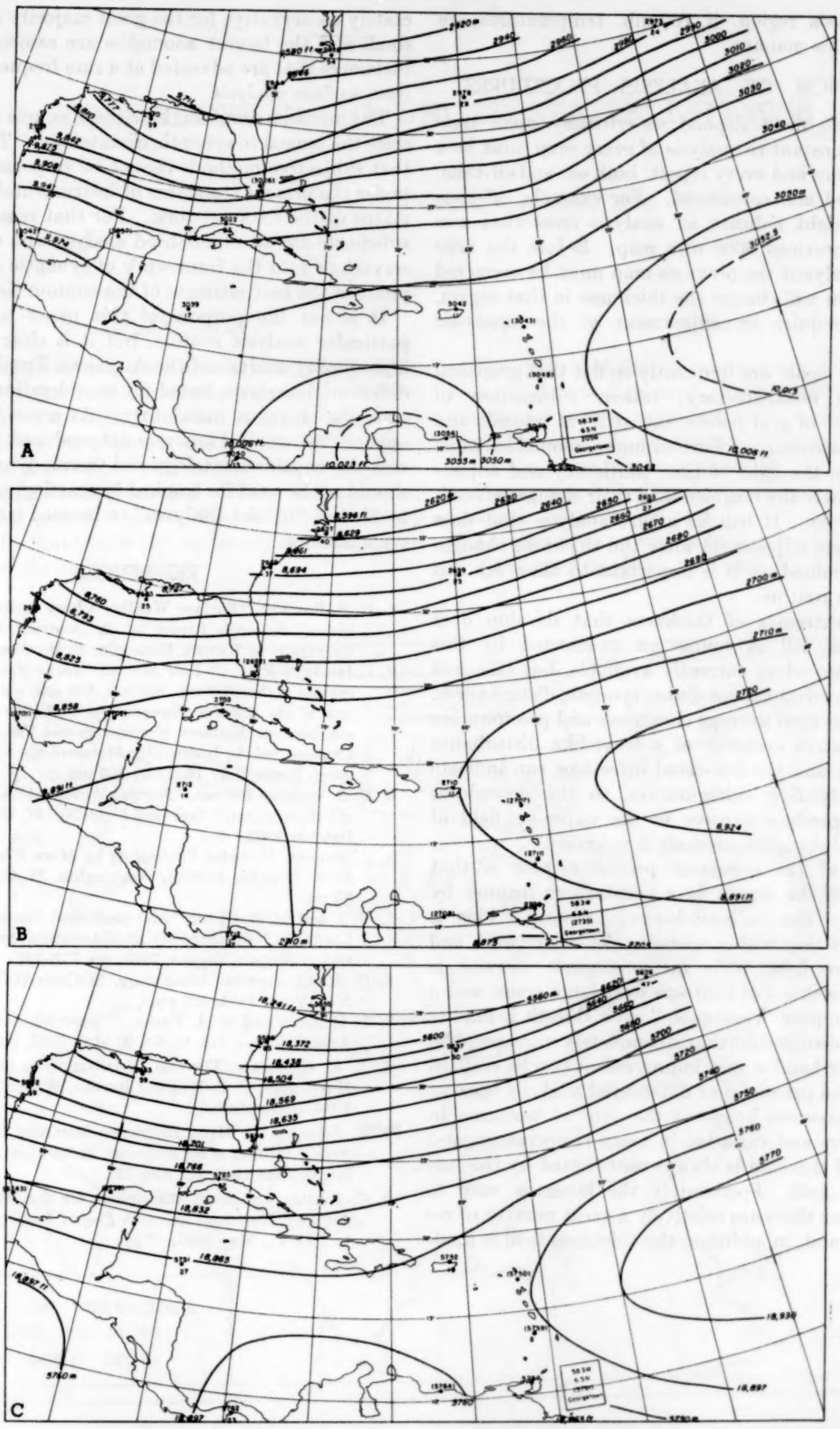

FIGURE 15.—Mean thickness and standard deviation of thickness (meters) for 1500 GMT for November. (A) 1000–700 mb. (ΔH_1), (B) 700–500 mb. (ΔH_2), and (C) 1000–500 mb. (ΔH_3).

over the analysis region, if 700-mb. temperatures are to be used in this manner.

6. DISCUSSION OF ANALYSIS PROCEDURES

Since analysis must depend so critically upon time continuity, a constant re-analysis of every map must be a routine procedure and every report, both on- and off-time, must be plotted and considered. For example, off-time ship reports might indicate an analysis error that was made on the previous 0000 GMT map. Before the 1200 GMT map is analyzed the previous map must be corrected and this in turn will change the thickness in that region, and perhaps require an adjustment of the upper-air map.

The contour fields are frequently so flat that graphical subtraction is unsatisfactory; rather, subtraction of heights at a net of grid points, say at 5° of latitude and longitude, is necessary. Furthermore, anomalies must be examined in the light of time continuity and adjustments made where the magnitude of their changes exceeds reasonable values. It will be a rare analysis that does not require some adjustment after the thickness changes have been examined, so it is important to allow for this in the analysis routine.

Important extremes of thickness that develop over data-free areas will of course go undetected by this or any other procedure currently available, but this does not mean the analyst cannot detect synoptic disturbances. Areas of greater than average cloudiness and precipitation are almost always evidence of a wave-like disturbance or a shear line and the low-cloud directions can indicate the most likely flow configuration, so the procedures outlined will produce a wave in the upper-air field of motion, even though the anomaly is unknown.

The point of the argument presented here is that contours cannot be drawn in a satisfactory manner by analyzing only the radiosonde-rawin reports. This is due to the fact that with a sparse upper-air network and a flat pressure field, little meteorological restraint is imposed on the shape of contours over large areas, and a pattern may appear "reasonable" even though it implies a temperature distribution that is completely unreasonable!

On the other hand a vast improvement can be realized by applying the principles of differential analysis because variation in pressure height is the sum of variation in surface pressure and variation in mean temperature, and a large part of this sum is always contributed by the surface pressure field. Fortunately the latter is easy to analyze because there are relatively a great number of reliable reports and, in addition, the thickness field is moderately conservative for the great majority of changes are small and the largest anomalies are associated with disturbances that are advected at a rate frequently deducible from surface analysis.

The methods discussed here are of course subjective, despite the appeal to synoptic climatology. The writer feels that subjective methods cannot be surpassed in this area under the present standards of instrumental accuracy and status of the data network. For that reason there is no substitute for an experienced analyst who can fit the observations into the framework of synoptic climatology to produce the best estimate of the contour field.

It is not the purpose of this paper to suggest any particular analysis routine, but it is clear that where a high-quality analysis of the American Tropics is required, differential analysis, based on considerations of the type presented here, is mandatory. As a corollary, it would appear that tropical analyses *not* produced under the control of synoptic climatology and thermodynamic restraints should *not* be used for tropical forecasting, nor should they be filed as "official analyses" to be used later by research organizations.

REFERENCES

1. C. S. Ramage, "Surface Weather Chart Analysis in Low Latitudes," *Scientific Report* No. 2, Contract AF 19(604)–1942, University of Hawaii, Honolulu, T. H., August 1957.
2. I. Jacobs, *5-Resp. 40-Year Monthly Means of the Absolute Topographies of the 1000 mb., 850 mb., 500 mb., and 300 mb. Levels and of the Relative Topographies 500/1000 mb. and 300/500 mb. over the Northern Hemisphere and Their Month-to-Month Changes*, vol. I., Institut für Meteorologie und Geophysik der freien Berlin, July 16, 1957, 305 pp.
3. U. S. Weather Bureau, "Normal Weather Charts for the Northern Hemisphere," *Technical Paper* No. 21, Washington, D. C., October 1952.
4. J. Namias, *Extended Forecasting by Mean Circulation Methods*, U. S. Weather Bureau, Washington, D. C., February 1947, 89 pp.
5. V. J. and M. B. Oliver, "Meteorological Analysis in the Middle Latitudes," *Compendium of Meteorology*, American Meteorological Society, Boston, 1951, pp. 715–727.
6. H. Riehl, *Tropical Meteorology*, McGraw-Hill Book Co., Inc., New York, 1954, 392 pp.
7. B. R. Döös and M. A. Eaton, "Upper-Air Analysis over Ocean Areas," *Tellus*, vol. 9, No. 2, May 1957, pp. 184–194.
8. A. K. Showalter, Thermal Distribution In and Near Tropical Hurricanes, U. S. Weather Bureau, Washington, D. C., June 1956, (unpublished).
9. E. Schacht, "A Mean Hurricane Sounding for the Caribbean Area," *Bulletin of the American Meteorological Society*, vol. 27, No. 6, June 1946, pp. 324–327.
10. C. Jordan, "A Mean Atmosphere for the West Indies Area," *National Hurricane Research Project Report*, No. 6, Washington, D. C., May 1957, 17 pp.

TORNADOES IN THE UNITED STATES, 1950–1956

J. T. LEE

Severe Local Storms Center, U. S. Weather Bureau, Kansas City, Mo.

[Manuscript received April 18, 1958]

1. INTRODUCTION

During the period 1950–1956 a total of 3,204 tornadoes was recorded in the United States as compared with 5,204 during the years 1916–1950 [1]. These data give an average of 458 tornadoes per year for the 1950–1956 period as compared with the 149 per year for the 1916–1950 period. Because of the increased number of observations during the more recent period, it was decided to study the distribution State by State, monthly and hourly, for comparison with results of the earlier study.

2. DATA

The 1950–1956 data were obtained from *Climatological Data, National Summary*. Every effort was made to include only those tornadoes which touched the ground. Funnel clouds aloft were not included because of the more likely chance of mistaken identity.

Due to the difficulty of determining in "family type" outbreaks whether the same tornado was sighted several times or whether several tornadoes developed, the material in *Climatological Data* was used to make the decision.

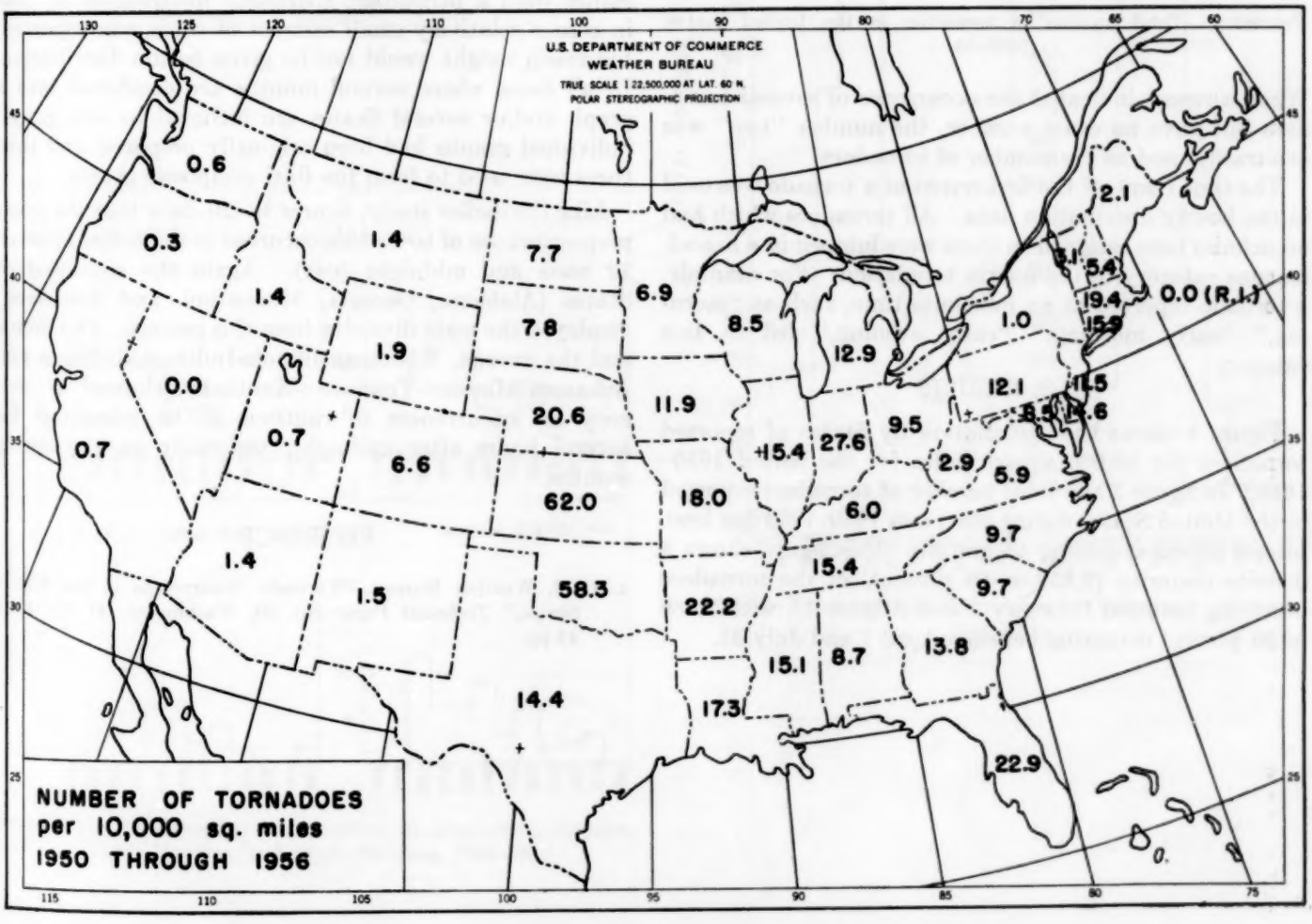

FIGURE 1.—Number of tornadoes per 10,000 square miles, 1950–56.

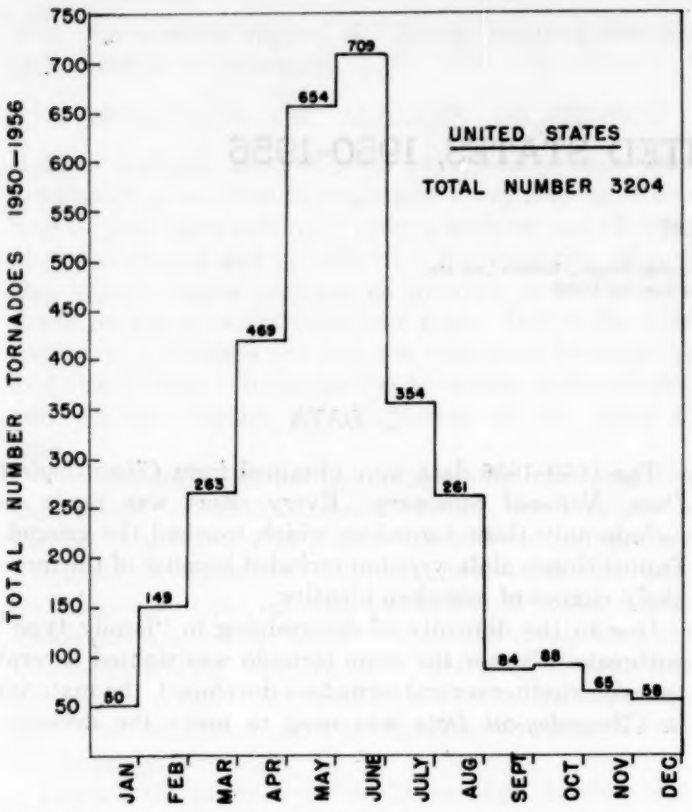

FIGURE 2.—Total number of tornadoes in the United States, 1950–56.

When a report indicated the occurrence of several tornadoes but gave no exact number, the number "two" was arbitrarily used as the number of tornadoes.

The time (CST) of the first report of a tornado was used in the hourly distribution data. All tornadoes which had no definite time assigned to them were lumped in a miscellaneous category in the hourly tabulation. For example, a tornado reported at an indefinite time, such as "morning," "early morning," "early evening," fell in this category.

3. RESULTS

Figure 1 shows the distribution by States of reported tornadoes per 10,000 square miles for the period 1950–1956. In figure 2 the total number of tornadoes reported in the United States during the years 1950–1956 has been broken down according to month. This figure shows a definite majority (2,859 or 89 percent) of the tornadoes occurring between February 1 and August 31, with 2,186 or 68 percent occurring between April 1 and July 31.

Figures 3 through 12 show the monthly distribution for each State, except the New England States and the Far West. In these two regions, insufficient tornado activity precluded a separate graph for each State. Graphs were not made for Rhode Island and Nevada, as no tornadoes were reported in these States during the period of study. States were not grouped as in previous studies because there was a significant shift in monthly tornado activity among States previously grouped together—such as the case of Florida, Alabama, and Georgia. This difference in the 1950–56 figures is also shown by the March maximum in Arkansas compared to a general March to May maximum in Missouri, a May maximum in Oklahoma, and a June maximum in Kansas. There is also the April maximum in Iowa compared to a July maximum in North Dakota.

The graphs of figures 3–12 were studied and grouped within the same geographical region according to similar hourly distribution curves. These groupings were then used in figures 13 through 20 for the hourly studies. Because the time of the first report of a tornado was used in compiling the hourly distributions, figures 13–20 might appropriately be interpreted as the time distribution of first reports of tornado activity.

The actual number of tornadoes reported was used rather than a percentage frequency distribution so that in case a relatively small number of cases was reported, too much weight would not be given to the distribution. In all cases where several months are combined into a graph and/or several States are included in one graph, individual graphs had been originally prepared and then these were used to form the final composite graph.

Like the earlier study, figures 13–20 show that the great preponderance of tornadoes occurred in the hours between 12 noon and midnight (CST). Again the southeastern States (Alabama, Georgia, Mississippi, and Louisiana) displayed the main diversity from this pattern. Oklahoma and the groups, Wisconsin-Illinois-Indiana-Michigan and Arkansas-Missouri-Tennessee-Kentucky, showed a tendency for occurrences to continue to be numerous for several hours after midnight, especially in the spring months.

REFERENCE

1. U. S. Weather Bureau, "Tornado Occurrences in the United States," *Technical Paper* No. 20, Washington, D. C., 1952, 42 pp.

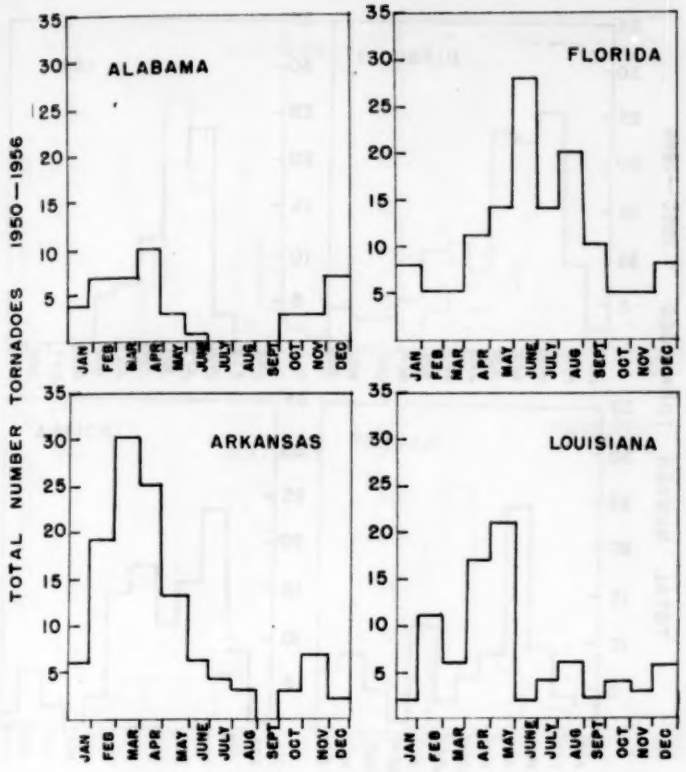

FIGURE 3.—Total number of tornadoes in Alabama, Florida, Arkansas, and Louisiana, 1950–56.

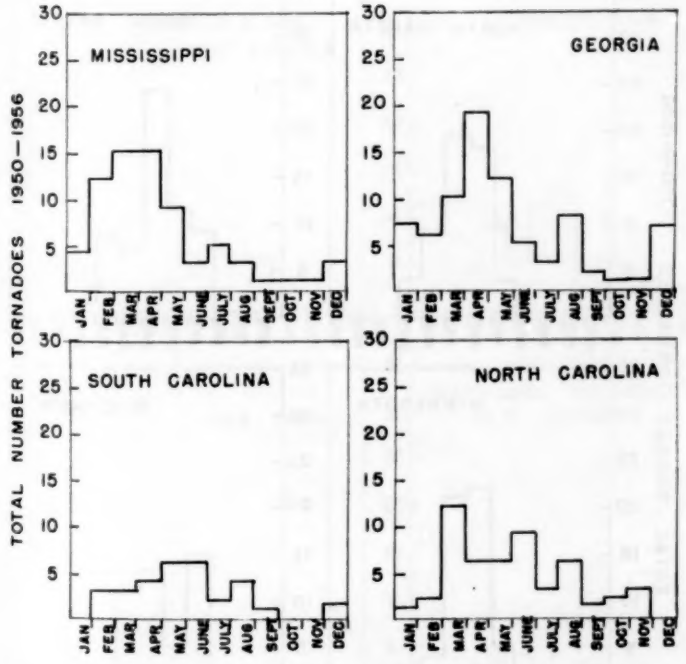

FIGURE 4.—Total number of tornadoes in Mississippi, Georgia, South Carolina, and North Carolina, 1950–56.

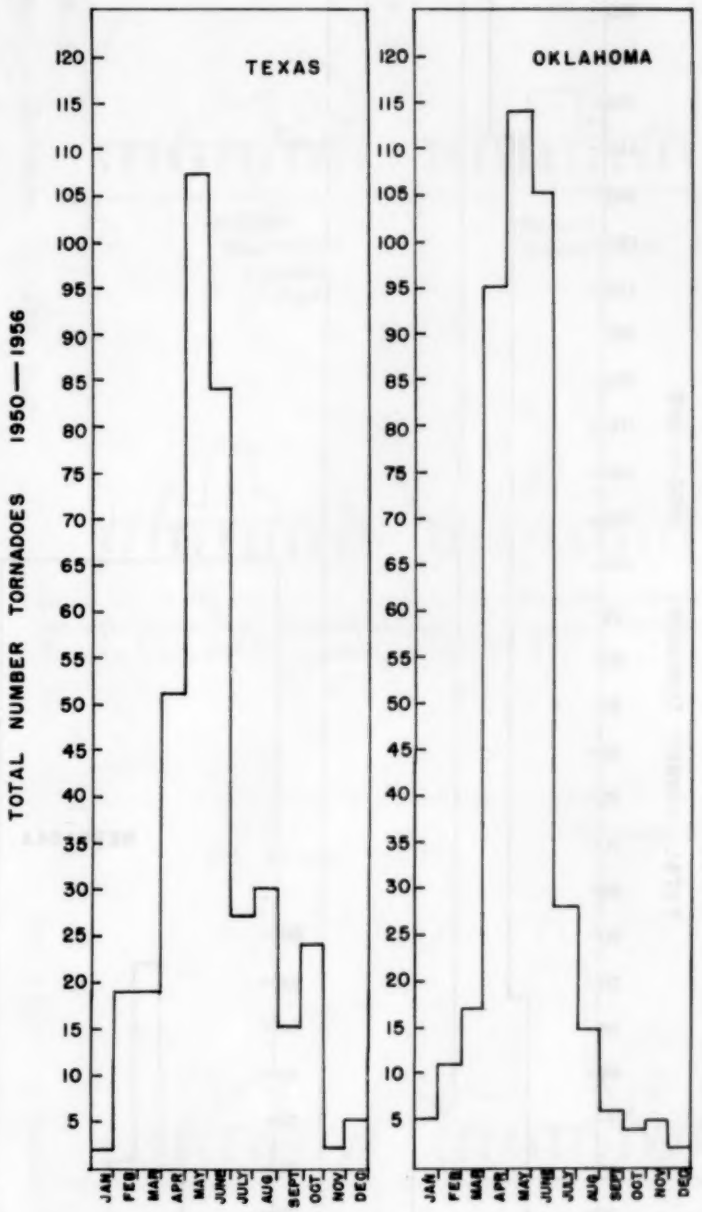

FIGURE 5.—Total number of tornadoes in Texas and Oklahoma, 1950–56.

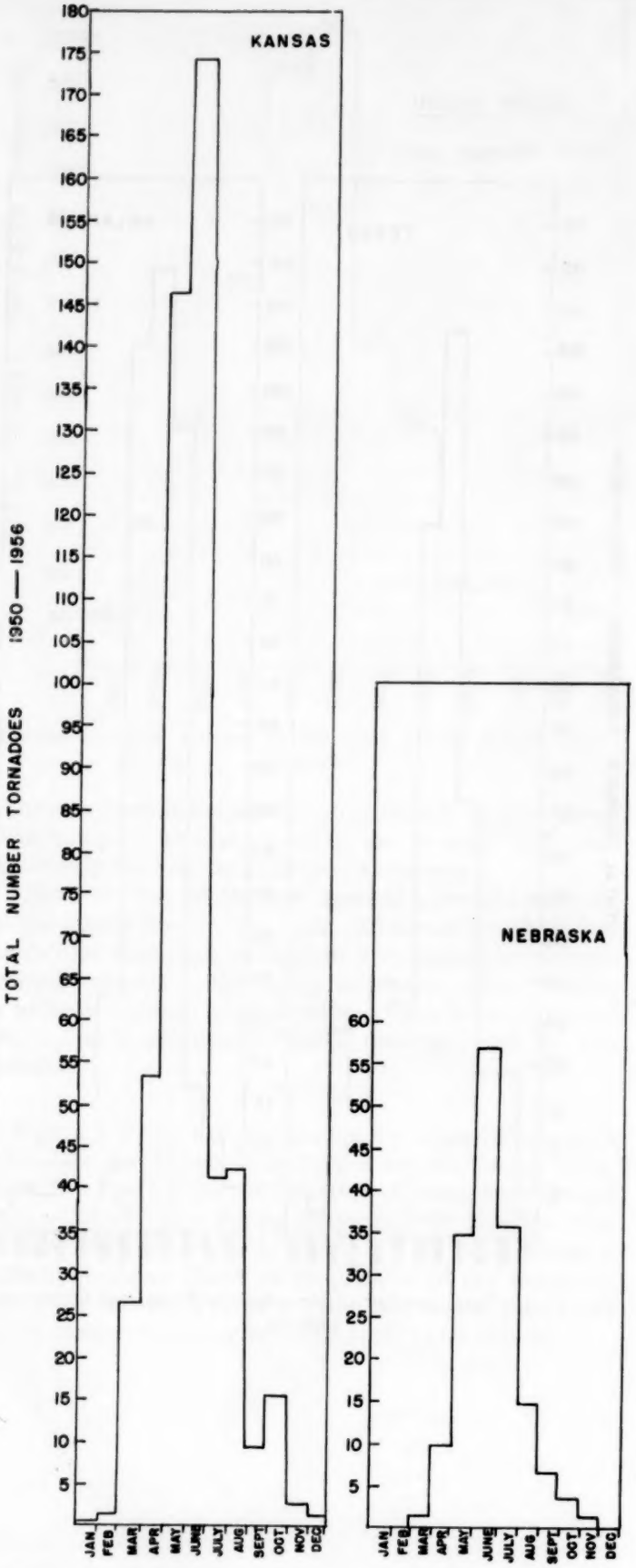

FIGURE 6.—Total number of tornadoes in Kansas and Nebraska, 1950–56.

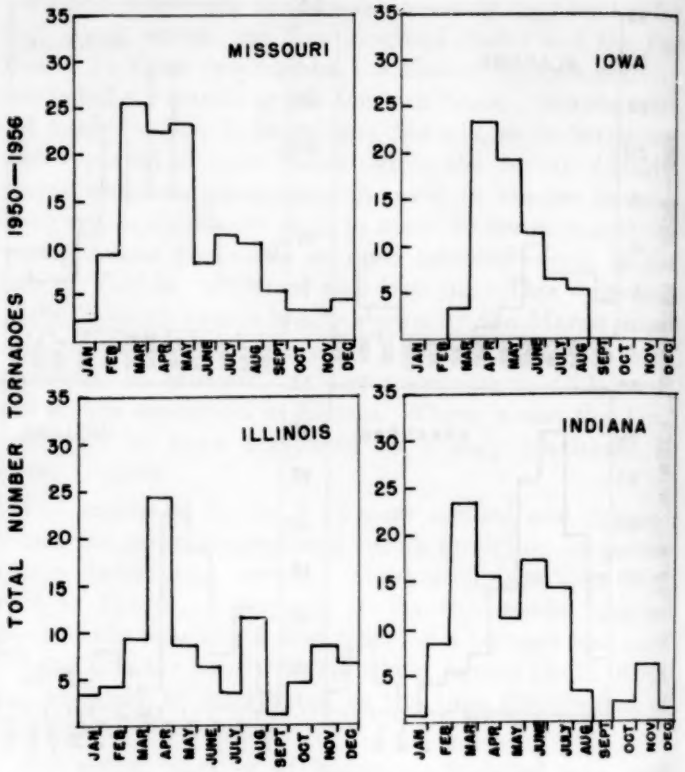

FIGURE 7.—Total number of tornadoes in Missouri, Iowa, Illinois, and Indiana, 1950–56.

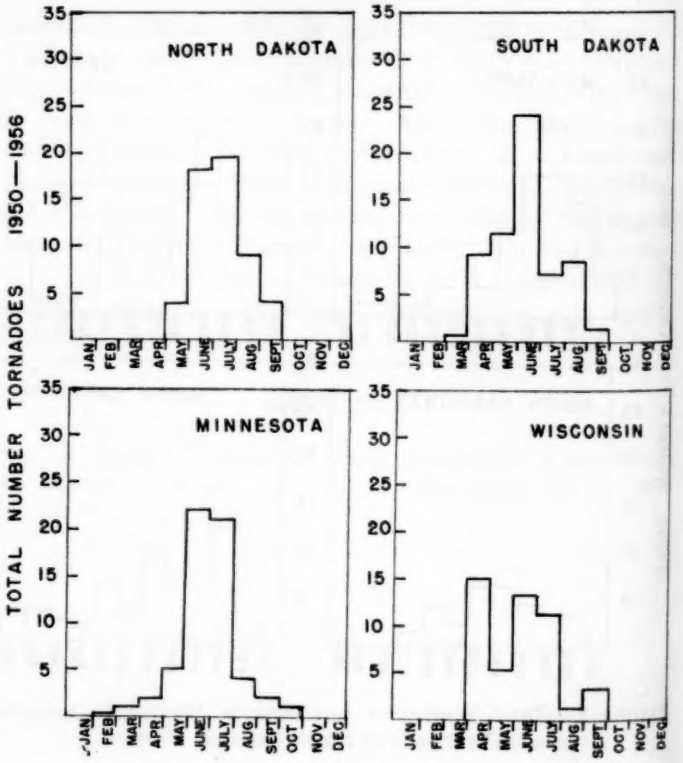

FIGURE 8.—Total number of tornadoes in North Dakota, South Dakota, Minnesota, and Wisconsin, 1950–56.

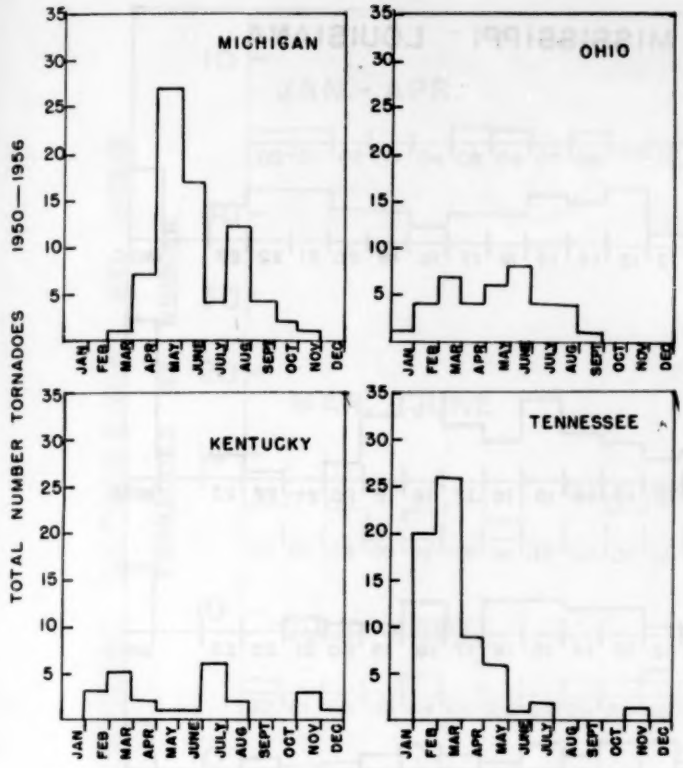

FIGURE 9.—Total number of tornadoes in Michigan, Ohio, Kentucky, and Tennessee, 1950–56.

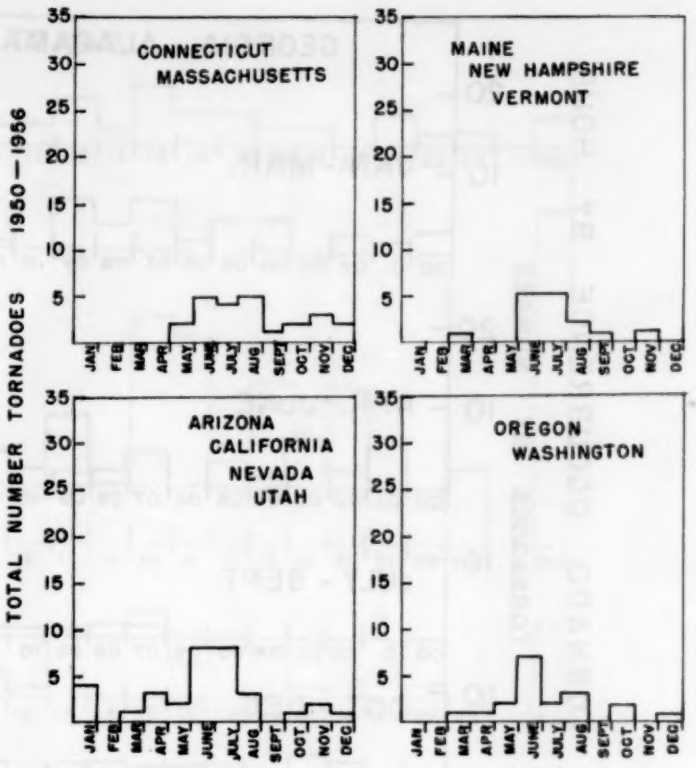

FIGURE 11.—Total number of tornadoes in Connecticut-Massachusetts-Maine-New Hampshire-Vermont, Arizona-California-Nevada, Utah, and Oregon-Washington, 1950–56.

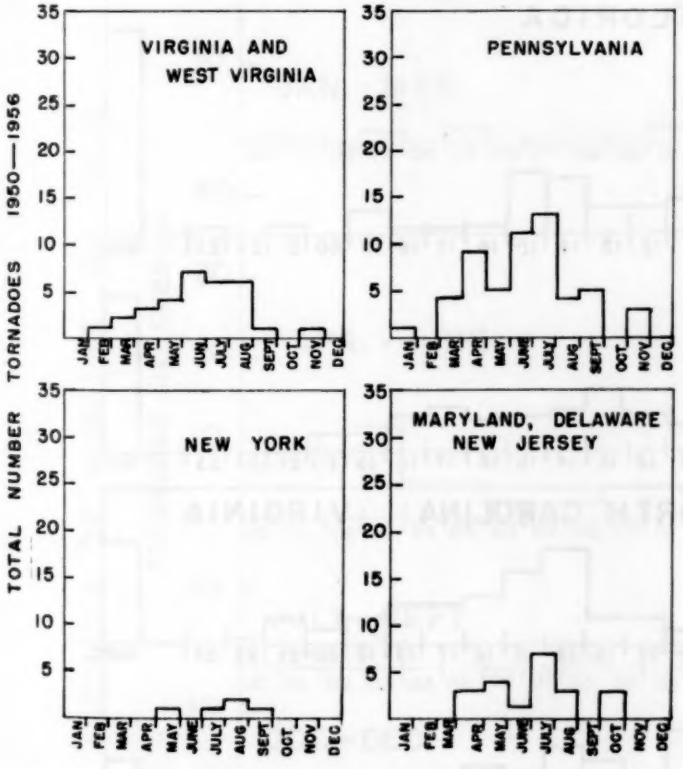

FIGURE 10.—Total number of tornadoes in Virginia-West Virginia, Pennsylvania, New York, and Maryland-Delaware-New Jersey, 1950–56.

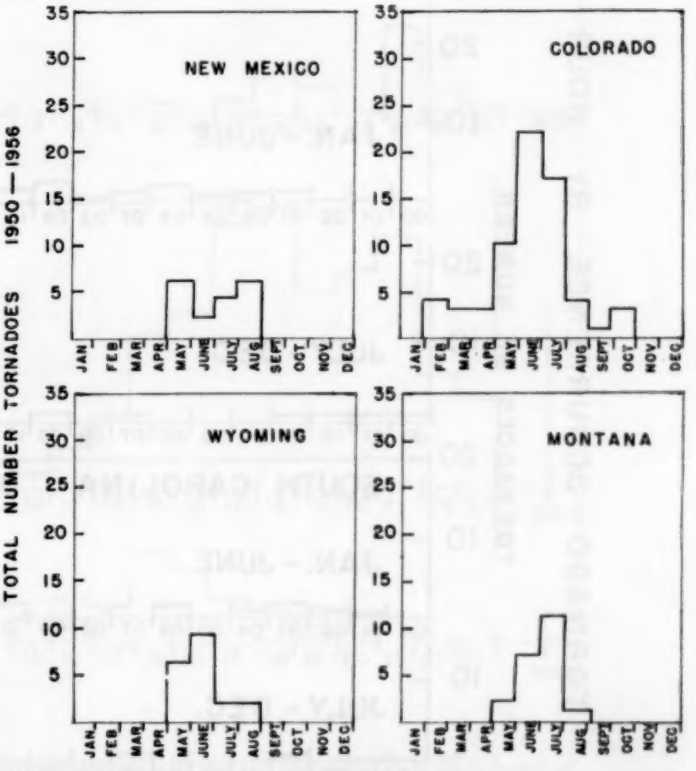

FIGURE 12.—Total number of tornadoes in New Mexico, Colorado, Wyoming, and Montana, 1950–56.

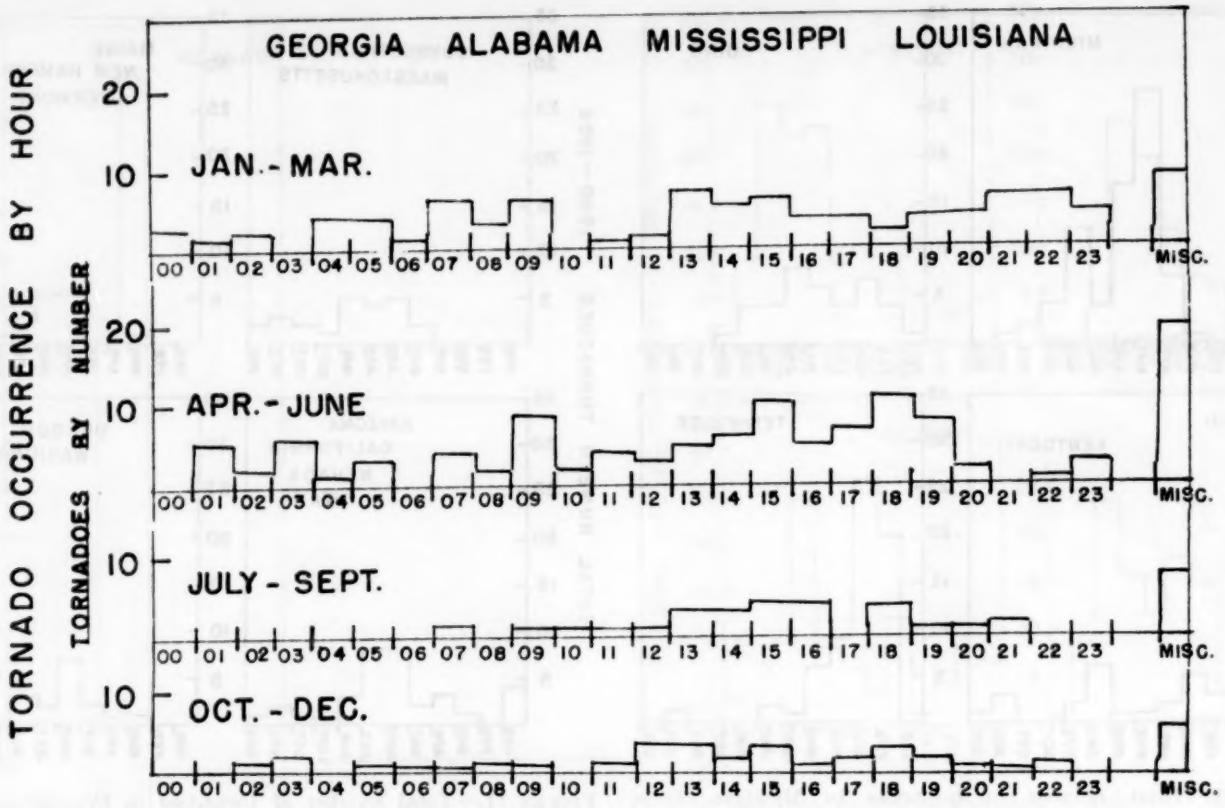
GEORGIA ALABAMA MISSISSIPPI LOUISIANA
JAN.-MAR.
APR.-JUNE
JULY-SEPT.
OCT.-DEC.
TORNADO OCCURRENCE BY HOUR
TORNADOES BY NUMBER
00 01 02 03 04 05 06 07 08 09 10 11 12 13 14 15 16 17 18 19 20 21 22 23 MISC.

FIGURE 13.—Tornado occurrence by the hour (CST) for Georgia-Alabama-Mississippi-Louisiana, 1950–56.

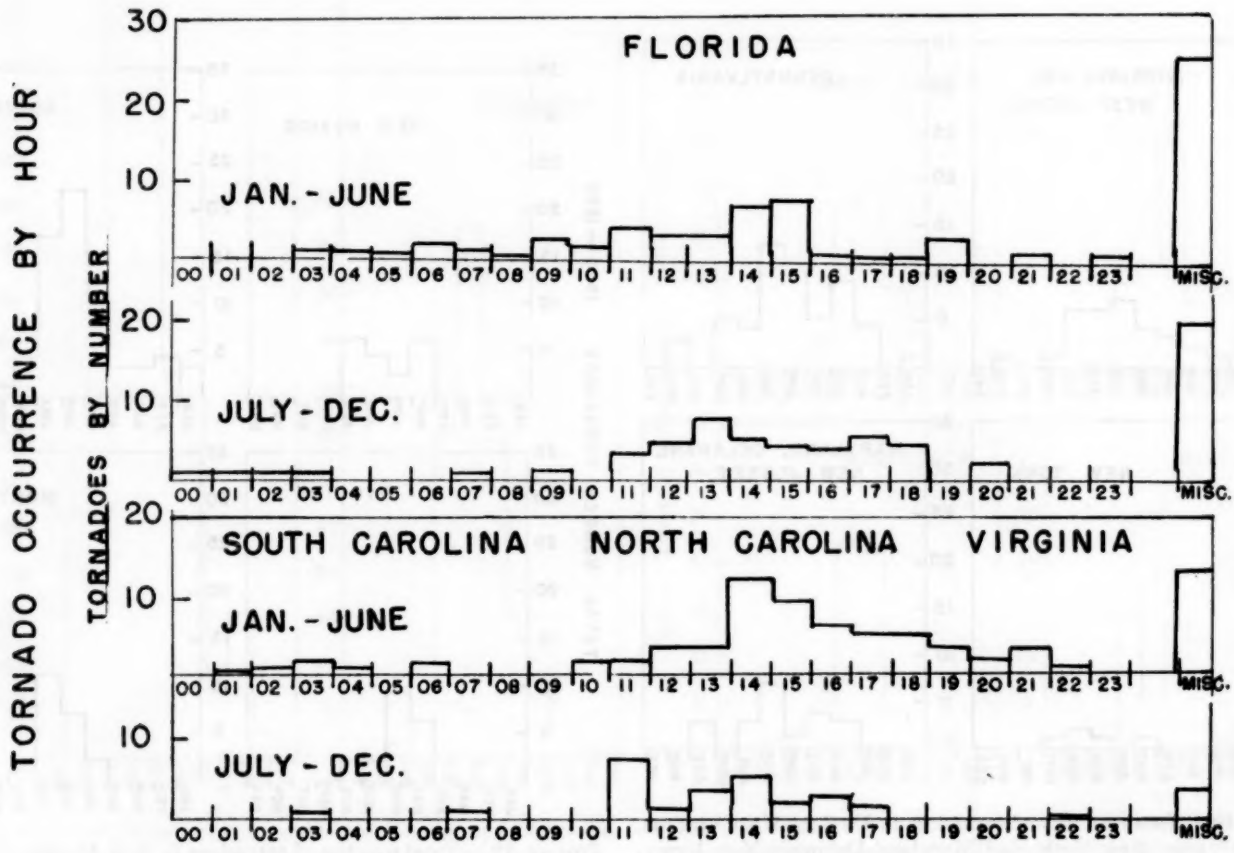
FLORIDA
JAN.-JUNE
JULY-DEC.
SOUTH CAROLINA NORTH CAROLINA VIRGINIA
JAN.-JUNE
JULY-DEC.
TORNADO OCCURRENCE BY HOUR
TORNADOES BY NUMBER
00 01 02 03 04 05 06 07 08 09 10 11 12 13 14 15 16 17 18 19 20 21 22 23 MISC.

FIGURE 14.—Tornado occurrence by the hour for Florida and South Carolina-North Carolina-Virginia, 1950–56.

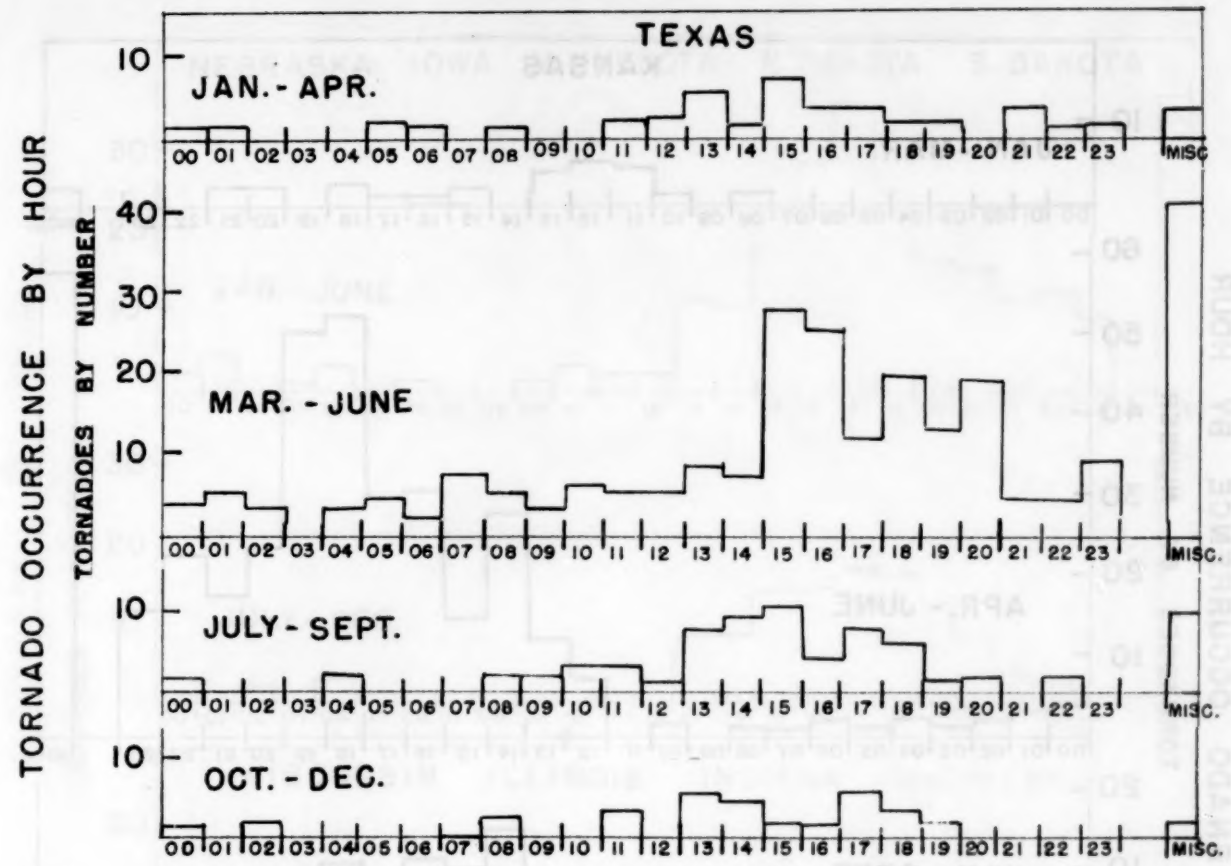
TEXAS
JAN. - APR.
MAR. - JUNE
JULY - SEPT.
OCT. - DEC.
TORNADO OCCURRENCE BY HOUR
TORNADOES BY NUMBER
00 01 02 03 04 05 06 07 08 09 10 11 12 13 14 15 16 17 18 19 20 21 22 23 MISC.
10
40
30
20

FIGURE 15.—Tornado occurrence by the hour for Texas, 1950–56.

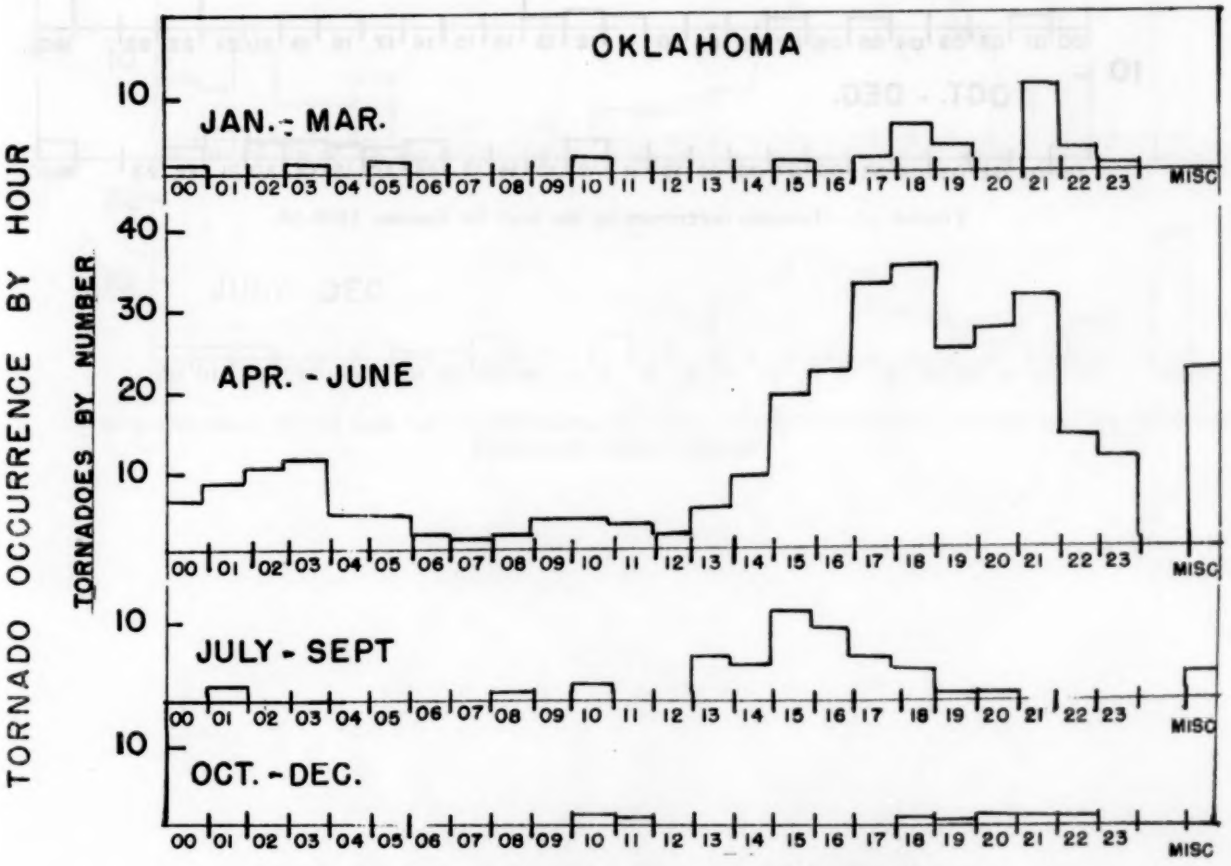
OKLAHOMA
JAN. - MAR.
APR. - JUNE
JULY - SEPT
OCT. - DEC.
TORNADO OCCURRENCE BY HOUR
TORNADOES BY NUMBER
00 01 02 03 04 05 06 07 08 09 10 11 12 13 14 15 16 17 18 19 20 21 22 23 MISC
10
40
30
20

FIGURE 16.—Tornado occurrence by the hour for Oklahoma, 1950–56

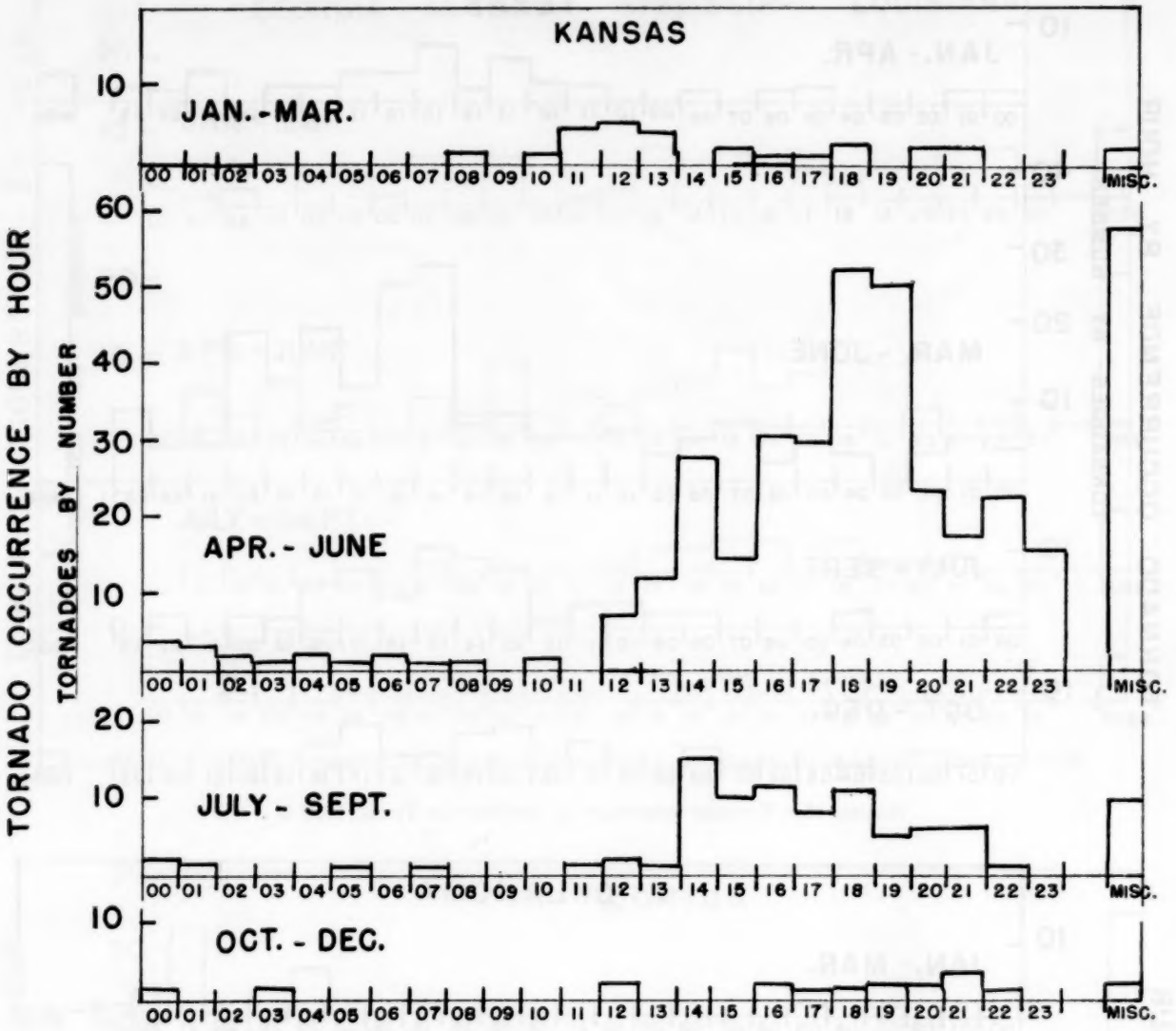
KANSAS
JAN.-MAR.
APR.-JUNE
JULY-SEPT.
OCT.-DEC.
TORNADO OCCURRENCE BY HOUR
TORNADOES BY NUMBER
00 01 02 03 04 05 06 07 08 09 10 11 12 13 14 15 16 17 18 19 20 21 22 23 MISC.

FIGURE 17.—Tornado occurrence by the hour for Kansas, 1950–56.

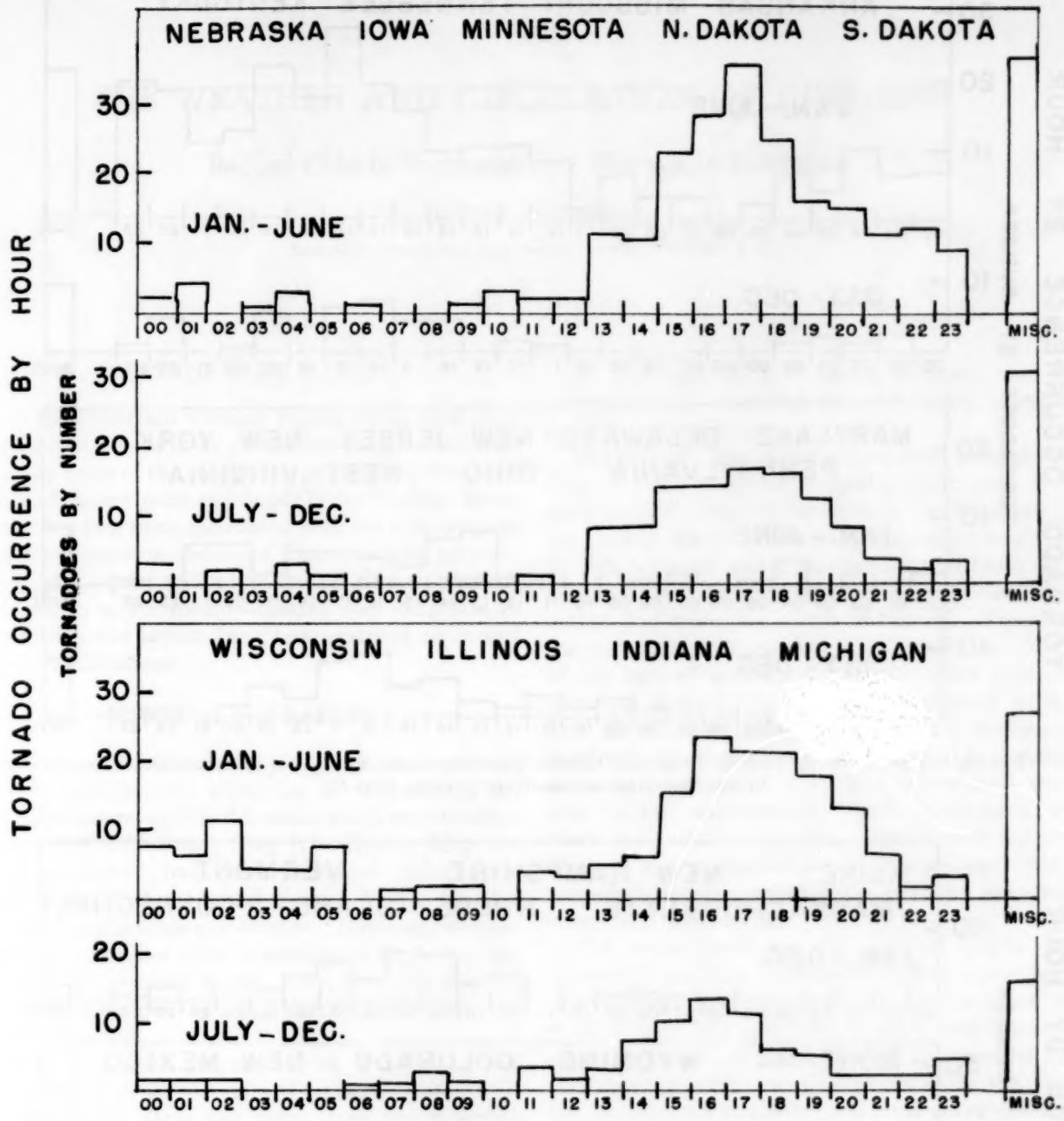
NEBRASKA IOWA MINNESOTA N. DAKOTA S. DAKOTA
JAN. - JUNE
JULY - DEC.
WISCONSIN ILLINOIS INDIANA MICHIGAN
JAN. - JUNE
JULY - DEC.
TORNADO OCCURRENCE BY HOUR
TORNADOES BY NUMBER
00 01 02 03 04 05 06 07 08 09 10 11 12 13 14 15 16 17 18 19 20 21 22 23 MISC.

FIGURE 18.—Tornado occurrence by the hour for Nebraska-Iowa-Minnesota-North Dakota-South Dakota and for Wisconsin-Illinois-Indiana-Michigan, 1950–56.

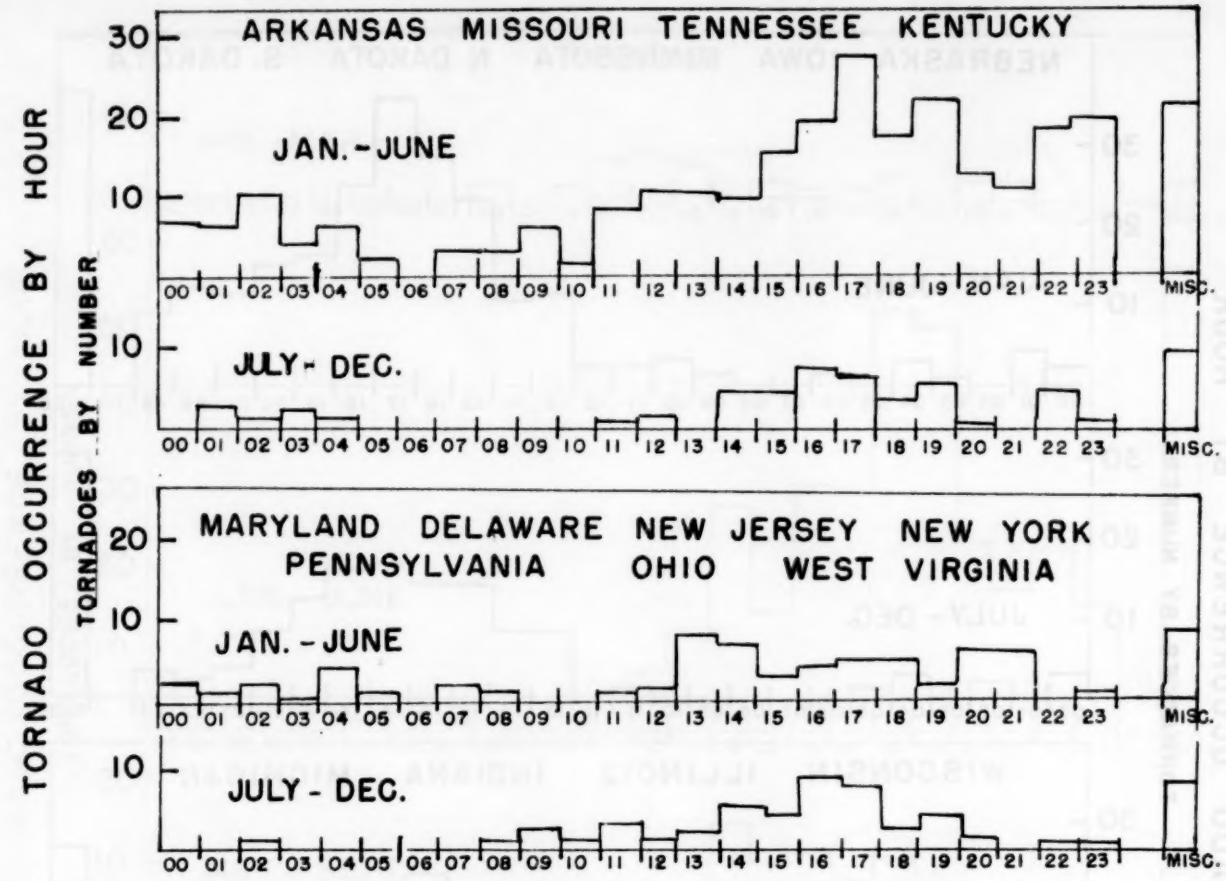
TORNADO OCCURRENCE BY HOUR
TORNADOES BY NUMBER
ARKANSAS MISSOURI TENNESSEE KENTUCKY
JAN.-JUNE
JULY-DEC.
MARYLAND DELAWARE NEW JERSEY NEW YORK
PENNSYLVANIA OHIO WEST VIRGINIA
JAN.-JUNE
JULY-DEC.
00 01 02 03 04 05 06 07 08 09 10 11 12 13 14 15 16 17 18 19 20 21 22 23 MISC.

FIGURE 19.—Tornado occurrence by the hour for Arkansas-Missouri–Tennessee-Kentucky and for Maryland-Delaware-New Jersey-New York-Pennsylvania-Ohio-West Virginia, 1950–56.

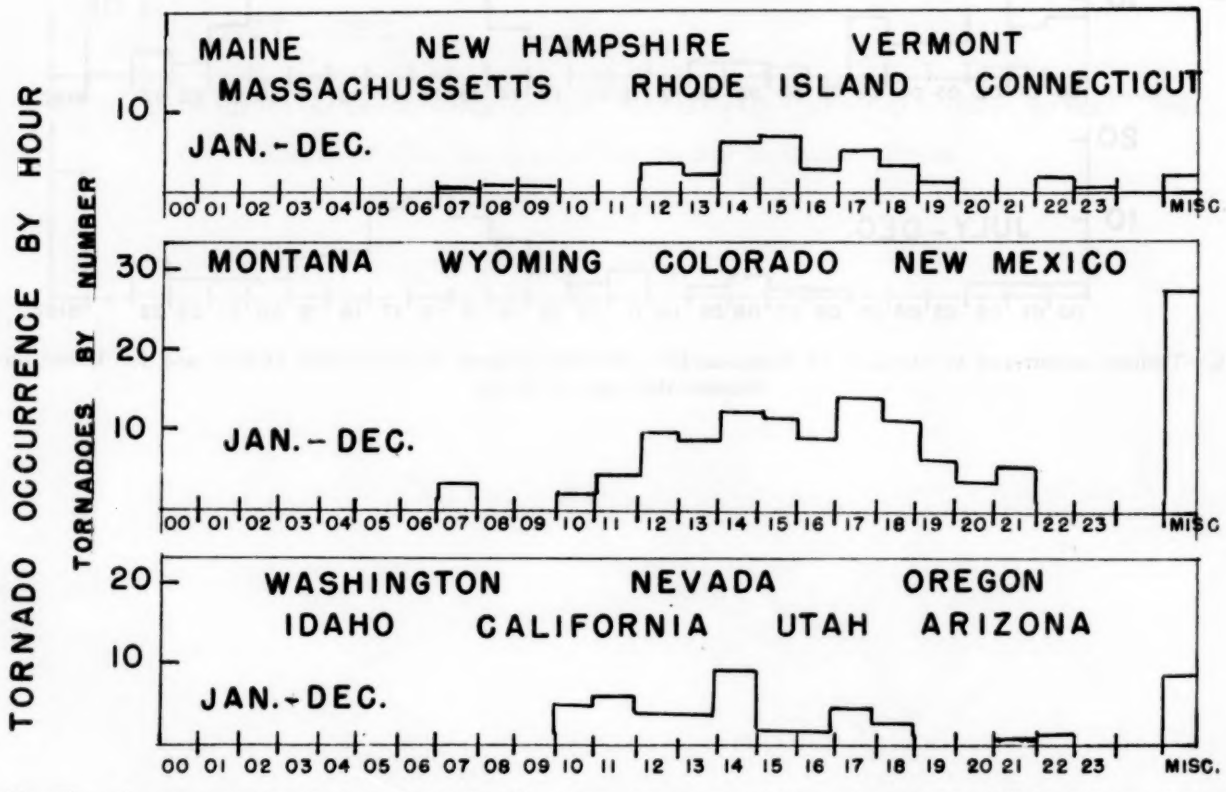
TORNADO OCCURRENCE BY HOUR
TORNADOES BY NUMBER
MAINE NEW HAMPSHIRE VERMONT
MASSACHUSSETTS RHODE ISLAND CONNECTICUT
JAN.-DEC.
MONTANA WYOMING COLORADO NEW MEXICO
JAN.-DEC.
WASHINGTON NEVADA OREGON
IDAHO CALIFORNIA UTAH ARIZONA
JAN.-DEC.
00 01 02 03 04 05 06 07 08 09 10 11 12 13 14 15 16 17 18 19 20 21 22 23 MISC.

FIGURE 20.—Tornado occurrence by the hour for Maine-New Hampshire-Vermont-Massachusetts-Rhode Island-Connecticut, Montana-Wyoming-Colorado-New Mexico, and Washington-Nevada-Oregon-Idaho-California-Utah-Arizona, 1950–56.

THE WEATHER AND CIRCULATION OF JUNE 1958[1]

Record Cold in Northeast and Warmth in Northwest

JAMES F. O'CONNOR

Extended Forecast Section, U. S. Weather Bureau, Washington, D. C.

1. WEATHER HIGHLIGHTS

Some of the important weather highlights of June 1958 over the United States were record-breaking cool conditions in many parts of the Northeast, particularly southern New England; heavy rains and floods in the Wabash Basin of Indiana; flooding rains associated with the first tropical storm of the season in southern Texas; severe tornado activity in the central and north-central States, particularly Wisconsin; and a record-breaking cool snap late in the month with the lowest June temperatures on record at many Texas locations.

2. GENERAL CIRCULATION

June 1958 was characterized by slightly above normal speed of the mid-latitude westerlies at 700 mb. in the Western Hemisphere, and in this sense was a continuation of the state achieved during May [1]. During May the circulation recovered from the prolonged index cycle which had influenced the weather over North America and adjacent oceans since mid-winter. However, in June the maximum westerlies receded southward from the high latitude of 47°N. reached during May, and this was accompanied by a general cooling relative to normal over most of the country.

The most important departures of the June 1958 circulation (fig. 1) from the normal pattern were:

(1) The strongly developed ridge from the Beaufort Sea southward into the eastern lobe of the Pacific subtropical high cell northeast of Hawaii. North of 50° N., this position represented a marked retrogression of the ridge normally located over Alberta, and south of 50°N. it represented an intensification of a feature barely discernible on the normal map [2] but well marked on charts showing the geographical frequency of 30-day mean ridges [3].

(2) The cyclonic center of action over Hudson Bay, which had a marked southward displacement from its normal location over the northern part of Baffin Island.

(3) The central Pacific trough, which tilted southeastward toward Hawaii, thereby tending to split the Pacific subtropical ridge into two cells.

(4) A trough in the eastern Atlantic, not normally present except along the coast of Africa, south of a depressed Icelandic Low.

The 700-mb. height departures from normal in figure 1 show a band of above normal heights with maxima in north-central Eurasia, Greenland, the Beaufort Sea, and the Gulf of Alaska. This band of positive height anomaly at high latitudes was a manifestation of blocking, a phenomenon normally associated with depressed centers of action and westerlies south of normal. Figure 2 shows the distribution of average wind speeds and the location of the axes of maximum speed for June 1958, with the principal axis of May 1958 superimposed as a dashed line for comparison. A southward displacement of maximum westerlies from May to June is indicated. An important feature of this chart is the split wind-speed axis in the northeastern Pacific associated with the block in the Gulf of Alaska. Downstream the confluence of these axes in the middle Mississippi and Ohio Valleys played an important part in the excessive rains and severe weather in these areas.

The widespread area of negative height departure associated with the depressed center of action at 700 mb. over Hudson Bay was reflected on the mean sea level chart (Chart XI) as a Low centered over Quebec instead of in the normal June position off the coast of Labrador. An additional feature of importance is the channel of low pressure on the mean sea level chart eastward from Labrador to the southern British Isles, indicating the prevailing storm track for the month. Normally this channel of low pressure is oriented northeastward north of the British Isles.

3. EVOLUTION OF THE CIRCULATION PATTERN

One of the major differences between the circulation in June (fig. 1) and the previous month [1] was the addition of a major trough in the central Pacific. As a block in the Siberian Arctic broke down during the first part of May the westerlies intensified in northeastern Siberia, forcing a major trough from Kamchatka eastward into the central Pacific. This trough was most strongly developed during the first half of June, as can be seen in figure 3 which shows the two 15-day averages which constituted the

[1] See Charts I-XVII following p. 244 for analyzed climatological data for the month.

474509—58——3

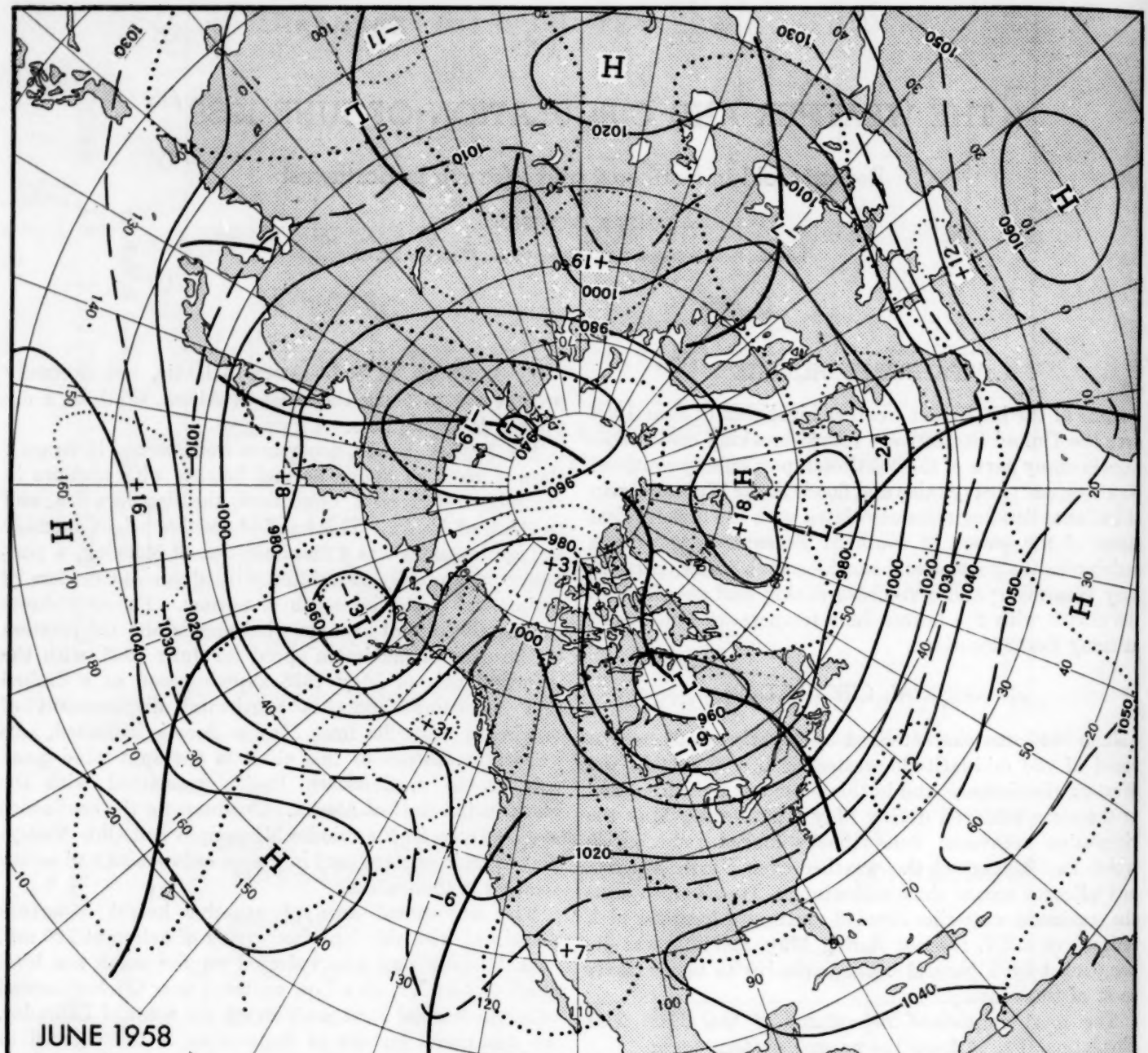

FIGURE 1.—Mean 700-mb. height contours (solid) and departures from normal (dotted) (both in tens of feet) for June 1958. Main features over North America were deep trough in East and confluence over western and central sections.

monthly mean 700-mb. circulation. The resultant shortening of the wavelength probably contributed to moving the eastern Pacific trough closer to the west coast of the United States than it had been during May. The strong blocking that persisted in the Gulf of Alaska tended to keep the coastal trough deeper than normal and temperatures over the interior of California below normal.

One of the most important features of the June circulation, a channel of negative anomaly from California to the Great Lakes, was primarily characteristic of the first half of the month (fig. 3A). It was a manifestation of a channel of cyclonic vorticity associated with a jet axis from southern California to the middle Mississippi Valley (fig. 2). This jet was much more strongly developed at the normal level of the jet core (about 200 mb.) than appears in figure 2. In fact, at 200 mb. the speed maximum over southern California averaged about 30 meters per second for the month, compared to 32 meters per second in the primary maximum which stretched from the middle Mississippi Valley to southern New England. It should also be noted that the southwestern jet maximum would show up even more strongly on a mean chart of the first 15 days, as can be deduced by comparing figure

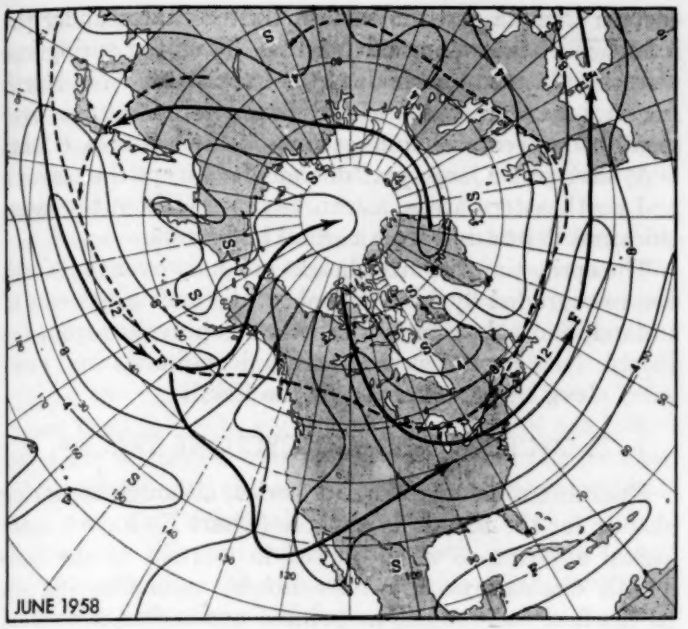

FIGURE 2.—Average 700-mb. wind speeds (meters per second) for June 1958. Solid arrows are axes of maximum speed (jets). Dashed line shows principal jet in May 1958. Major feature is confluence near lower Great Lakes.

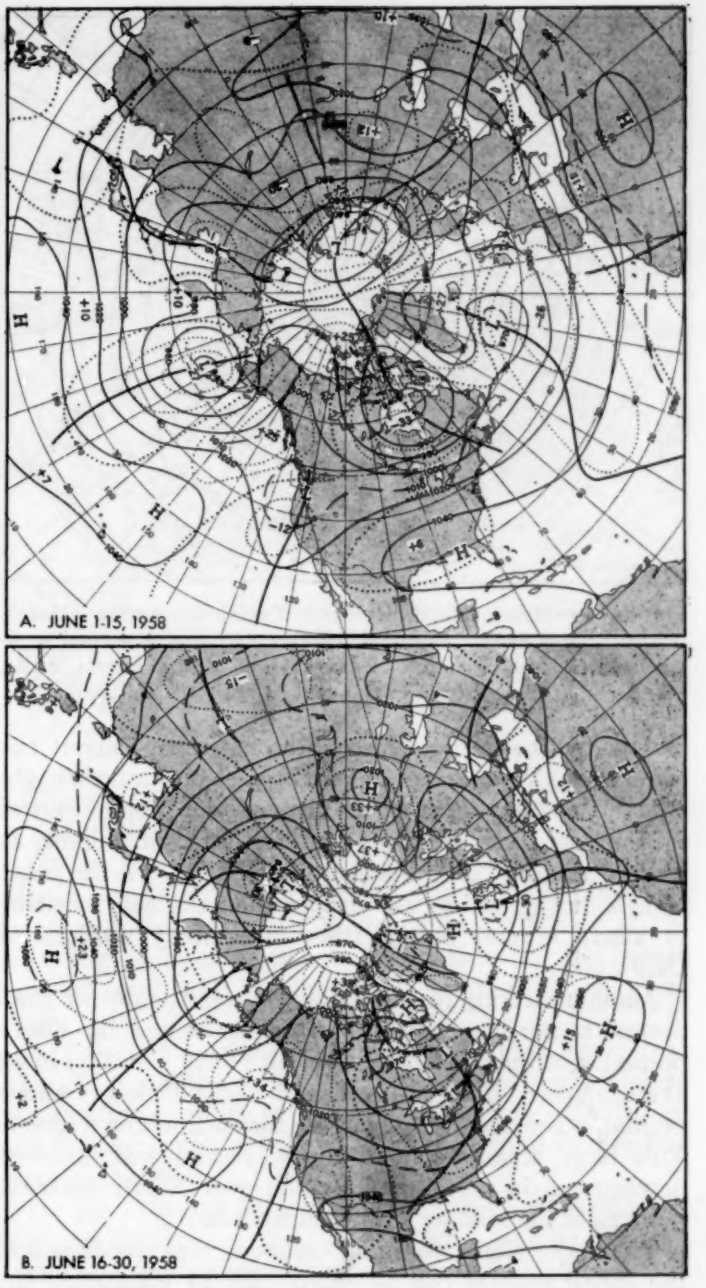

FIGURE 3.—Fifteen-day mean 700-mb. contours (solid) and departures from normal (dotted) (both in tens of feet) for (A) June 1–15, 1958 and (B) June 16–30, 1958. Deep Pacific coastal trough and marked confluence during the first half of June were followed by development of ridge in West and trough in East during the second half of the month.

3A with figure 1, since a rather marked change occurred in the second half of the month. The strongly confluent pattern which characterized the circulation during the first 15 days of June made a strong contribution to the severe weather which occurred in the Mississippi and Ohio Valleys during this time.

Figure 3 also shows the southward migration of the negative height anomaly from Hudson Bay in the first half of the month to the Great Lakes and St. Lawrence Valley in the second half. During the second half of the month marked filling of the Pacific coastal trough and change to a widespread northerly anomalous flow over the midsection of the country were responsible for flooding the country east of the Rockies with record-breaking cool air.

In the Gulf of Alaska the positive height departures shown in figure 3B were a manifestation of marked retrogression in the second half of the month. Five-day mean charts during this period (not shown) disclosed that the trough in mid-Pacific returned to the western Pacific where it had been early in May. For example, a strong positive height anomaly center was near the British Columbia coast along the 135th meridian on the 5-day mean chart of June 19–23, and a week later it was observed along the 155th meridian. This retrogression near month's end was important in redeveloping the western United States trough and spreading warm air eastward to end the cool wave in the central and eastern parts of the country, which dominated the last half of the month.

4. COMPARISON OF JUNE WITH THE SPRING MONTHS

Figure 4 is a mean of the 700-mb. circulation for the spring months of 1958, March, April, and May. The most striking anomaly of spring was the tremendous positive departure from normal height over eastern Canada. In fact, a general circumpolar area of positive anomaly existed, but centered near the magnetic pole rather than the geographic pole. This area was girdled to the south by a wide band of negative height anomalies and depressed westerlies around practically the entire hemisphere except the central Pacific. This band was associated with below normal spring temperatures over

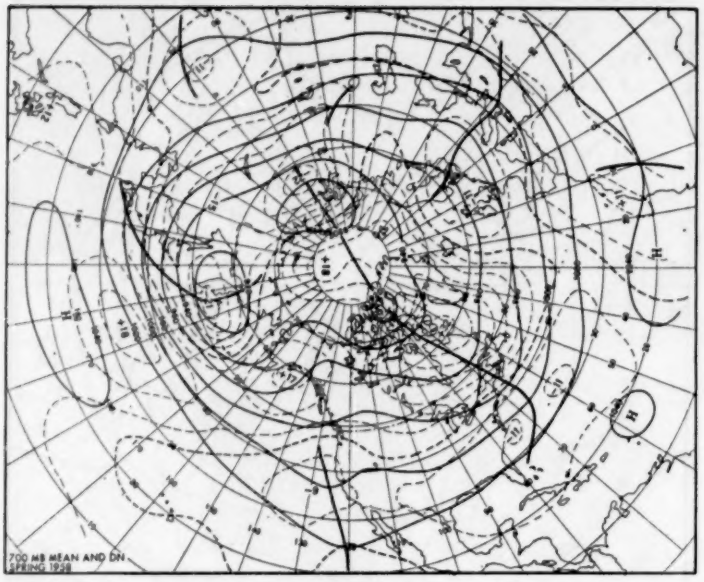

FIGURE 4.—Mean 700-mb. contours (solid) for spring (March, April, May) 1958. Principal features were above normal westerlies south of Kamchatka, blocking in Gulf of Alaska and Canada, and deeper than normal Pacific and Atlantic coastal troughs.

practically the entire United States south of about the latitude of Chicago, and abundant precipitation throughout the country except for the extreme north central sections, southern Michigan and northeastern Indiana, as well as extreme southeastern Texas. The Pacific coast trough during spring was deeper than normal, resulting in above normal precipitation over many sections of California.

Another striking feature of spring was the deeper than normal center of action near Kamchatka and the above normal subtropical High to the south of it, resulting in an average speed of the westerlies of about 10 knots above normal, a considerable departure for such a long average. This large abnormality of the westerlies was manifest downstream in persistent blocking over North America, perhaps in the manner suggested by Rex [4].

The major similarities and contrasts between June and the spring months can be determined by comparing the 700-mb. height departure from normal patterns in figure 1 with those in figure 4. By way of similarity the California coastal trough continued deeper than normal during June as it had been in spring and resulted in similar temperature anomaly patterns; i. e., above normal along the California coast and below normal in Nevada and interior California. The springtime above normal heights in the Gulf of Alaska were also strongly developed during June, together with much above normal temperatures in the Pacific Northwest States. A zone of above normal heights southeastward from this area was associated with above to much above normal temperatures in June over much of Utah, Colorado, Arizona, and New Mexico, where in spring it had been mostly below normal.

In eastern North America the strong springtime Canadian block centered near Hudson Strait retreated northwestward to the Arctic Ocean during June, leaving southeastern Canada and the eastern United States under the influence of below normal heights. Thus the springtime warmth relative to normal north of about 40° N. in North America gave way to below normal temperatures over most of the central and eastern United States (Chart I–A) and over a large part of Canada, except the western and northeastern areas, as can be inferred from the mean thickness departures from normal in figure 5.

The springtime negative height anomaly over the North Sea retrograded by June to a short distance southwest of Ireland, and below normal thicknesses prevailed from the British Isles northeastward across Scandinavia and eastward along the Arctic coast of the USSR.

5. CYCLONE AND ANTICYCLONE TRACKS

Cyclone tracks over North America, although appearing chaotic for the month as a whole (Chart X) have a more logical appearance when viewed in relation to the half-month circulations and their height anomalies (fig 3). In the first half-month, as pointed out earlier, a channel of negative height anomaly existed from California northeastward into the large negative anomaly center over Hudson Bay, together with a confluent jet pattern (fig 2). The cyclone tracks for the first half of the month were entirely compatible with this large-scale circulation, with cyclonic centers on about the 1st, 3d, 6th, and 9th emanating from the Rocky Mountain area in the southern branch of the split westerlies and proceeding northeastward across the Great Lakes, thence northward around the eastern periphery of the center of action over Hudson Bay. During this same period, additional cyclonic centers were propagated southeastward in the northern branch of the westerlies along the tracks clustered in the Great Bear Lake area of western Canada, also terminating in the Hudson Bay center of action. The track emanating from the western United States on about the 9th was considerably farther north than previous tracks, perhaps suggesting a tendency for a change in the circulation. On the 13th and 14th the strongest cyclonic development of the month occurred in southeastern Canada, and lingered over this area for almost a week. This marked the beginning of the major change in the general circulation over North America which was to dominate the latter half of the month. The confluence over northern United States, which had favored systems moving northeastward from the Plateau in the first half of the month, receded southward and ended this storm track until near the month's end.

The circulation during the second half of the month (fig. 3B) was characterized by an abnormally strong trough system in the East, together with an abnormally strong ridge in the West. With above normal northwesterly flow keeping the eastern United States flooded with cold air, a new storm path more characteristic of the colder seasons developed. This path is indicated by the cluster of tracks shown in Chart X along the middle Atlantic coast, extending eastward across the Atlantic in the mean sea level trough (Chart XI).

The tracks of anticyclones over North America for the month as a whole (Chart IX), although emanating from a rather narrow zone near Great Slave Lake in northwestern Canada, became widely dispersed as they turned eastward over central North America, ranging from a path across James Bay in the first part of the month, to a path across Arkansas in the latter part of the month.

No clear-cut track of maritime polar anticyclones occurred this month from the northern Rockies toward the Great Lakes Region, an area ordinarily traversed by a "principal" track of Highs during June [5]. When the tracks for the whole month were divided into half-monthly groups, the northernmost tracks across the Great Lakes region were found to occur in the first half of the month when the westerlies were closer to their normal position. During this period the actual tracks were in closer agreement with the "principal" tracks [5].

However, the anticyclone tracks which characterized the second half of the month were the southernmost ones which dipped southward into Kansas, Arkansas, Kentucky, etc. These tracks, which were well south of the "principal" track for June, were associated with the abnormally deep mean trough in the eastern United States in the second half of the month. Record-breaking cool temperatures occurred over many sections as strong northerly flow over central sections deployed successive polar anticyclones farther and farther south during this period. Actually the anticyclone tracks in the second half of June were more characteristic of late winter or early spring [5] than of early summer.

6. CHRONOLOGY OF SURFACE WEATHER SYSTEMS

The first storm of the month emerged from Utah into the Northern Plains on the 4th with heavy rains and local flooding in southeastern Minnesota and northwestern Wisconsin. Severe tornadoes in Wisconsin killed at least 28 persons, with hundreds injured and homeless and property losses tremendous.

This storm was followed by a polar anticyclone from Manitoba which moved into the Northern Plains on the 5th, thence rapidly eastward across southern New England on the 7th, with record low temperatures and frosts in parts of Michigan, Pennsylvania, New York, and New England. Norfolk, Va. reported a new record for minimum temperature on the 8th.

On the 6th and 7th another cyclonic system emerged from Idaho to the Dakotas and merged over the Great Lakes with a cold front sweeping southeastward from Canada on the 8th. The marked confluence aloft caused this front to strengthen and become stationary across Ohio, Indiana, and Illinois, while still another Low emerged from the Plateau into the Central Plains on the 9th and 10th producing an abnormally strong low-level southerly flow of extremely moist tropical air against the stationary front. This resulted in flood-producing rains over north central Indiana, and locally severe thunderstorms and tornadoes in a zone from Kansas to the east coast on the 10th. At least 15 died from a tornado at

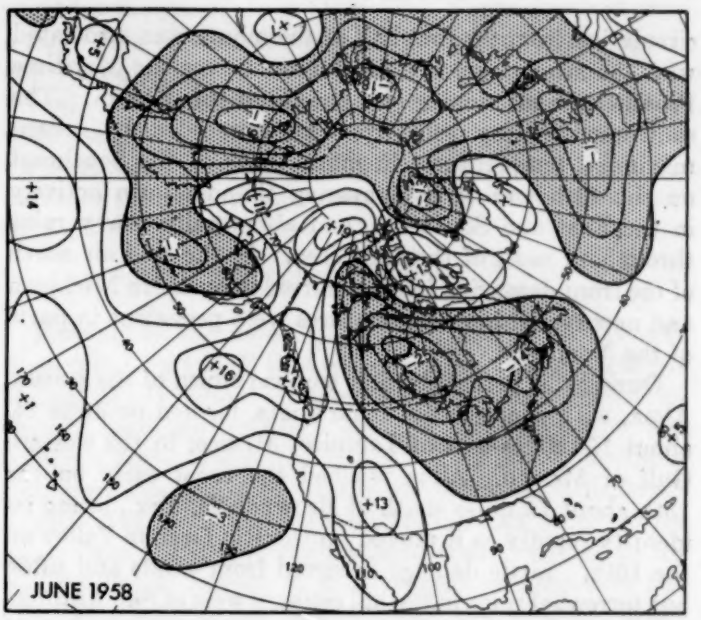

FIGURE 5.—Mean departures from normal of 1000–700-mb. thicknesses for June 1958 (tens of feet). Outstanding feature was below normal thickness (shaded) over large part of North America.

El Dorado, Kans. on the 10th, which also caused millions of dollars damage.

On the 11th the front started moving eastward from the Mississippi Valley to the mid-Atlantic coast, accompanied by heavy showers and squalls, with Philadelphia, Pa. reporting 73 m. p. h., a new record there for the fastest mile of wind, and Washington County, Md., reporting winds up to 100 m. p. h.

A polar anticyclone which moved across the Great Lakes from Alberta on the 11th and 12th set new minimum temperature records in parts of Wisconsin, Minnesota, and Pennsylvania, and provided a respite from the flooding rains in the Wabash Basin of Indiana.

On the 12th and 13th another cyclonic center emerged from the Plateau into the Central Plains, tending to merge with a deepening Low moving southeastward across James Bay, similar to the situation on the 8th. Heavy rains spread rapidly across the country in the strong confluent jet flow aloft across northern sections of the country, being particularly heavy in the central Mississippi and Ohio Valleys. The earlier flood conditions in Indiana were aggravated, and damaging thunderstorm activity occurred in the Ohio Valley on the 13th.

On the 14th, under the influence of very strong deepening of the merged cyclonic centers near the Gulf of St. Lawrence, a strong anticyclone pushed slowly southward across the North Central States, preceded by a strong cold front and prefrontal squall line moving across the mid-Atlantic States. This front continued slowly southward to near the Gulf coast during the next four days under the influence of the major trough aloft in the East and ridge in the West which developed strongly during this period. This major change in the general

circulation from the first half of the month was associated with the strong cyclonic development over the Maritime Provinces and ridging in the Gulf of Alaska. The southward-moving cold front was preceded by record maximum temperatures in many parts of the Southeast on the 13th and 14th, damaging thunderstorm activity in the East and Southeast, and abnormally heavy rains throughout most of the Gulf area. In the cold air north of the front damaging frosts occurred in northern Michigan and new record low temperatures were prevalent in parts of the Northeast.

During this period the first tropical storm of the season, Alma, with winds of about 50 knots, formed on June 14, about 150 miles east of Tampico, Mexico, in the western Gulf of Mexico. Alma reached the coast early on the 15th about 75 miles south of Brownsville, Tex., losing its identity rapidly as it moved up the Rio Grande Valley on the 16th. Little damage occurred from winds and tides, but torrential rains in the hill country west of San Antonio, Tex., in excess of 7 inches, and with some measurements as high as 20 inches, produced locally heavy flood damage.

Under the influence of the persistent broad trough in the East and northerly flow over central sections aloft emanating from the strong ridge over the western Plateau, another surge of polar air associated with a surface anticyclone made its way southeastward from Alberta on the 19th across Missouri to the east coast on the 23d. Heavy to torrential rains in some places in the Southern Plains, lower Mississippi Valley, and Gulf coastal areas accompanied the southward progress of the leading edge of the cold air. New record low temperatures were reported in many places during this period over a wide area embracing Montana, Nebraska, Minnesota, Wisconsin, Ohio, and Pennsylvania, with damaging freezes in parts of Wisconsin and Michigan. In contrast, record high temperatures were occurring in the Pacific Northwest, with Pendleton, Oreg., reporting 103° F. and Yakima, Wash., 102° F. on the 22d.

On the 24th a fresh outbreak of cold air from Alberta and Saskatchewan began protruding southward into the north central sections of the country, associated with a rapidly developing storm over the Great Lakes on the 25th and 26th. During the period from the 24th to the 29th, the most southerly trajectory of any polar anticyclone during the month occurred, producing record low temperatures on as many as four successive days in some places in the Southern Plains and generally much below to record low temperatures over most of the United States east of the Rockies. As the leading edge of this cool wave swept eastward to the coast on the 26th and 27th, heavy showers were general throughout much of the eastern United States and damaging thunderstorms were widespread, especially up and down the east coast. Rochester, N. Y. Airport recorded gusts to 103 m. p. h. on the evening of the 25th with widespread damage in part of the city. By way of contrast, in the western Plateau, Salt Lake City reported a record high of 102° F. on the 27th. A detailed study of this unusually cold outbreak from June 24–27 by Jordan and Lowry [6] can be found in an adjoining article in this issue.

The remainder of the month was relatively dry as the polar anticyclone in the East became transformed into a warm extension of the Bermuda High, and a strong warm ridge in the westerlies aloft replaced the large trough which had dominated the East since mid-month. This major change in the circulation was accompanied by marked cooling in the West as a strong maritime cold front in a major trough aloft moved eastward across the Rockies, associated with a new series of storms moving into the northern Plains and upper Mississippi Valley.

7. TEMPERATURE

The southward migration of the maximum westerlies from the May position was accompanied by general cooling relative to normal over most of the country, with the greatest cooling in the North Central States. The only stations reporting warmer temperatures than the previous month, relative to normal, were in Texas. The Pacific Northwest and the Colorado, Utah, Arizona, and New Mexico area remained well above normal.

Many cities from the upper Mississippi Valley eastward reported the coldest June of record; e. g., Green Bay, Wis., Youngstown, Ohio, Pittsburgh, Pa., Albany, N. Y., Newark, N. J., Hartford, Conn., and Providence, R. I. Second coldest June of record was reported by Escanaba, Mich., Indianapolis, Ind., Akron, Ohio, Portland, Maine, and Burlington, Vt.; the third coldest June, at St. Cloud, Minn., Rochester, N. Y., and Richmond, Va.

By way of contrast, this June was the warmest on record at many places in the Pacific Northwest such as Olympia and Seattle, Wash., and Meacham, Oreg., while Pendleton, Oreg., equalled the June record for warmth. Second warmest of record was reported by San Francisco and Los Angeles, Calif., and Houston, Tex.

The mean 1000–700-mb. thickness anomalies given in figure 5 summarize the large-scale departures from normal of the low-level thermal field. Comparing figure 5 with Chart I–A shows the correspondence between average thickness departures and reported monthly temperature anomalies. In the Northeast, for example, average thicknesses 50 ft. or more below normal were associated with much below normal average monthly surface temperatures, and in the West thicknesses roughly 100 ft. or more above normal were associated with much above normal surface temperatures.

A map of the number of days with fronts for a network of squares covering North America (not shown) revealed that the mean position of the polar front in June was in close agreement with the zero average thickness departure line in figure 5, running from Alberta southward to the Texas Panhandle and eastward through the Gulf States to the Carolinas. This was certainly an abnormally depressed location for the mean polar front near the beginning of summer.

In local areas the correspondence between mean thick-

ness and surface temperature anomalies occasionally may be poor, even in as long an average as a month. For example, tongues of slightly above and below normal average surface temperatures alternated across the Gulf States where the monthly thickness departures appeared to be uniform. These variations are probably due in part to the variations in precipitation; e. g., along the southern Appalachians below normal precipitation favored warmer surface temperature.

Perhaps the most interesting temperature anomaly pattern in Chart I–A is the below normal area in Nevada and interior California, while the coastal area of California reported much above normal, this being the second or third warmest June on record along the coast. A similar contrast also appeared in the spring anomalies, although May was above normal in the interior as well as along the coast. The deeper than normal California coastal trough in June (fig. 1) as well as in spring (fig. 4) resulted in California and Nevada being persistently under the influence of cooler than normal maritime polar air. At Fresno, Calif., an interior station, while the daily mean temperatures averaged about 3° below normal for June, the maximum temperatures averaged about 5° below normal. With near normal sunshine and sky cover, the cool air aloft kept the lapse rates steep, thus keeping the maximum temperatures considerably below normal.

Across the mountains on the coast however, San Francisco City Office and Los Angeles Airport reported this June was the second warmest on record. This occurred despite their exposure to about the same gross synoptic conditions aloft as in the interior where temperatures were below normal.

Normally, cool conditions in the interior are associated with diminished onshore winds along the coast, thus reducing the cooling effect of the sea breeze, but this could not be the explanation of the above normal conditions on the coast in this case, for the San Francisco City Office average surface winds were about one mile per hour above normal. Also on 20 days when the westerly winds averaged above normal, the daily mean temperatures averaged about 3° above normal. Likewise, Los Angeles Airport reported winds above normal on almost every day, together with above normal temperatures on every day during the month.

As far as sky cover was concerned, San Francisco averaged above normal sky cover from sunrise to sunset, resulting in the greater contribution to the monthly positive anomaly by the minimum temperatures. At Los Angeles, the daytime sky cover averaged considerably below normal with the greater contribution to the anomaly by the maximum temperatures. Thus contributions were made by both daytime and nighttime temperatures, the greater effect depending on the sky cover.

These facts suggest that abnormal sea-surface temperatures played a dominant role in the much above normal temperatures reported along the coast during June. That this was probable may be seen by referring to charts of anomalies of sea-surface temperatures off the California coast for the period June 11–20 [7]. These charts showed a large area of ocean surface off the coast with temperatures ranging up to 8° F. above normal during the period. On the other hand, in the interior, the abnormally warm sea surface had little effect upon surface temperatures because interior sections are separated from the influence of ocean temperatures by the coastal mountain range.

8. PRECIPITATION

Turning to the monthly precipitation pattern, it can be seen in Chart II–B that one of the major areas of above normal precipitation extended from northern California, Oregon, and northwestern Nevada through Idaho and southern Nevada into the Plains. This heavy precipitation area was produced by the vertical motion fields accompanying the numerous vorticity maxima which propagated from the deeper than normal coastal trough in the well-developed current of moist southwesterlies over this area, especially in the first part of the month. Many stations such as Winnemucca, Nev., Boise, Idaho, Missoula, Mont., and Red Bluff, Calif., reported the wettest or near wettest June of record. Boise received 2.24 inches of rain in one 24-hour period on the 11th and 12th, a new record for 24-hour rainfall in June.

Another major area of precipitation was the middle Mississippi and Ohio Valleys. Some stations in this area reported the wettest or near wettest June on record, such as Fort Wayne, Ind., with 8.29 inches, and Columbus, Ohio with 9.75 inches, the greatest June amount and second largest ever recorded there in one month. The major contribution to the heavy amounts in this area was the marked confluence during the first half of the month, and particularly during the second week, as the cyclonic systems of about the 8th and 13th dumped flooding rains over some sections, particularly the Wabash Basin.

During about the 3d week of the month, due to the major change in circulation aloft near mid-month (i. e., trough development in the East and ridge development in the West) the confluence zone shifted southward to the Southern Plains and lower Mississippi Valley, associated with a strong frontal zone across southern portions of the country east of the Rockies. This change shifted the heavy precipitation areas southward, resulting in weekly totals up to 20 inches west of San Antonio, Tex. (due to tropical storm Alma), 4 inches in parts of Oklahoma and southern Kansas, 5 inches in Arkansas, and 6 inches in interior Louisiana. Jackson, Miss. reported the 6th wettest June on record with 8.77 inches, only 0.58 inch below the record amount in June 1900. About 7.37 inches of this amount occurred during the 3d week.

Most of the rainfall during the last week occurred as moist tropical air was lifted along the strong cold front which moved across the country in advance of the major cool wave which overspread the East in the latter part of the month.

Areas of lighter or below normal precipitation were the

Appalachian region which was generally west of the mean trough, the upper Mississippi Valley and extreme northern border areas westward to the Pacific coast which were persistently under the influence of northerly flow, the Central Plains which was somewhat south of the northern confluence zone and also to some extent in a "rain shadow" or zone of dessication of the Pacific moist tongue east of the Rockies. Another dry area extended from the extreme Southwest northeastward into Utah, due to the prevalence of anticyclonic vorticity east of the Pacific coastal trough. Extreme southern Texas was also dry under strong anticyclonic vorticity aloft just south of the southern confluence zone.

REFERENCES

1. J. F. Andrews, "The Weather and Circulation of May 1958—Reversal from a Long-Period Regime," *Monthly Weather Review*, vol. 86, No. 5 May 1958, pp. 177–185.
2. U. S. Weather Bureau, "Normal Weather Charts for the Northern Hemisphere," *Technical Paper* No. 21, Washington, D. C., Oct. 1952.
3. W. H. Klein and J. S. Winston, "Geographical Frequencies of Troughs and Ridges on Mean 700-mb. Charts," to be published in *Monthly Weather Review*, vol. 86, 1958.
4. D. F. Rex, "An Aerological Study of Blocking Action," *Tellus*, vol. 2, No. 3, 1950, pp. 196–211.
5. W. H. Klein, "Principal Tracks and Mean Frequencies of Cyclones and Anticyclones in the Northern Hemisphere," U. S. Weather Bureau, *Research Paper* No. 40, Washington, D. C., 1957.
6. H. M. Jordan and D. A. Lowry, "Late-Season Cold Outbreak, June 24–27, 1958," *Monthly Weather Review*, vol. 86, No. 6, June 1958, pp. 237–244.
7. R. J. Callaway and E. W. Mendiola, *Charts of Anomaly of Sea Surface Temperature*, Saltonstall-Kennedy Albacore Project, Pacific Ocean Fisheries Investigations, Fish and Wildlife Service, U. S. Department of Interior, 1958.

Weather Note

WORLD RECORD LOW TEMPERATURE

A report of a new low temperature record for the world* was received from Mr. Morton J. Rubin, U. S. Weather Bureau meteorologist stationed with the Soviet IGY Antarctic expedition at Mirny, Antarctica. Three successive records were set: at Vostok (78°27′ S., 106°52′ E., elevation approximately 3500 meters) on June 15, −113.3° F. (−80.7° C.) was recorded; at Sovetskaya (78°24′ S., 87°35′ E., elevation approximately 3700 meters) on June 19 the temperature fell to −113.8° F. (−81.0° C.), and on June 25 to −117.4° F. (−83.0° C.). The new record at Sovetskaya is "taken from corrected weekly thermograph trace with 3-hourly comparisons during periods of extreme temperatures." The following further information regarding the conditions under which these temperatures occurred is taken from Mr. Rubin's dispatches.

June 15 Vostok reading of −80.7° C.: From 0000 GMT, June 14 the temperature at Vostok fell from −69° C., with a surface wind from the southwest at 6 to 4 kt. and partly cloudy skies with altocumulus, to −78° C. with west wind at 2 kt. and clear skies at 1200 GMT on June 15. By 1800 GMT on June 15 the temperature had fallen to −79° C. with northwest wind of 2 to 4 kt. and clear skies. The minimum (−80.7° C.) was recorded between 1800 GMT, June 15 and 0000 GMT, June 16. During the same period at Komsomolskaya (74°08′ S., 97°17′ E., elevation approximately 3200 meters) temperatures dropped to −70° to −72° C. with southerly surface winds at 6–8 kt. and clear skies. At Sovetskaya temperatures fell from −67° to −75° C. with northeast winds at 8 kt. and clear skies. There was a 500-mb. col in the region of 80° S., 95° E. with generally weak westerly flow. At 300 mb. a Low was located near 80° S., 120° E. with a col stretching from 80° S. southeastward to 80.8° S., and weak west-southwesterly flow.

June 19 Sovetskaya low of −81.0° C.: At Sovetskaya the temperature fell from −69° C. at 0000 GMT, June 18 to −81° C. at 0000 GMT, June 19, with variable surface winds, northeast to east, at 8–10 kt. and clear skies during the entire period. Komsomolskaya's temperature dropped from −63° to −72° C. with east-southeast to south winds dropping from 8 to 4 kt. and partly cloudy conditions becoming clear at the end of the period. At Vostok the temperature rose from −79° to −74° C. while the wind changed from northwest at 8 kt. to west at 6 kt. with clear skies. Conditions at 500 and 300 mb. were approximately the same, with a ridge along 70° E. and a trough along 120° E. with marked south-southwest flow.

June 25 Sovetskaya low of −83.0° C.: Beginning at 0000 GMT, June 25 temperature at Sovetskaya fell from −72° to −80° C. at 0000 GMT, June 26; a surface wind from the east dropped from 12 kt. to 8 kt. under clear skies. The minimum temperature (−83.0° C.) was recorded at approximately 2200 GMT, June 25. At Komsomolskaya at the same time under clear skies the temperature dropped from −66° to −68° C., with a wind from the south-southeast changing from 12 to 10 kt. Vostok's temperature fell from −73° to −75° C. The wind there changed from southwest at 8 kt. to west at 4 kt.; skies were partly cloudy with altocumulus.

*See *Monthly Weather Review*, vol. 85, No. 11, Nov. 1957, p. 383, for the previous record low also recently reported from Antarctica.

LATE-SEASON COLD OUTBREAK, JUNE 24–27, 1958

HAROLD M. JORDAN AND DALE A. LOWRY

National Weather Analysis Center, U. S. Weather Bureau, Washington, D. C.

1. INTRODUCTION

June was an abnormally cold month for much of the central United States. Elsewhere in this issue O'Connor [1] discusses in detail the monthly circulation and weather. The most severe of a series of cold outbreaks which contributed to the delay of summer weather occurred June 24 to 27. Many long-standing daily temperature records at numerous stations as far south as Texas tumbled to lower levels with this intrusion of Canadian air. Crops were generally retarded and a few small areas where temperatures dropped below freezing suffered actual crop damage. However, the surge occurred so late in the season that strong modifying influences served to temper the onerous effects that cold air earlier would have imposed upon man's activities.

A review of the general synoptic features of the pertinent weather maps for this period, some noteworthy details of frontal reorganization, and some prognostic problems related to the temperature patterns are the main subjects of this article.

2. ANTECEDENT DEVELOPMENTS

Prior to June 24 a cold filling Low on the surface chart meandered in the vicinity of Hudson Bay. North of the Low an extensive area of high pressure was building over Baffin Island, upper Northwest Territories, and the Beaufort Sea. This mass of cold air had a lobe poised over Baffin Island with a ridge westward toward Baker Lake then southwestward toward Montana. The Arctic airmass forming this lobe of high pressure was bounded on the southern edge by an Arctic front moving slowly southward toward Montana and North Dakota. The entire United States east of the Divide except the Gulf States was under the weakening influence of a previous cold surge. The front at the leading edge of the weakened surge became nearly stationary along a line from Georgia to Texas then northwestward parallel to the Divide.

At 500 mb. a semipermanent Low over northern Hudson Bay drifted southwestward through Churchill toward La Pas coming into phase with a short-wave trough moving around a long-wave ridge in Yukon and British Columbia.

The 1000–500-mb. thickness charts showed a cool pool whose central positions coincided with and moved with the 500-mb. Low. Warm air bulged northward from Arizona through Washington to Yukon. Contour gradients demonstrated a rather sharp discontinuity along the main polar front and a weak Arctic front through British Columbia.

3. EARLY DEVELOPMENTS

At 0000 GMT, June 24 (fig. 1A) the surface chart showed the main polar front along the Gulf Coast to southern Texas then north-northwestward to Montana. The pressure pattern was very weak throughout the United States. A previous cold High had decreased in intensity and all that remained was an unusual lack of pressure gradient. The Arctic front had moved through North Dakota, while an innocuous, inactive-appearing Low drifted into northern Minnesota.

At 500 mb. (fig. 1A), the deep cold Low near La Pas, then in phase with the short wave, was ready to move southeastward into the long-wave position in eastern United States.

The 1000–500-mb. thickness analysis (fig. 1B) displays a well organized thermal wind discontinuity along the main polar front. In the Dakotas and Montana a further increase in thickness gradient at the Arctic front corroborated its existence and intensity. The intensity of fronts is defined by NAWAC in terms of thickness gradient, or thermal wind discontinuity. Strong fronts are defined by discontinuities across the fronts of 75 kt. or more, moderate fronts by 50 to 75 kt., and weak fronts by 25 to 50 kt. in the 1000–500-mb. thermal winds. In addition, the analyst may upgrade or downgrade by one degree of intensity depending on the existence or absence of active weather.

The analysis of thickness departure from monthly normal (fig. 1B) demonstrates the same gradient discontinuities as the thickness. The large magnitude of the negative departure near La Pas revealed the threat of a cold surge into the United States.

By 1200 GMT, June 24 (fig. 2A) the surface chart changed only slightly. The main polar front was still fairly stationary through the Gulf States toward northern Texas then northwestward to Montana. The pressure pattern remained very weak and the Low near Lake Superior continued to fill. The trough in which the Arctic front had been carried was diffused through all of South Dakota, Nebraska, and Kansas. Any thermal discontinuity which had previously existed along this front had disintegrated. Cooling ahead of the front and warming farther to the

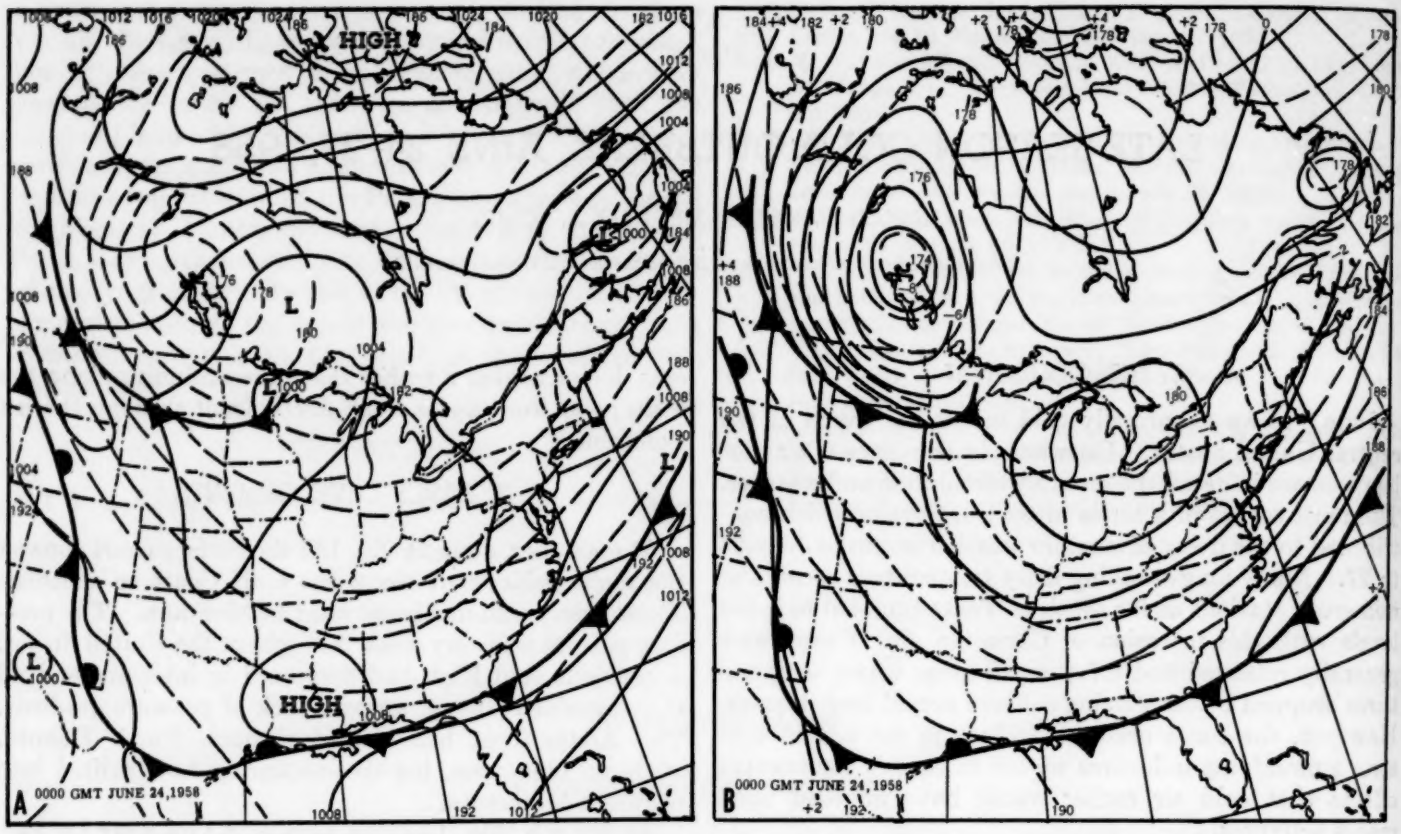

FIGURE 1.—0000 GMT, June 24, 1958. (A) Surface analysis with 500-mb. contours in dashed lines. (B) 1000–500-mb. thickness contours (dashed) and their departure from normal (solid); surface fronts are also shown.

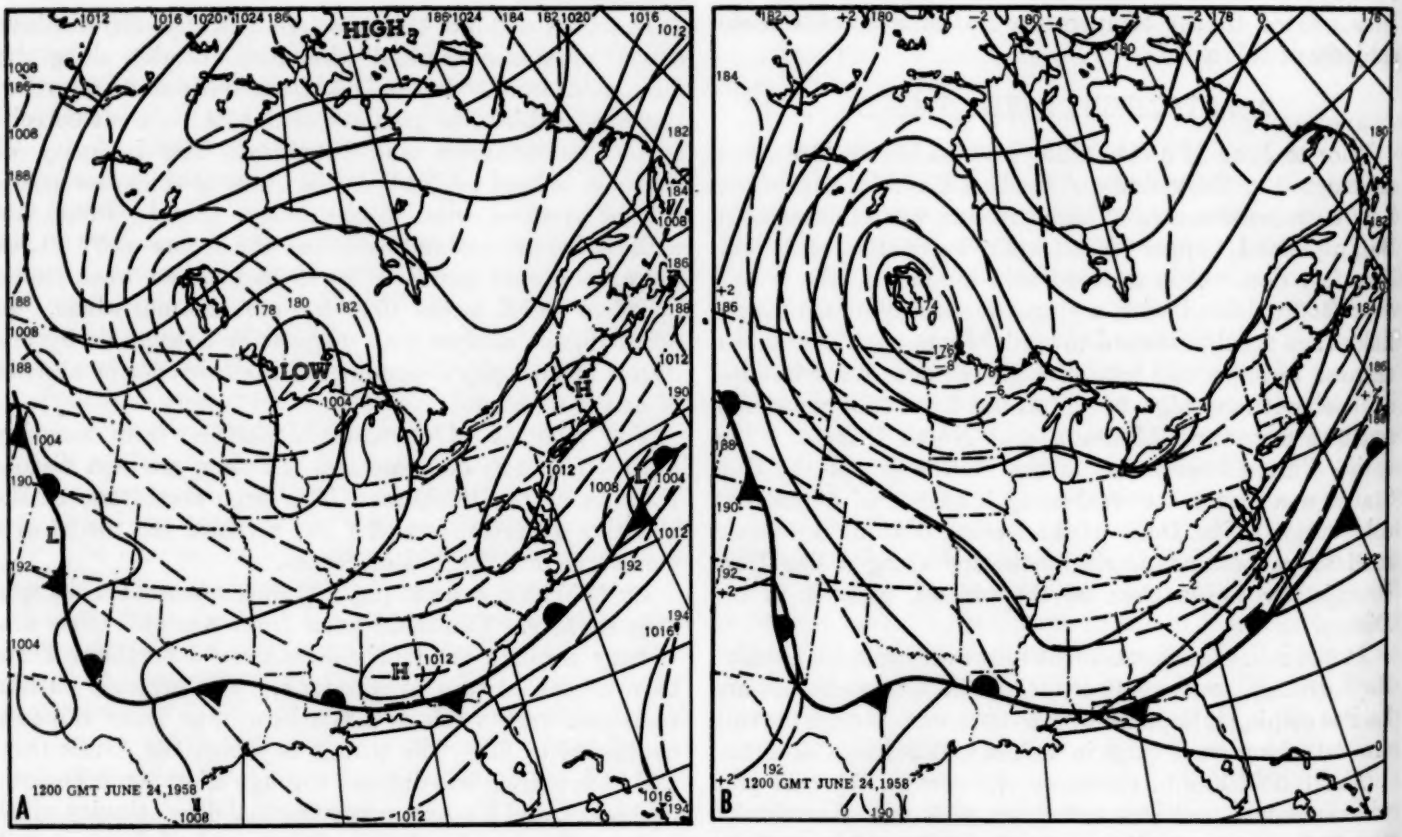

FIGURE 2.—1200 GMT, June 24, 1958. (A) Surface analysis with 500-mb. contours in dashed lines. (B) 1000–500-mb. thickness contours (dashed) and their departure from normal (solid); surface fronts are also shown.

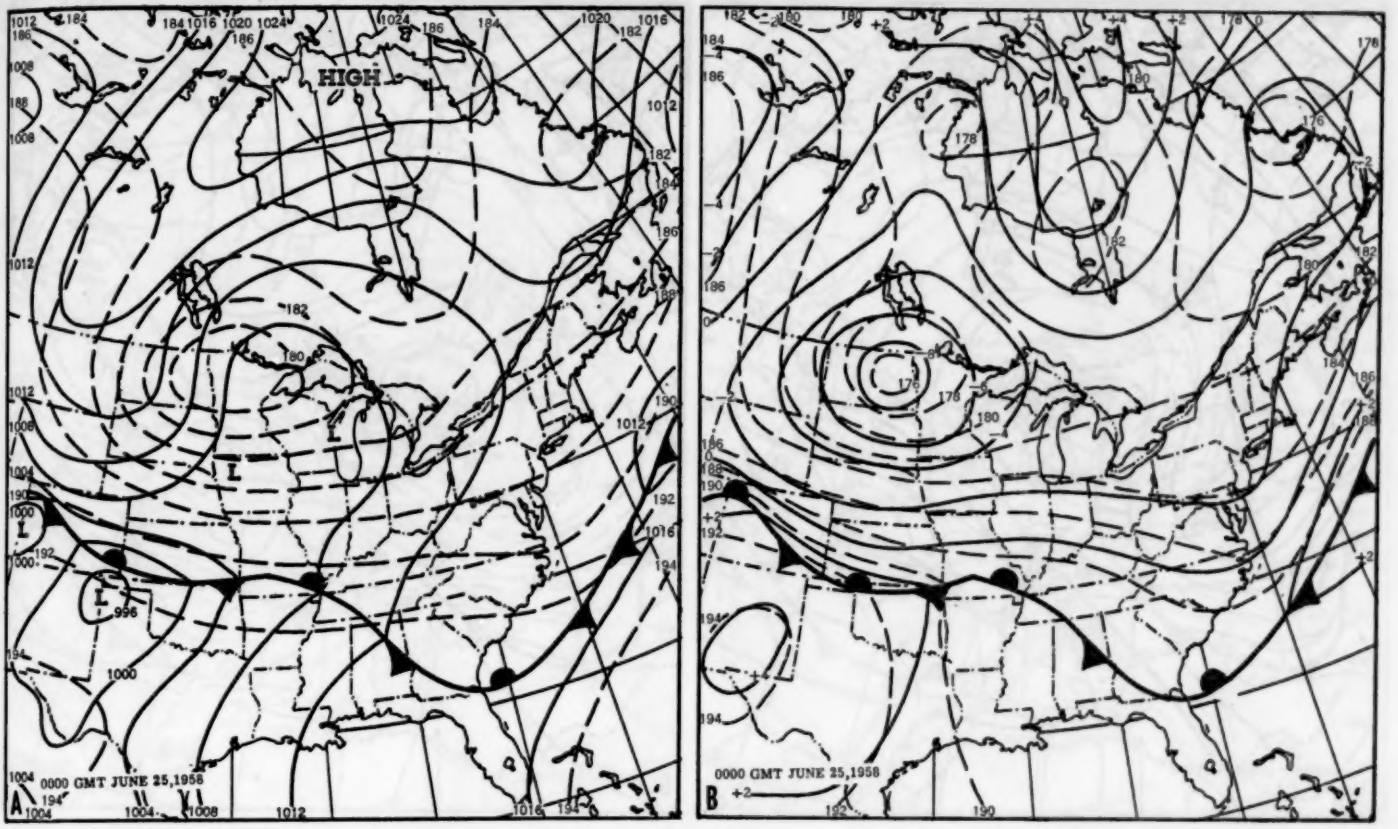

FIGURE 3.—0000 GMT, June 25, 1958. (A) Surface analysis with 500-mb contours in dashed lines. (B) 1000–500-mb. thickness contours (dashed) and their departure from normal (solid); surface fronts are also shown.

south served to increase the thickness gradient ahead of the front. This process left no line of thermal wind discontinuity anywhere north of the portion of the main polar front in Texas.

The thickness chart (fig. 2B) at that time, however, does show a gradually increasing gradient northward from Texas, suggesting that a reorganization of the frontal structure was occurring somewhere near the northern Oklahoma border between the main polar front and the diffuse trough to the north. Along the line where the frontolysed Arctic front had been, all surface pressure tendency discontinuity was gone, and only widely scattered precipitation was observed. At the 850- and 700-mb. levels the isotherm patterns were quite similar to the thickness.

At 500 mb. (fig. 2A) the deep cold Low was moving southeast over Lake Winnepeg. The most striking feature of the circulation was the strong northwest flow from Montana and the Dakotas to the Kentucky, Tennessee, and Alabama area.

An examination of gradients on the thickness departure from normal analysis (fig. 2B) substantiated the lack of definition to any Arctic front in the Dakotas or Nebraska. Still impressive, however, was the large negative anomaly over Lake Winnipeg.

By 0000 GMT, June 25 (fig. 3A), all that remained of the Low then over Wisconsin was a large amorphous area of low pressure with no well defined center. The advective and in situ warming over northern Texas and Oklahoma caused frontolysis of the polar front in northern Texas. The warming to the south together with the cooling to the north through Kansas, Nebraska, and Colorado caused reorganization of the temperature field into the intensifying frontal zone near the northern Oklahoma border. Afternoon temperatures in northern Texas, New Mexico, and western Colorado, ranged from the middle 90's to over 100° F., while temperatures in the Dakotas were in the 50's. An incipient wave in southern Missouri did not at that time appear very important because a more active Low with better upper-air support was moving into the Texas-Oklahoma Panhandle.

At 500 mb. the principal Low had continued to fill southeastward and was centered over northern Minnesota. An area of height rises centered over Kentucky changed the flow to more westerly over the Central States. The strong short-wave trough had moved south and was observed over North Dakota and Montana.

The thickness patterns (fig. 3B) showed the moderate to strong single frontal organization. The cool pool had moved more southerly than the 500-mb. Low and was centered in northeastern North Dakota.

4. MATURE OUTBREAK

Reintensification of the surface Low in Wisconsin began at 1200 GMT, June 25 (fig. 4A). The weak wave

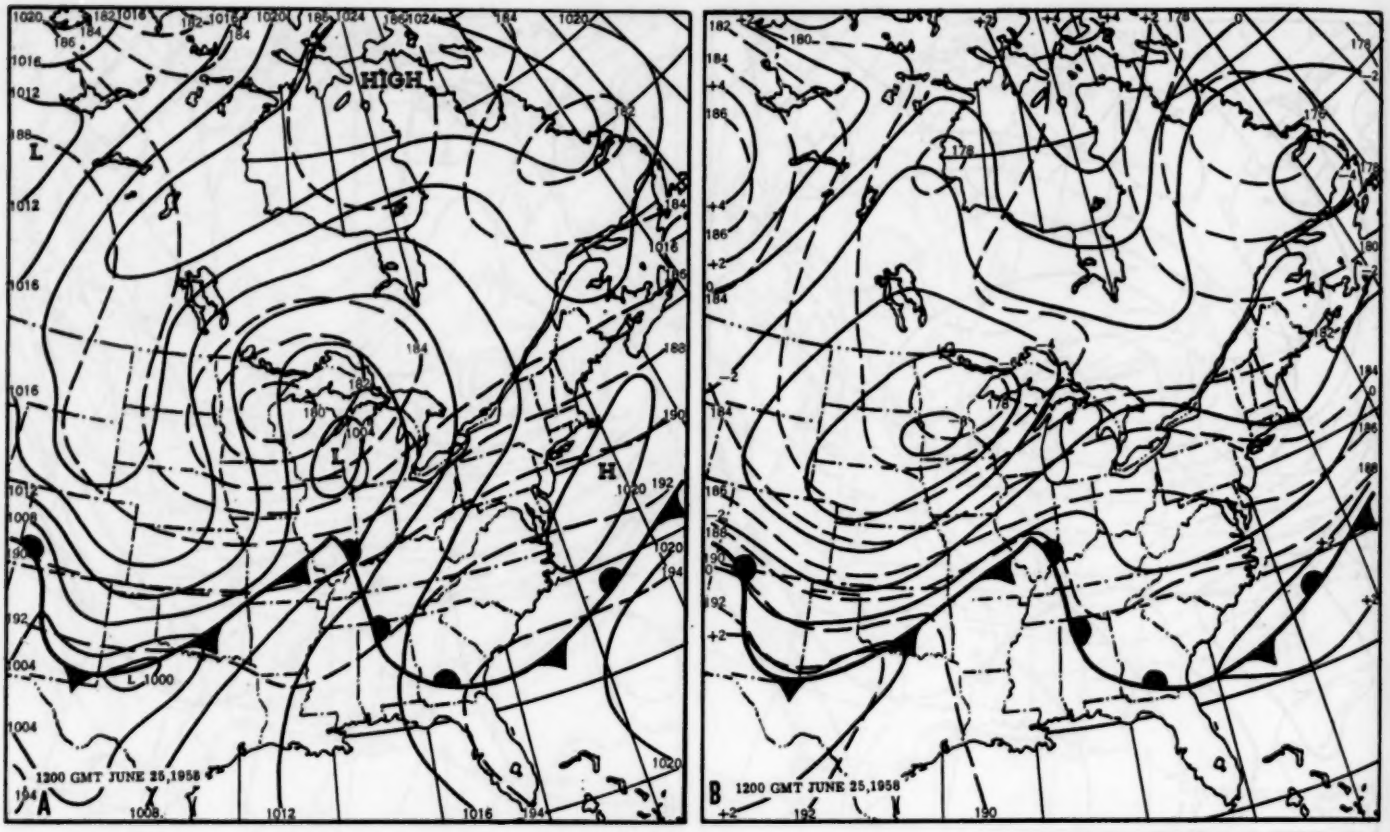

FIGURE 4.—1200 GMT, June 25, 1958. (A) Surface analysis with 500-mb. contours in dashed lines. (B) 1000–500-mb. thickness contours (dashed) and their departure from normal (solid); surface fronts are also shown.

which had been in southern Missouri moved to central Illinois without much increase in circulation but with a marked increase in amplitude. The cold front from the crest of the wave southwestward through eastern Oklahoma to southern New Mexico appeared exceptionally strong even at that early morning hour. Temperatures in the high 70's were present south of the front in Texas while readings in the mid 40's were observed 200 miles to the north in Kansas and Colorado. Considerable precipitation, thunderstorms, strong gusty shifting winds, and marked pressure tendency discontinuities attended the cold frontal passage. The Low in the Panhandle filled as the cold air streamed southward into Nebraska, Kansas, Oklahoma, and northwestern Texas, breaking many temperature records enroute. In figure 5 the stations marked with heavy dots reported in the *Local Climatological Data* various kinds of new temperature records during June 25. Also shown are isotherms of departure of average daily temperature from daily normal. The entire area from the western Great Lakes south to Arkansas, west to Colorado, and north to Montana showed average temperature for the 24-hour period of June 25 to be much below normal.

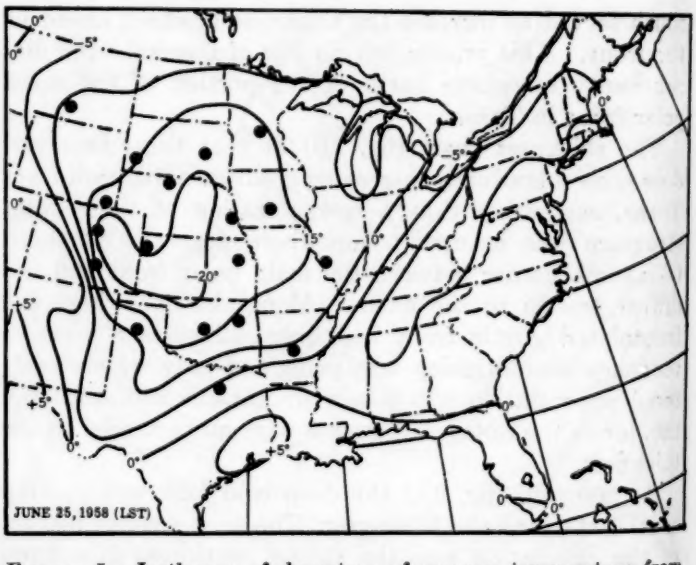

FIGURE 5.—Isotherms of departure of average temperature from normal for June 25, 1958 (local standard time). Heavy black dots indicate stations which reported record-breaking temperatures.

The similarity of the isotherms of departure from normal temperature (fig. 5) to the contours of thickness departure from normal for 1200 GMT of the same day (fig. 4B) suggests that the latter may be useful in describing the large-scale temperature field. In a case study, Kibler, Lennahan, and Martin [2] demonstrated some areal relationships between surface temperatures and 1000–500-mb. thickness, especially where a fresh outbreak of cold air was moving into an area. Ellis and Allen [3], Showalter [4], and Boyden [5] have accumulated

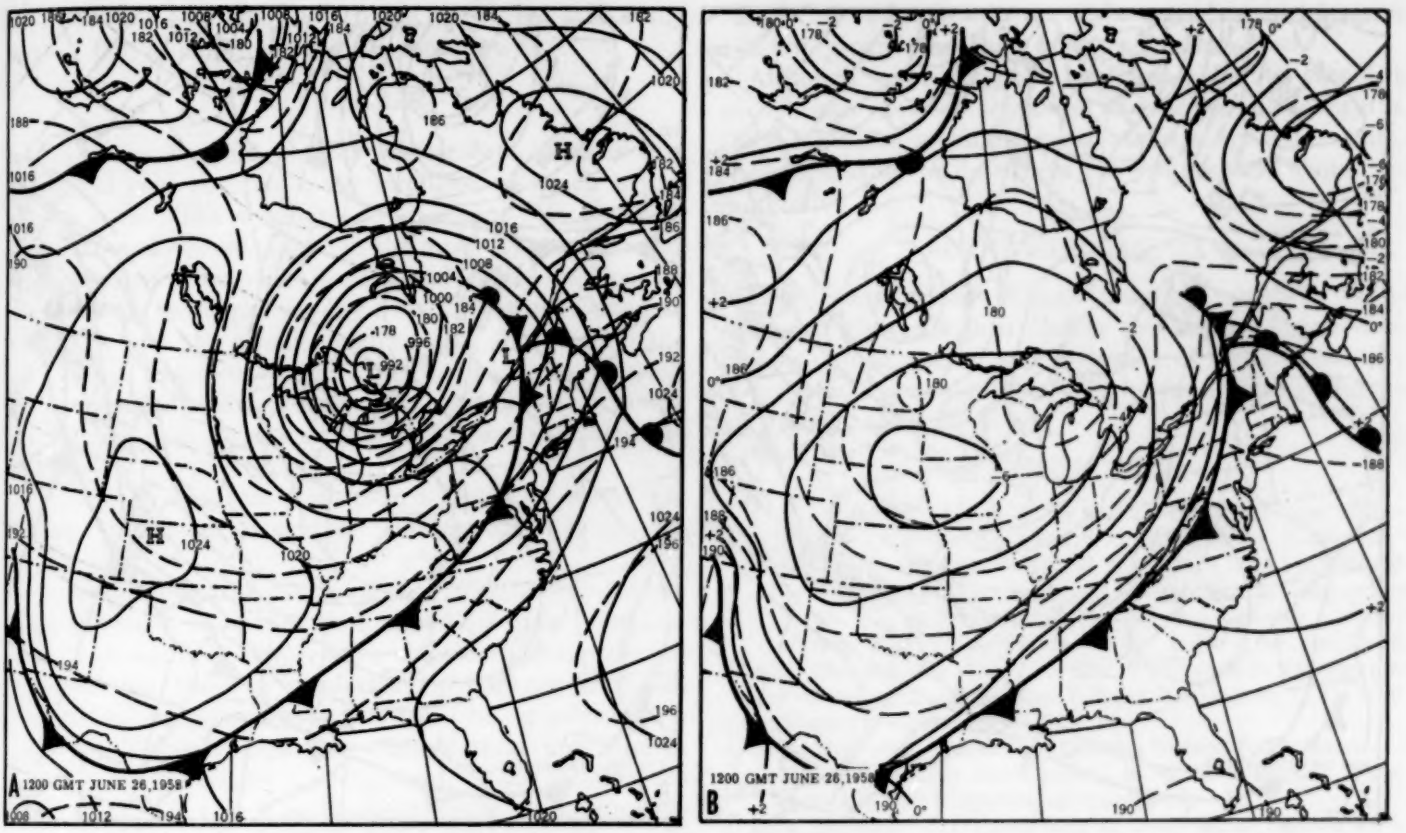

FIGURE 6.—1200 GMT, June 26, 1958. (A) Surface analysis with 500-mb. contours in dashed lines. (B) 1000–500-mb. thickness contours (dashed) and their departure from normal (solid); surface fronts are also shown.

correlations between observed individual surface temperatures and thicknesses. However, the differences between the patterns suggest that other parameters are also necessary to relate the two. Deviations from average lapse rate, cloud cover, presence of precipitation, diurnal changes of temperature, elevation of the station, and local exposures are all important considerations for local temperature forecasting.

At 500 mb. (fig. 4A) the Low was centered near Duluth, Minn., with a trough southwestward toward Wyoming moving around the Low.

The thickness cool pool (fig. 4B) was over central Minnesota. Extremely strong thickness gradients were observed south of the Low extending to the cold front. The large gradient discontinuity along the front confirmed its strong thermal intensity.

By 1200 GMT, June 26 (fig. 6A), the surface Low attained its maximum intensity and depth. The central pressure was down to 990 mb. north of Sault Ste. Marie. The strong northwesterly flow behind the Low had carried cold air as far east as New York and Pennsylvania and as far south as central Texas. Most indications by the surface observations—active thunderstorms, copious precipitation, and large temperature changes—attested to the strong intensity of the front. A portion of the ridge of high pressure which had been in Montana and the Dakotas formed a cold migratory High that moved southeastward into Kansas.

FIGURE 7.—Isotherms of departure of average temperature from normal for June 26, 1958 (local standard time). Heavy black dots indicate stations which reported record-breaking temperatures.

At 500 mb. the Low had deepened and become vertical over the surface Low as the cool pool on the thickness chart lost its definition near the center. The short-wave trough had moved around the Low and was approaching a long-wave position through the Central States.

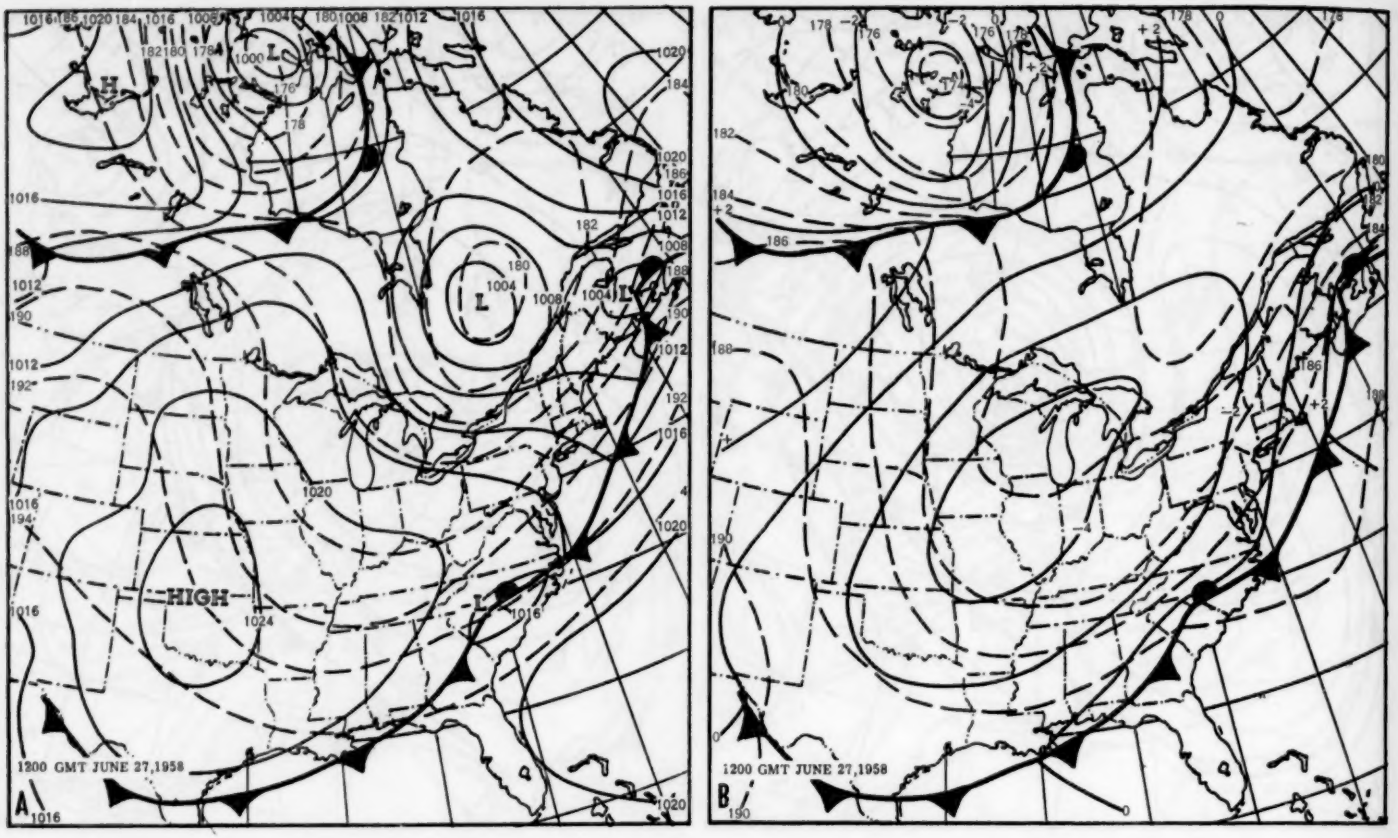

FIGURE 8.—1200 GMT, June 27, 1958. (A) Surface analysis with 500-mb. contours in dashed lines. (B) 1000–500-mb. thickness contours (dashed) and their departure from normal (solid); surface fronts are also shown.

The center of the maximum negative departure from normal of the 1000–500-mb. thickness (fig. 6B) was quite remote from the surface or 500-mb. Low. Both the thickness and the thickness departure from normal still showed a strong gradient discontinuity along the front. However, there was a tendency for the magnitude of thickness departure to decrease. Associated with the decrease was also a tendency for the departure of surface temperatures from normal to lessen (fig. 7). While many stations measured temperatures more than 20° F. below normal on June 25, the largest departures observed on June 26 were about 16° F. The daily records continued to tumble, however, in spite of the modifying forces already in effect.

The surface map at the end of this series, 1200 GMT, June 27 (fig. 8A) shows the filling Low in western Quebec. Northwesterly flow had diminshed in speed but had extended to the Atlantic coast through New England and southward to Virginia. The high pressure cell became quite flat over Oklahoma and Kansas and the cold airmass continued to modify as it moved southward under the increasing influence of the high angle of the summer sun.

The 500-mb. Low remained nearly vertical with and moved with the surface Low, while the short-wave trough passed through the long-wave position in the eastern United States. The thickness gradients (fig. 8B)

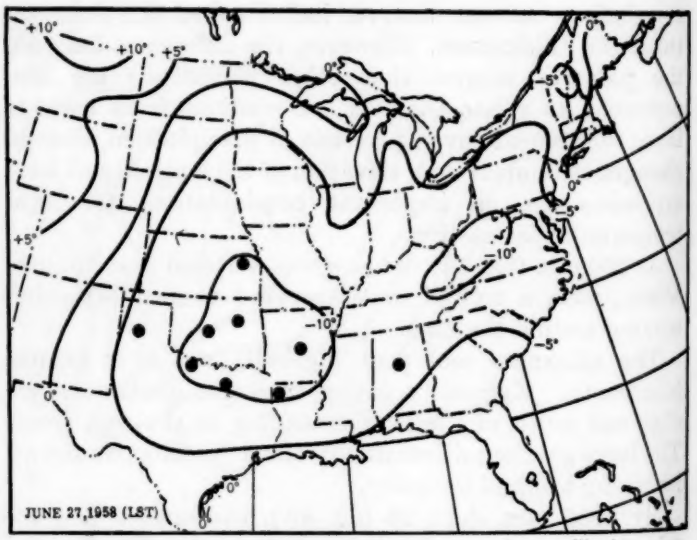

FIGURE 9.—Isotherms of departure of average temperature from normal for June 27, 1958 (local standard time). Heavy black dots indicate stations which reported record-breaking temperatures.

showed further weakening of the frontal intensity and the cool pool no longer had clear identity.

Centered over Illinois there remained a diminishing closed cell of thickness departure which still identified the cold air over the central and eastern portions of the country. The departures of the surface temperatures

(fig. 9) were only about −10° to −12° F.; still many records fell, some for the third consecutive day.

5. SUMMARY

The unusually cold weather during June was the sum of several cold outbreaks, the strongest of which is presented here. The sequence of events in this outbreak was the usual one even though the intensity was extreme. First a mass of cold air formed and cooled in Canada. Then a Low developed rapidly near the central Canadian border. Next the strong northwesterly flow behind the Low forced the cold air into the States in a rapid surge which plunged temperatures to record-breaking levels. Finally the cold airmass moved southward and began to modify.

During the early stages the reorganization of the frontal systems presented an analysis problem which frequently occurs.

An examination of charts of the 1000–500-mb. thickness, thickness departure from normal, surface temperature, and surface temperature departure from normal suggests that there is a relationship between thickness and surface temperature, or perhaps a better relationship between thickness departure from normal and surface temperature departure from normal. This relationship further suggests that a first approximation to a temperature forecast might be found in a thickness forecast. One of the routine charts prepared at NAWAC is a prognostic 1000–500-mb. thickness chart which is not transmitted but is implicit in the 30-hour surface and 36-hour 500-mb. prognostic charts which are transmitted.

Although some research has been done to establish correlations between thickness and surface temperature, further studies including local variation of other influences operating to determine the temperature should be productive.

ACKNOWLEDGMENTS

The authors wish to thank the staff members of the National Meteorological Center for helpful suggestions, preparation of charts, and reviewing of the article. We also thank the Daily Map Unit of the Weather Bureau for drafting the figures.

REFERENCES

1. J. F. O'Connor, "The Weather and Circulation of June 1958—Record Cold in Northeast and Warmth in Northwest," *Monthly Weather Review*, vol. 86, No. 6, June 1958, pp. 229–236.
2. C. L. Kibler, C. M. Lennahan, and R. H. Martin, "Temperature Forecasting as an Implicit Feature in Prognostic Charts," *Monthly Weather Review*, vol. 83, No. 1, Jan. 1955, pp. 23–30.
3. J. O. Ellis and R. A. Allen, The Use of Thickness in Temperature Forecasting, U. S. Weather Bureau, Washington, D. C., 1958. (Unpublished manuscript)
4. A. K. Showalter, Correlations between Surface Temperature and 1000–500 Millibar Thickness, U. S. Weather Bureau, Washington, D. C. (Unpublished manuscript)
5. C. J. Boyden, "The Forecasting of Daily Mean Surface Temperature from 1000–500 Millibar Thickness Lines," *The Meteorological Magazine*, vol. 87, No. 1030, Apr. 1958, pp. 98–105.

DESCRIPTION OF CHARTS

CHART I. *A. Average Temperature (°F.) at Surface. B. Departure of Average Temperature from Normal.*—The average monthly temperature presented in Chart I–A is computed from the average daily maximum and the average daily minimum which in turn are computed from the daily maximum and minimum temperatures reported by some 225 first-order Weather Bureau stations and 700 cooperative stations. The departures from normal are presented in Chart I–B. They are based on the 30-year normals (1921–50) for the first-order Weather Bureau stations and on means of 25 years or more (mostly 1931–55) for the cooperative stations.

CHART II. *Total Precipitation.*—

CHART III. *A. Departure of Precipitation from Normal (inches). B. Percentage of Normal Precipitation.*—Chart II is based on daily precipitation records at about 800 Weather Bureau and cooperative stations. In Chart III the anomaly in the month's precipitation is shown as a departure from the normal total and as a percentage of the normal total. These anomalies show the deviations from the 30-year normals (1921–50) for about 225 first-order Weather Bureau stations in Charts III A and B, supplemented in Chart III–A by the deviation from means of 25 years or more (mostly 1931–55) for about 700 cooperative stations.

CHART IV. *Total Snowfall.*—

CHART V. *A. Percentage of Normal Snowfall. B. Depth of Snow on Ground.*—Chart IV gives the total depth in inches of unmelted snowfall as reported during the month by Weather Bureau and cooperative stations. This is converted in Chart V–A into a percentage of the normal total amount computed for each Weather Bureau station having at least 10 years of record. The depth of snow on ground is that reported by both Weather Bureau and cooperative stations as of 7:00 a. m. EST on the last Monday of the month. This is reported only for the months December through April. The snowfall charts are presented each month November through April.

CHART VI. *A. Percentage of Sky Cover Between Sunrise and Sunset. B. Percentage of Normal Sky Cover Between Sunrise and Sunset.*—These charts are based on visual observations made hourly at Weather Bureau stations and averaged for the month. Sky cover includes, in addition to cloudiness, obscuration of the sky by fog, smoke, etc. Normal amount of sky cover is computed for stations having at least 10 years of record.

CHART VII. *A. Percentage of Possible Sunshine. B. Percentage of Normal Sunshine.*—Chart VII–A shows the amount of sunshine received in terms of percentage of the total hours of sunshine possible during the month. In Chart VII–B this is shown as a percentage of the normal number of hours of sunshine received. Normals are computed for Weather Bureau stations having at least 10 years of record.

CHART VIII. *Average Daily Values of Solar Radiation, Direct and Diffuse.*—Plotted on the chart are the monthly means of daily total solar radiation, both direct and diffuse, in langleys (gm. cal. $cm.^{-2}$) for all Weather Bureau stations which record this element. Supplementary data, for which limits of accuracy are wider than for those data shown, are drawn upon in making the analysis. The inset shows the percentages of the mean based on the period 1951–55.

CHART IX. *Tracks of Centers of Anticyclones at Sea Level.*—

CHART X. *Tracks of Centers of Cyclones at Sea Level.*—Centers which can be identified for 24 hours or more are tracked in these charts. Semipermanent features such as the Great Basin and Pacific Highs and Colorado and Mexico Lows are not shown. The 7:00 a. m. EST positions are shown by open circles, with the intermediate positions at 6-hour intervals shown by solid dots. The date is given above the circle and the central pressure to whole millibars below. A dashed track indicates a regeneration rather than actual movement to the next position. Solid squares indicate position of stationary center for period shown beside it.

CHART XI. *Average Sea Level Pressure (mb.) and Surface Windroses.*—The average monthly sea level pressure is obtained from the averages of the 7:00 a. m. and 7:00 p. m. EST pressures reported at Weather Bureau stations. Windroses are based on the hourly wind directions (to 16 points of the compass) reported by Weather Bureau stations, each circle or arc indicating 5 percent of the time. The inset shows the departure of the average pressure from the normal average computed for each station having at least 10 years record and for each 10° intersection in a diamond grid over the oceans from interpolated values read from the Historical Weather Maps for the 20 years of best coverage prior to 1940.

CHARTS XII–XVII. *Average Height, Temperature, and Resultant Winds, 850, 700, 500, 300, 200, and 100 mb.*—Height is given in geopotential meters and temperature in degrees Celsius. These are the averages of the 1200 GMT radiosonde reports. Wind speeds are given in knots; flag represents 50 knots, full feather 10 knots, and half feather 5 knots. Directions are shown to 360° of the compass. Winds are based on rawins at 1200 GMT.

NOTE. Tabulations of exact values of most of these charted elements for Weather Bureau stations are printed each month in *Climatological Data—National Summary*, and annual averages are presented in the Annual Issue of that publication each year.

U. S. GOVERNMENT PRINTING OFFICE: 1958

Chart I. A. Average Temperature (°F.) at Surface, June 1958.

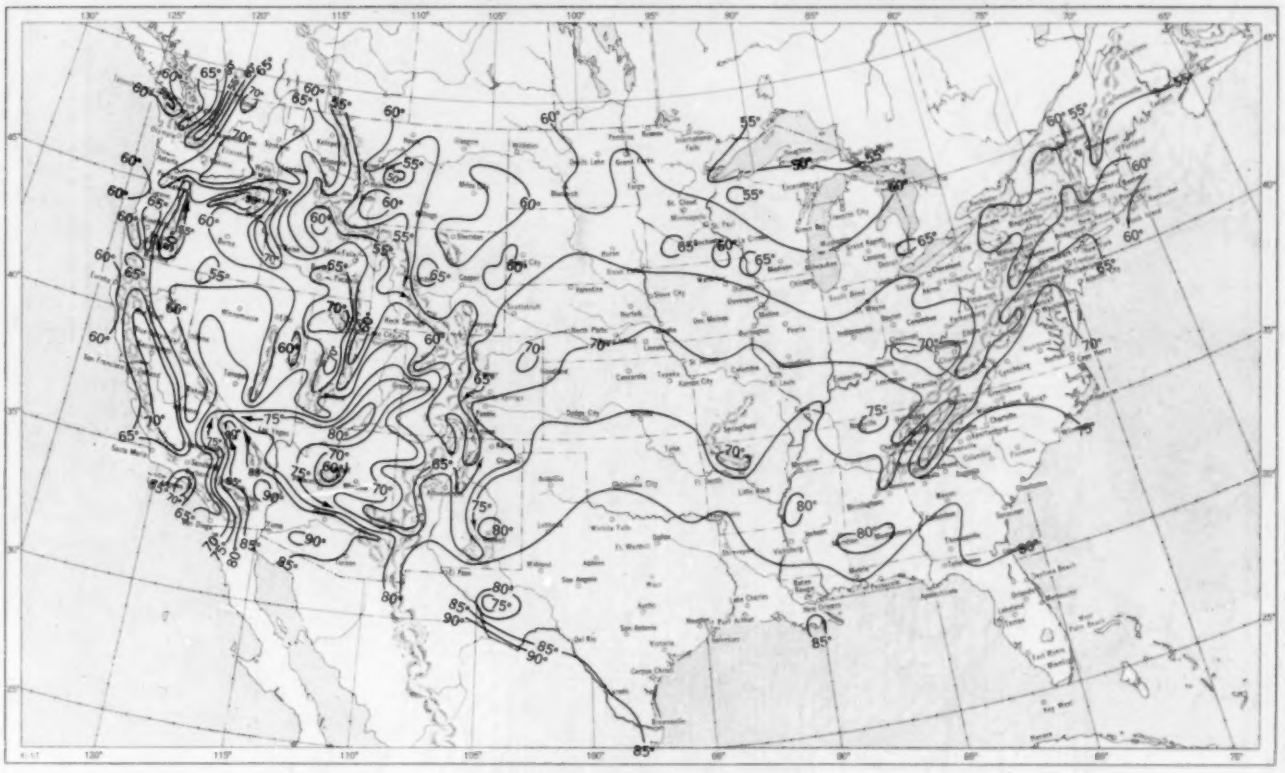

B. Departure of Average Temperature from Normal (°F.), June 1958.

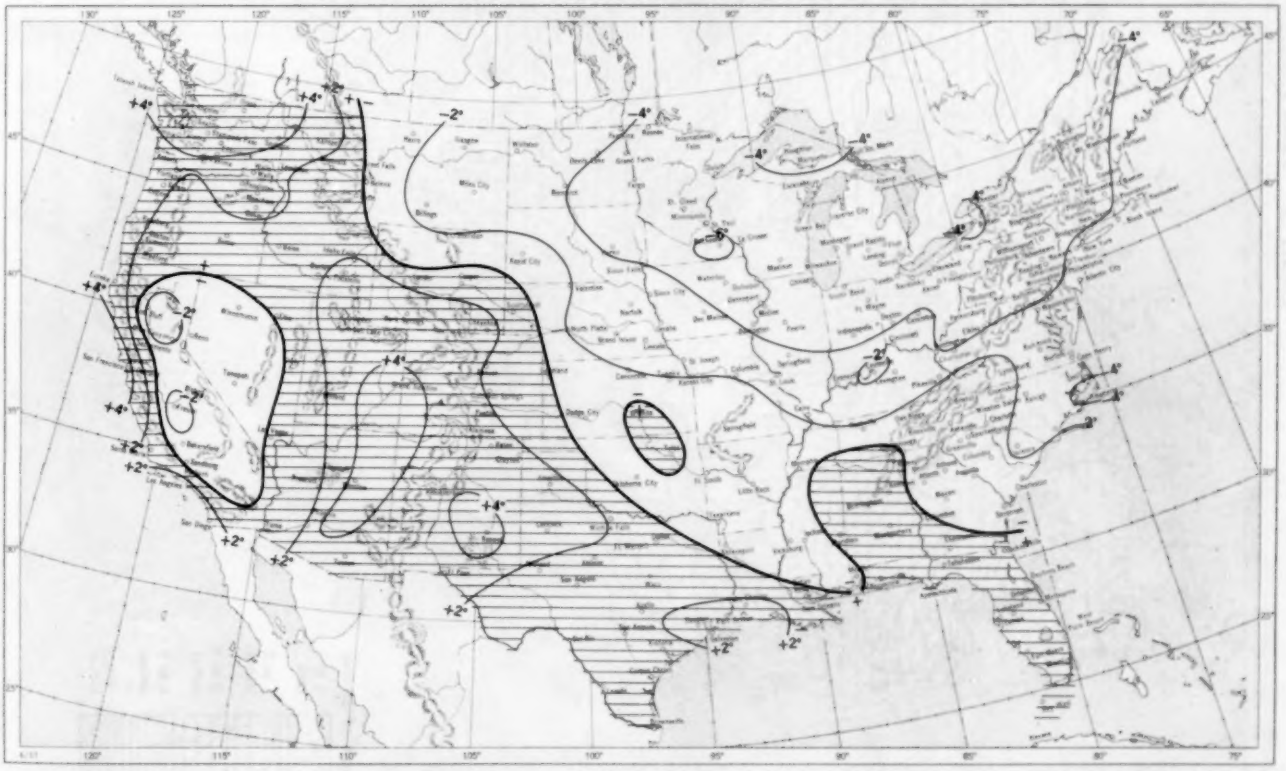

A. Based on reports from over 900 Weather Bureau and cooperative stations. The monthly average is half the sum of the monthly average maximum and monthly average minimum, which are the average of the daily maxima and daily minima, respectively.

B. Departures from normal are based on the 30-yr. normals (1921-50) for Weather Bureau stations and on means of 25 years or more (mostly 1931-55) for cooperative stations.

Chart II. Total Precipitation (Inches), June 1958.

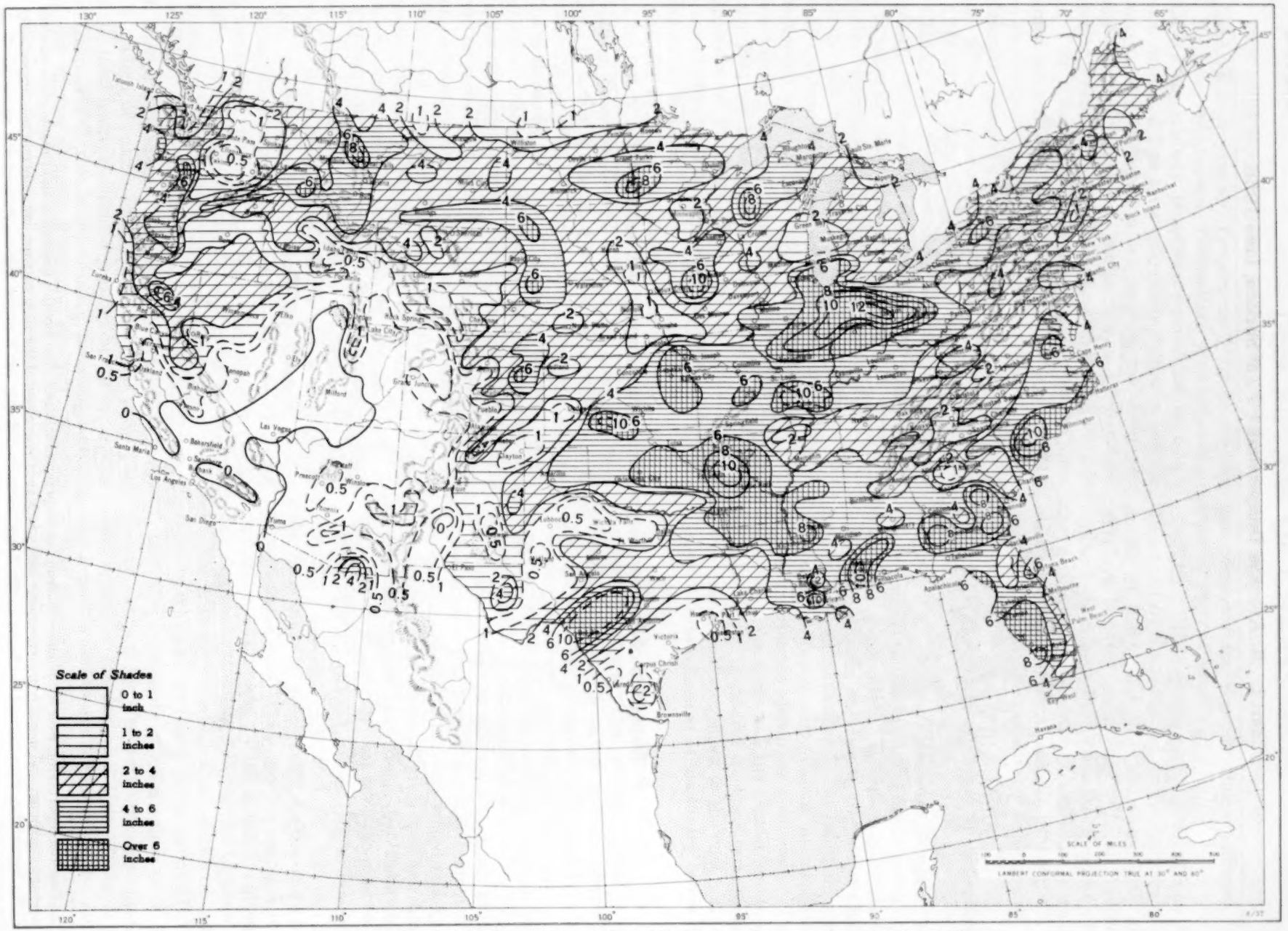
Scale of Shades
0 to 1 inch
1 to 2 inches
2 to 4 inches
4 to 6 inches
Over 6 inches
SCALE OF MILES
LAMBERT CONFORMAL PROJECTION TRUE AT 30° AND 60°

Based on daily precipitation records at about 800 Weather Bureau and cooperative stations.

Chart III. A. Departure of Precipitation from Normal (Inches), June 1958.

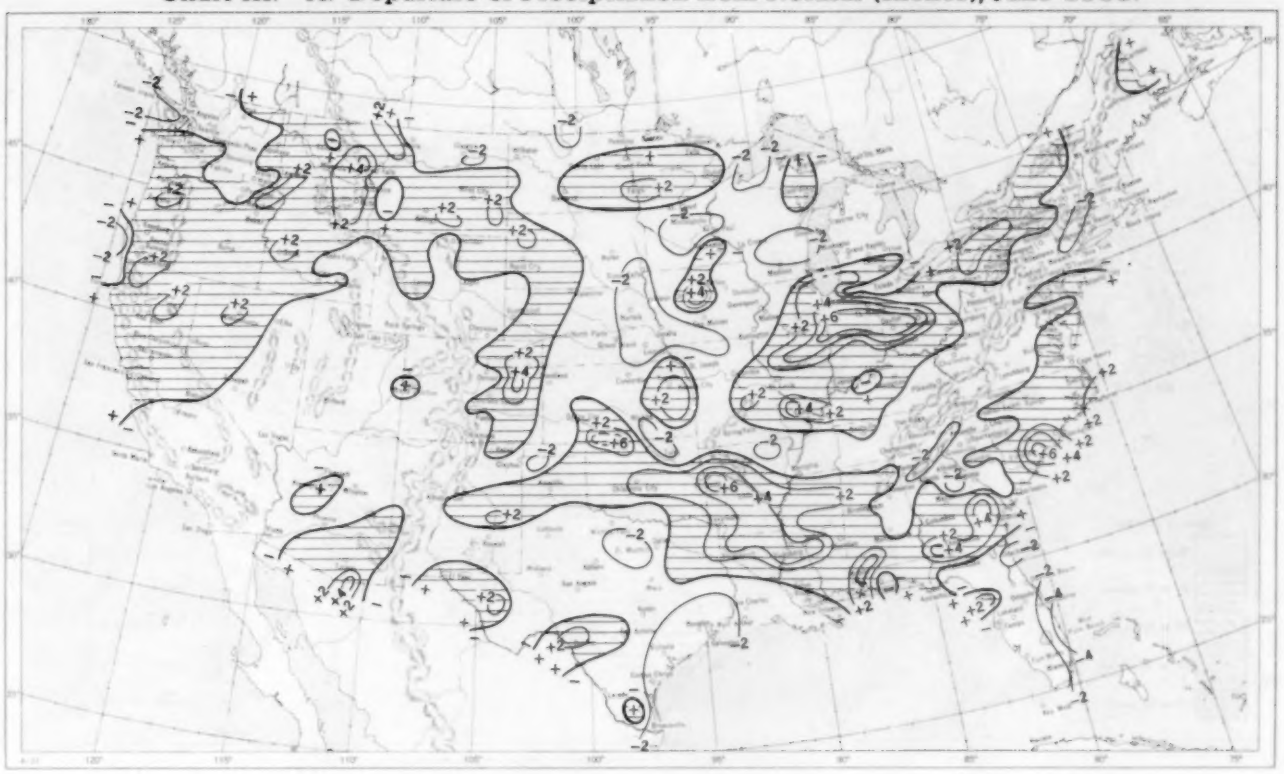

B. Percentage of Normal Precipitation, June 1958.

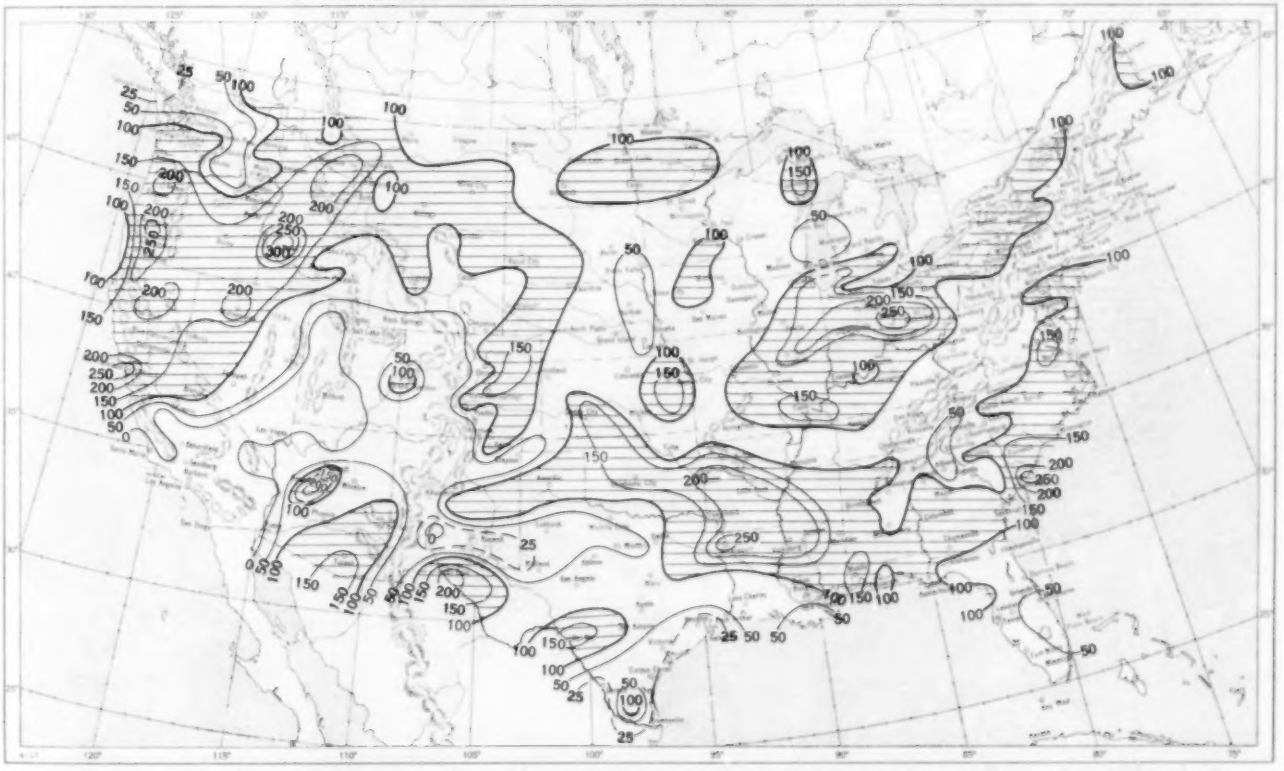

Normal monthly precipitation amounts are computed from the records for 1921-50 for Weather Bureau stations and from records of 25 years or more (mostly 1931-55) for cooperative stations.

Chart VI. A. Percentage of Sky Cover Between Sunrise and Sunset, June 1958.

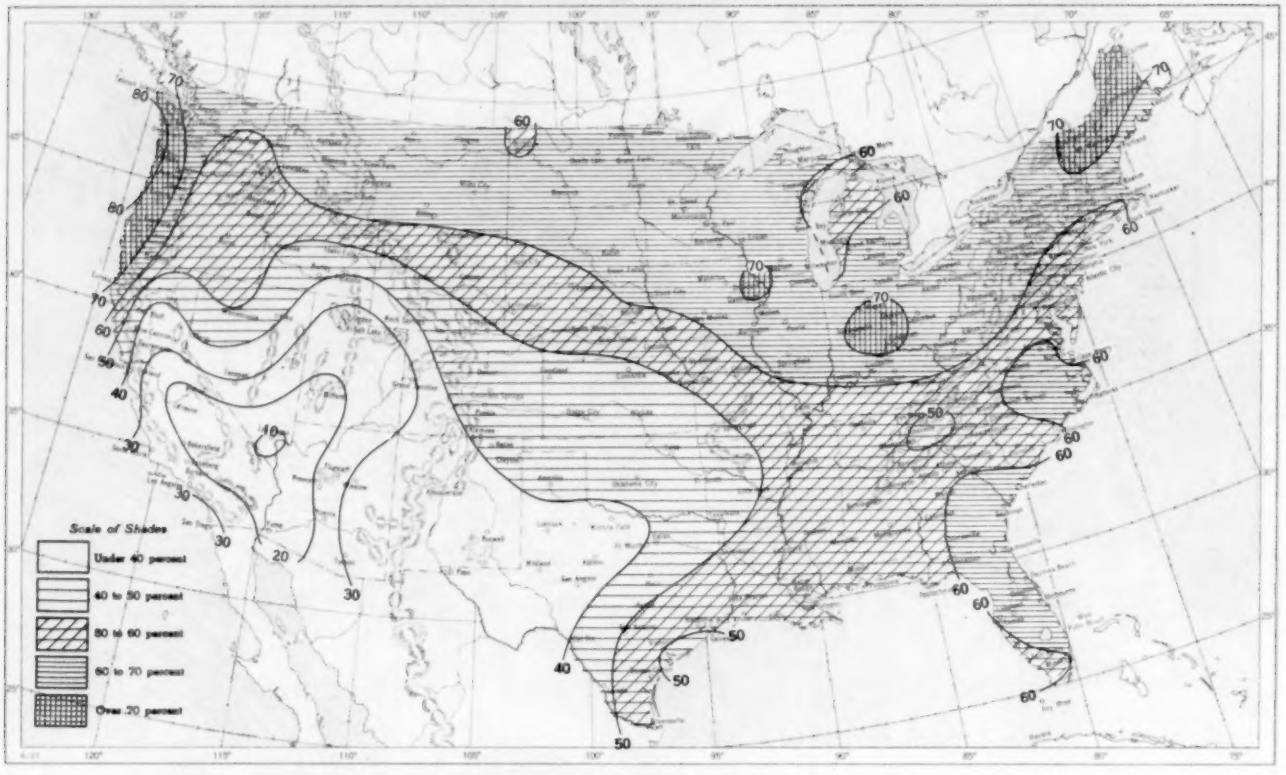

B. Percentage of Normal Sky Cover Between Sunrise and Sunset, June 1958.

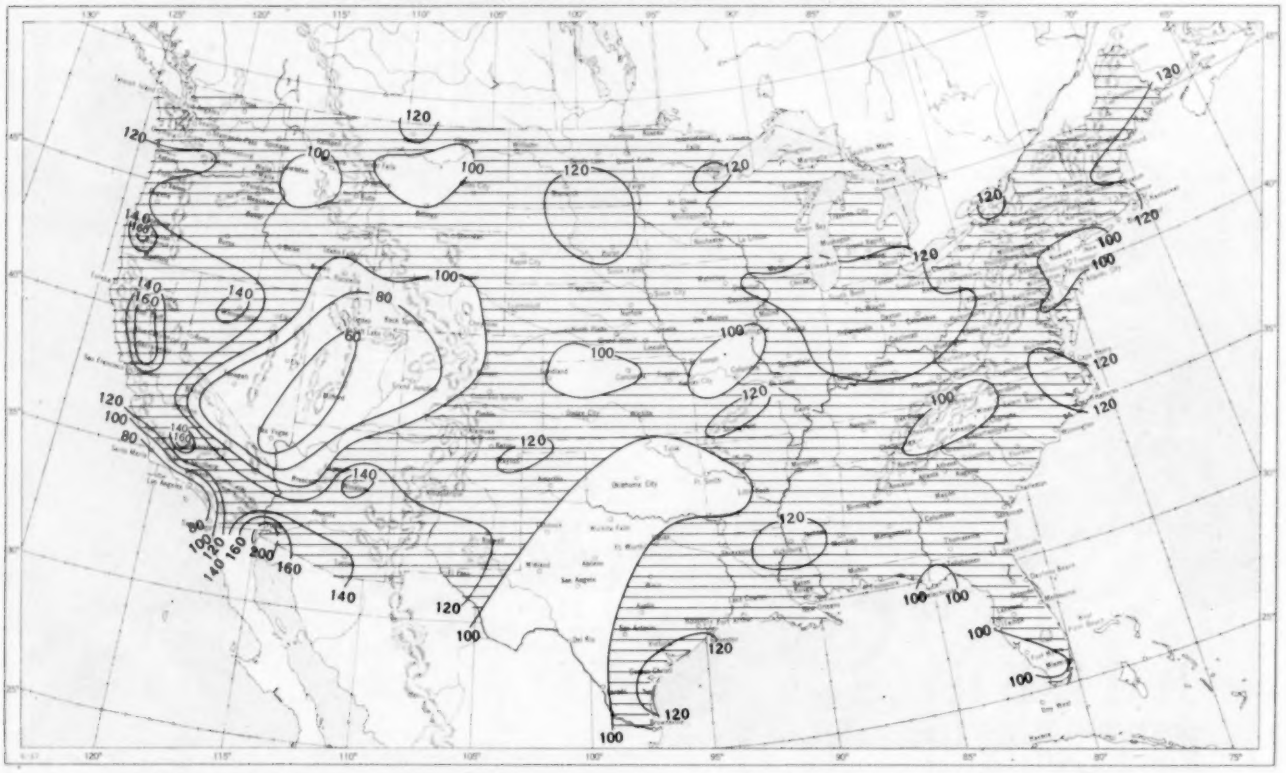

A. In addition to cloudiness, sky cover includes obscuration of the sky by fog, smoke, snow, etc. Chart based on visual observations made hourly at Weather Bureau stations and averaged over the month. B. Computations of normal amount of sky cover are made for stations having at least 10 years of record.

Chart VII. A. Percentage of Possible Sunshine, June 1958.

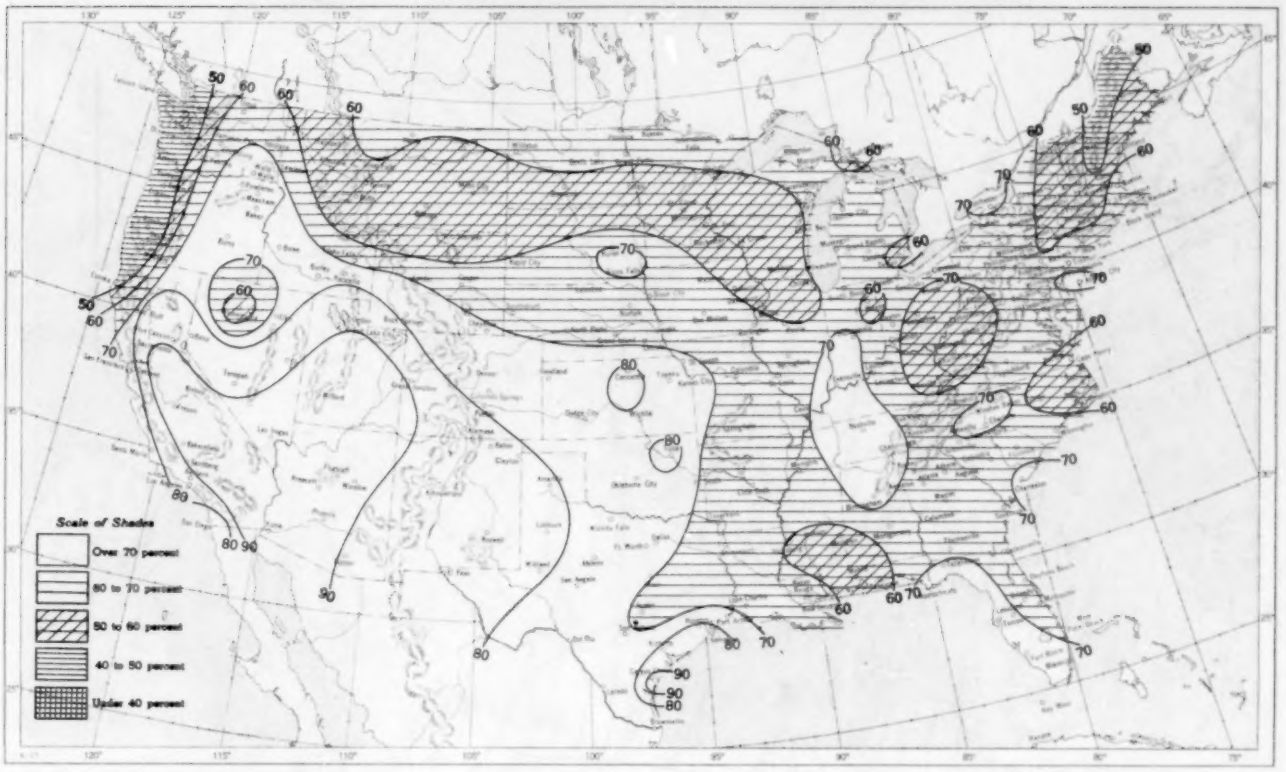

B. Percentage of Normal Sunshine, June 1958.

A. Computed from total number of hours of observed sunshine in relation to total number of possible hours of sunshine during month. B. Normals are computed for stations having at least 10 years of record.

Chart VIII. Average Daily Values of Solar Radiation, Direct + Diffuse, June 1958. Inset: Percentage of Mean Daily Solar Radiation, June 1958. (Mean based on period 1951-55.)

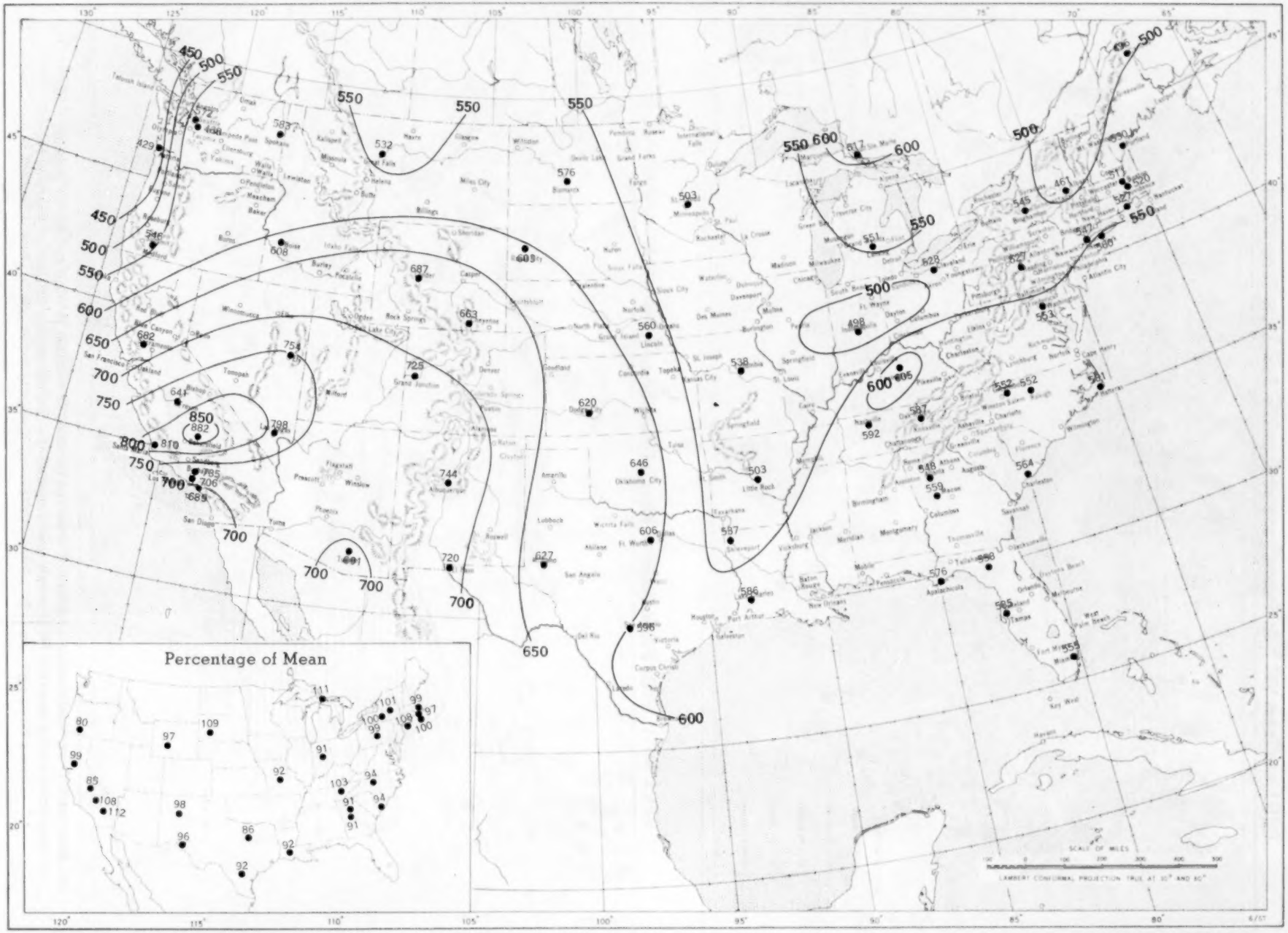

Chart shows mean daily solar radiation, direct + diffuse, received on a horizontal surface in langleys (1 langley = 1 gm. cal. cm. $^{-2}$). Basic data for isolines are shown on chart. Further estimates are obtained from supplementary data for which limits of accuracy are wider than for those data shown. The inset shows the percentage of the mean based on the period 1951-55.

Chart IX. Tracks of Centers of Anticyclones at Sea Level, June 1958.

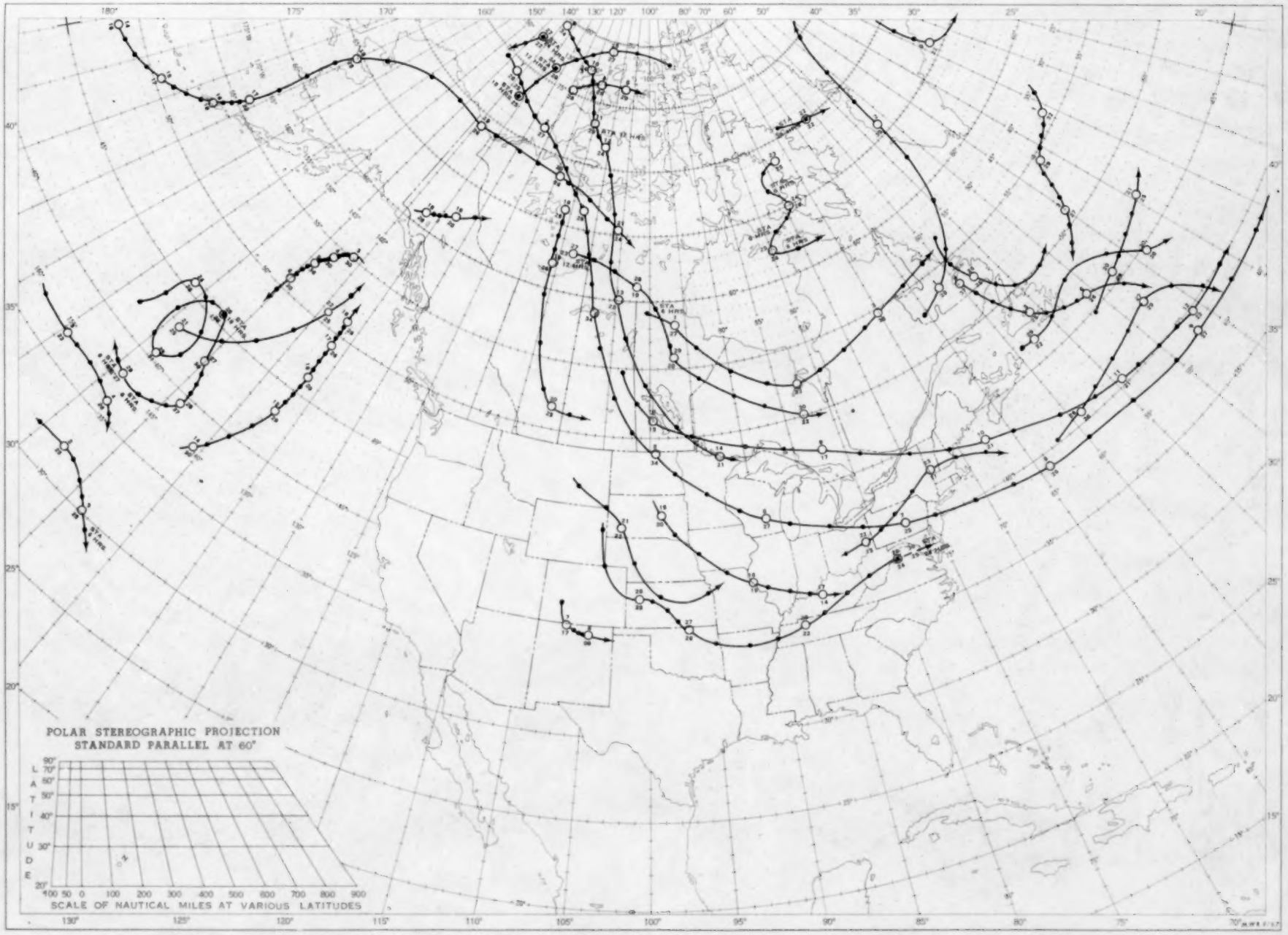
POLAR STEREOGRAPHIC PROJECTION
STANDARD PARALLEL AT 60°
LATITUDE
90° 70° 60° 50° 40° 30° 20°
100 50 0 100 200 300 400 500 600 700 800 900
SCALE OF NAUTICAL MILES AT VARIOUS LATITUDES

Circle indicates position of center at 7:00 a. m. E. S. T. Figure above circle indicates date, figure below, pressure to nearest millibar. Dots indicate intervening 6-hourly positions. Squares indicate position of stationary center for period shown. Dashed line in track indicates reformation at new position. Only those centers which could be identified for 24 hours or more are included.

Chart X. Tracks of Centers of Cyclones at Sea Level, June 1958.

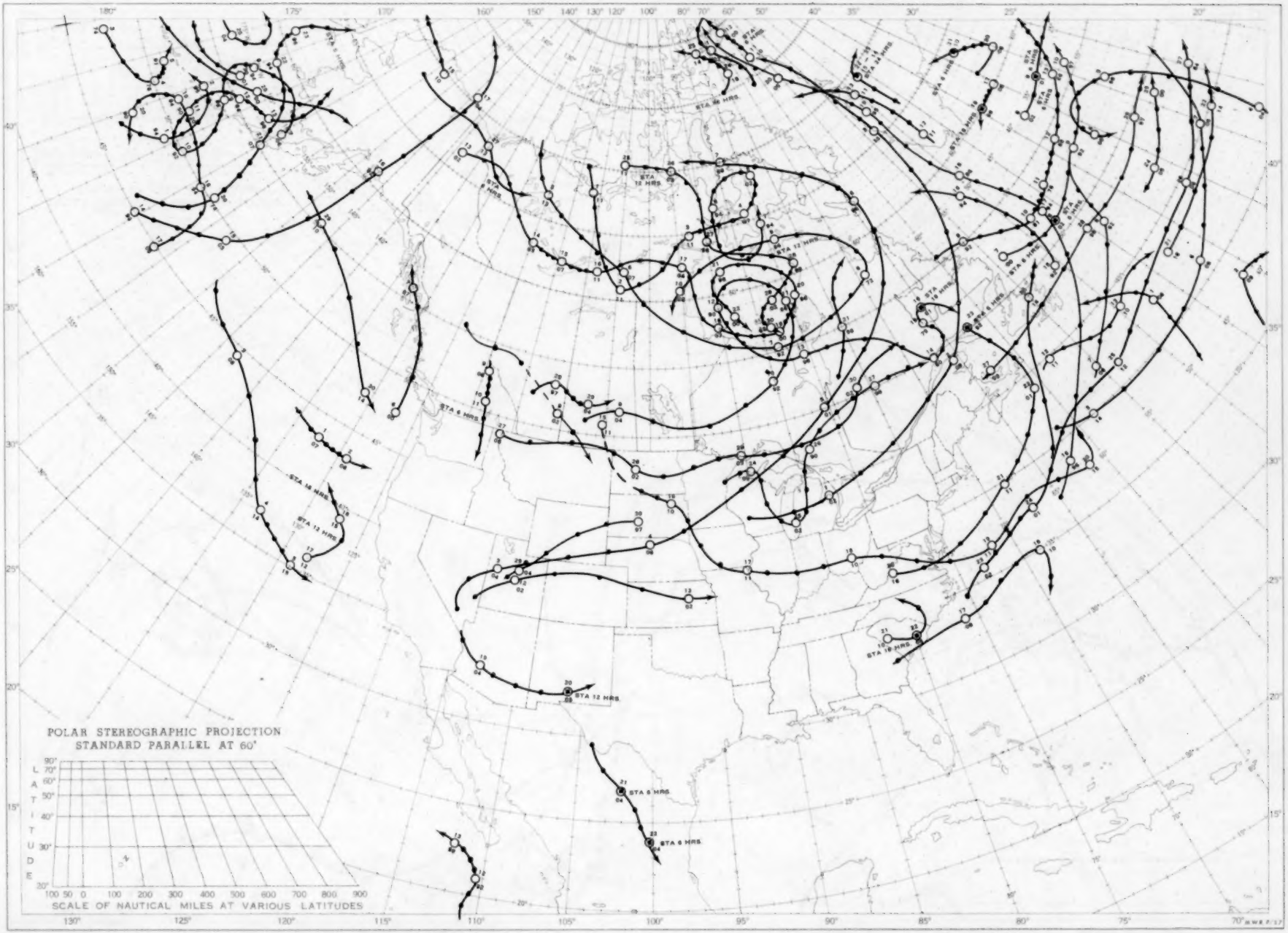

Circle indicates position of center at 7:00 a. m. E. S. T. See Chart IX for explanation of symbols.

Chart XI. Average Sea Level Pressure (mb.) and Surface Windroses, June 1958. Inset: Departure of Average Pressure (mb.) from Normal, June 1958.

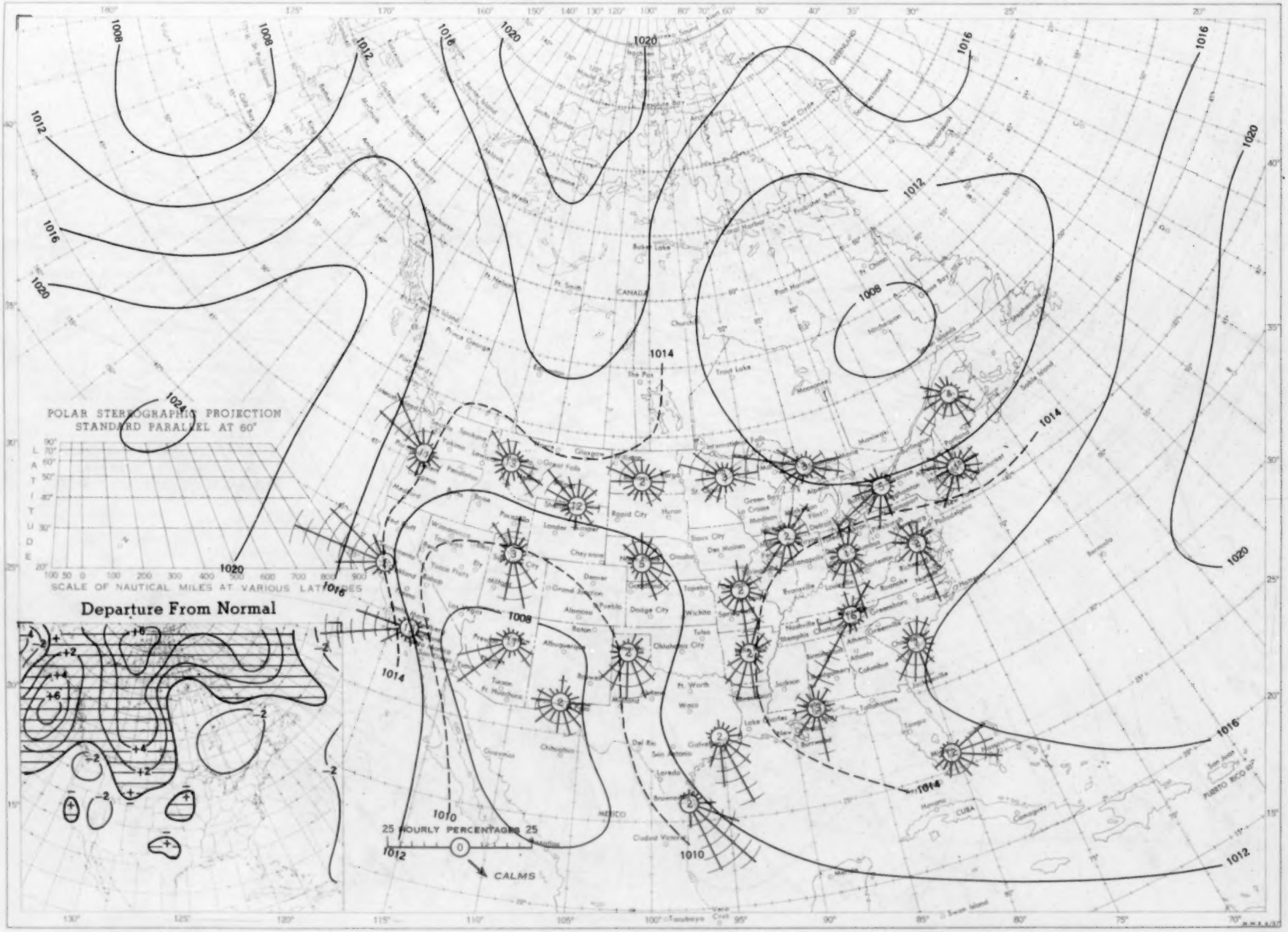

Average sea level pressures are obtained from the averages of the 7:00 a. m. and 7:00 p. m. E. S. T. readings. Windroses show percentage of time wind blew from 16 compass points or was calm during the month. Pressure normals are computed for stations having at least 10 years of record and for 10° intersections in a diamond grid based on readings from the Historical Weather Maps (1899-1939) for the 20 years of most complete data coverage prior to 1940.

Chart XII. 850-mb. Surface, 1200 GMT, June 1958. Average Height and Temperature, and Resultant Winds.

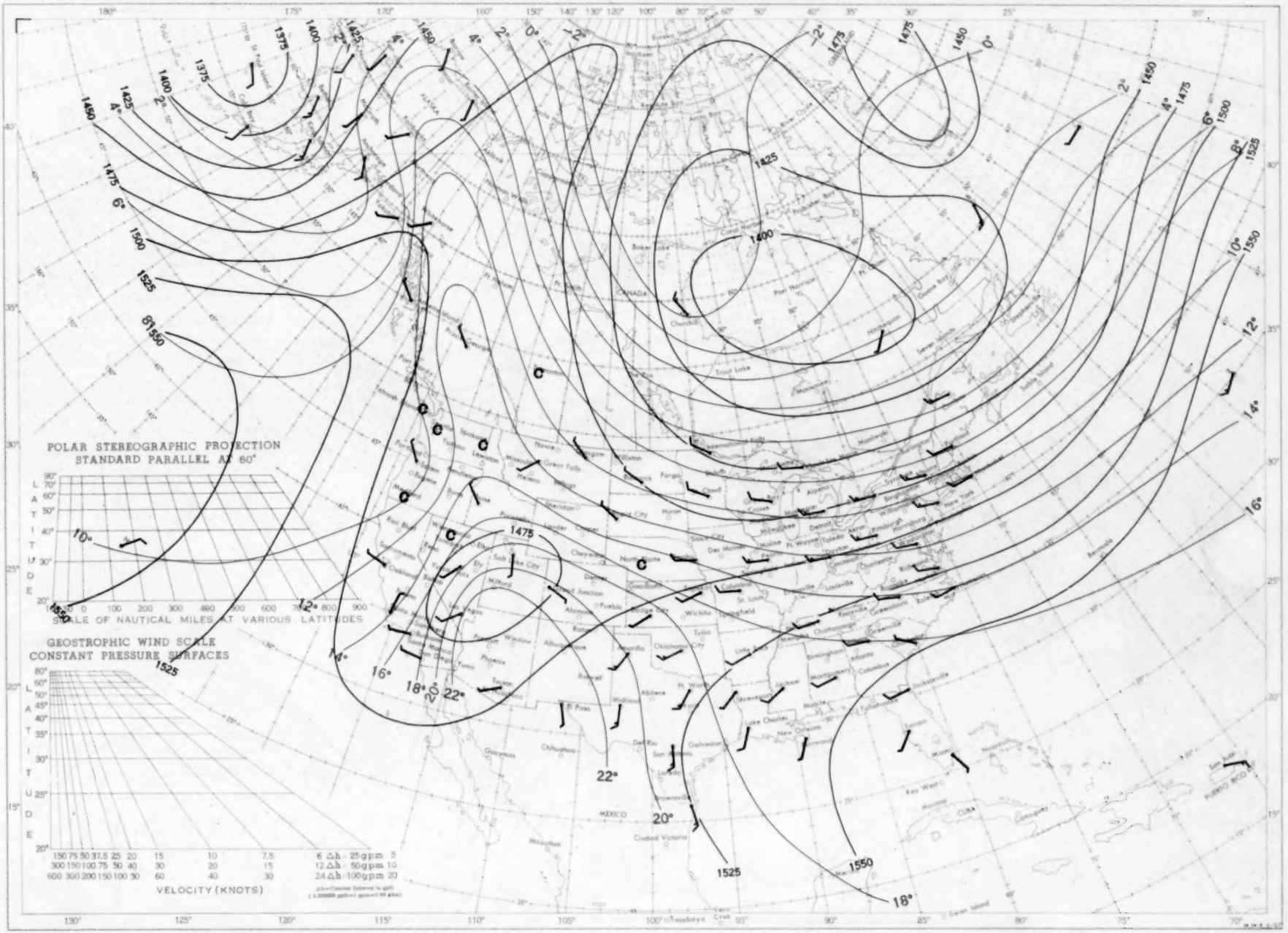

Height in geopotential meters (1 g.p.m. = 0.98 dynamic meters). Temperature in °C. Wind speed in knots; flag represents 50 knots, full feather 10 knots, and half feather 5 knots. All wind data are based on rawin observations.

Chart XIII. 700-mb. Surface, 1200 GMT, June 1958. Average Height and Temperature, and Resultant Winds.

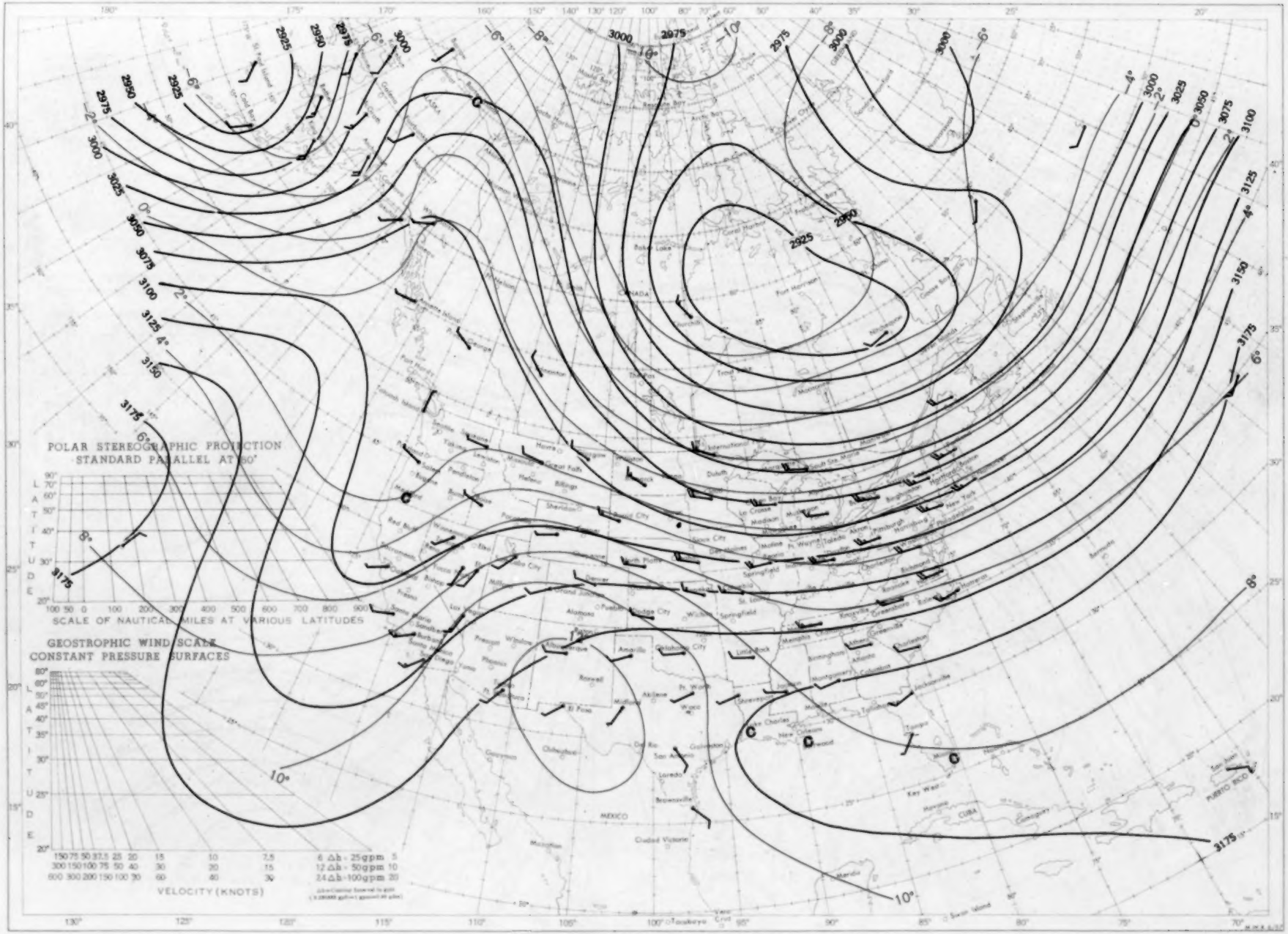

See Chart XII for explanation of map.

Chart XIV. 500-mb. Surface, 1200 GMT, June 1958. Average Height and Temperature, and Resultant Winds.

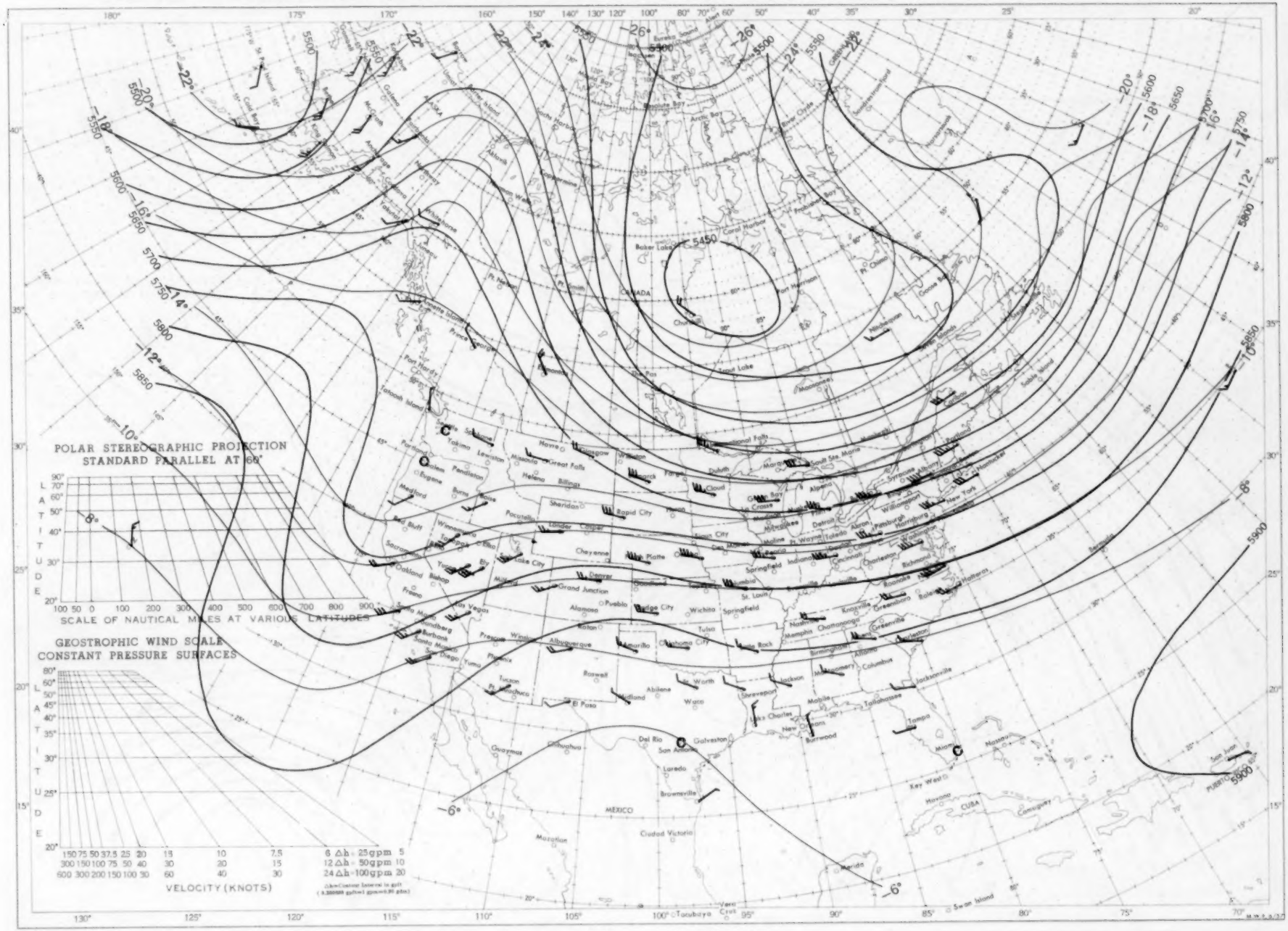

See Chart XII for explanation of map.

Chart XV. 300-mb. Surface, 1200 GMT, June 1958. Average Height and Temperature, and Resultant Winds.

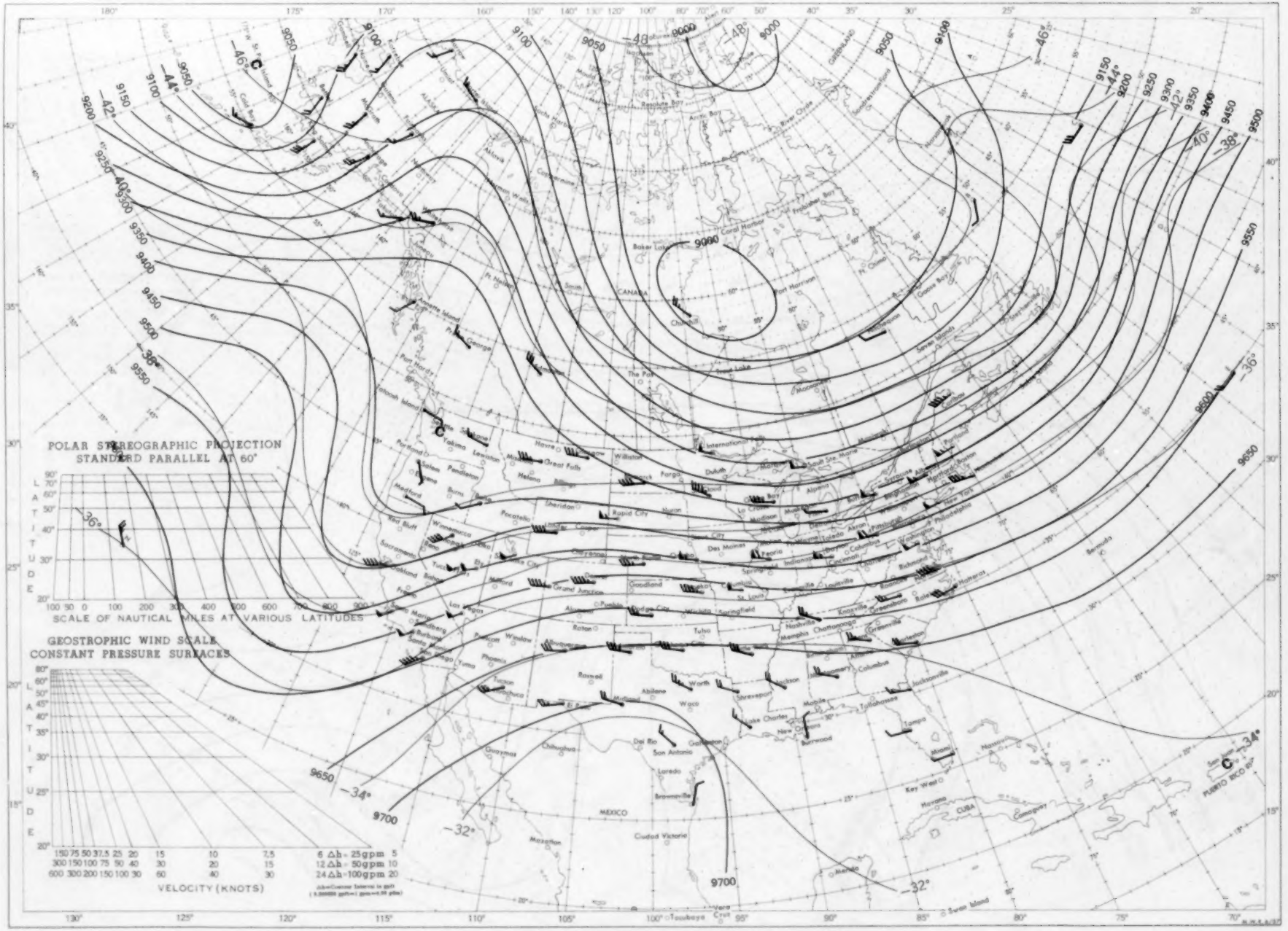

See Chart XII for explanation of map.

Chart XVI. 200-mb. Surface, 1200 GMT, June 1958. Average Height and Temperature, and Resultant Winds.

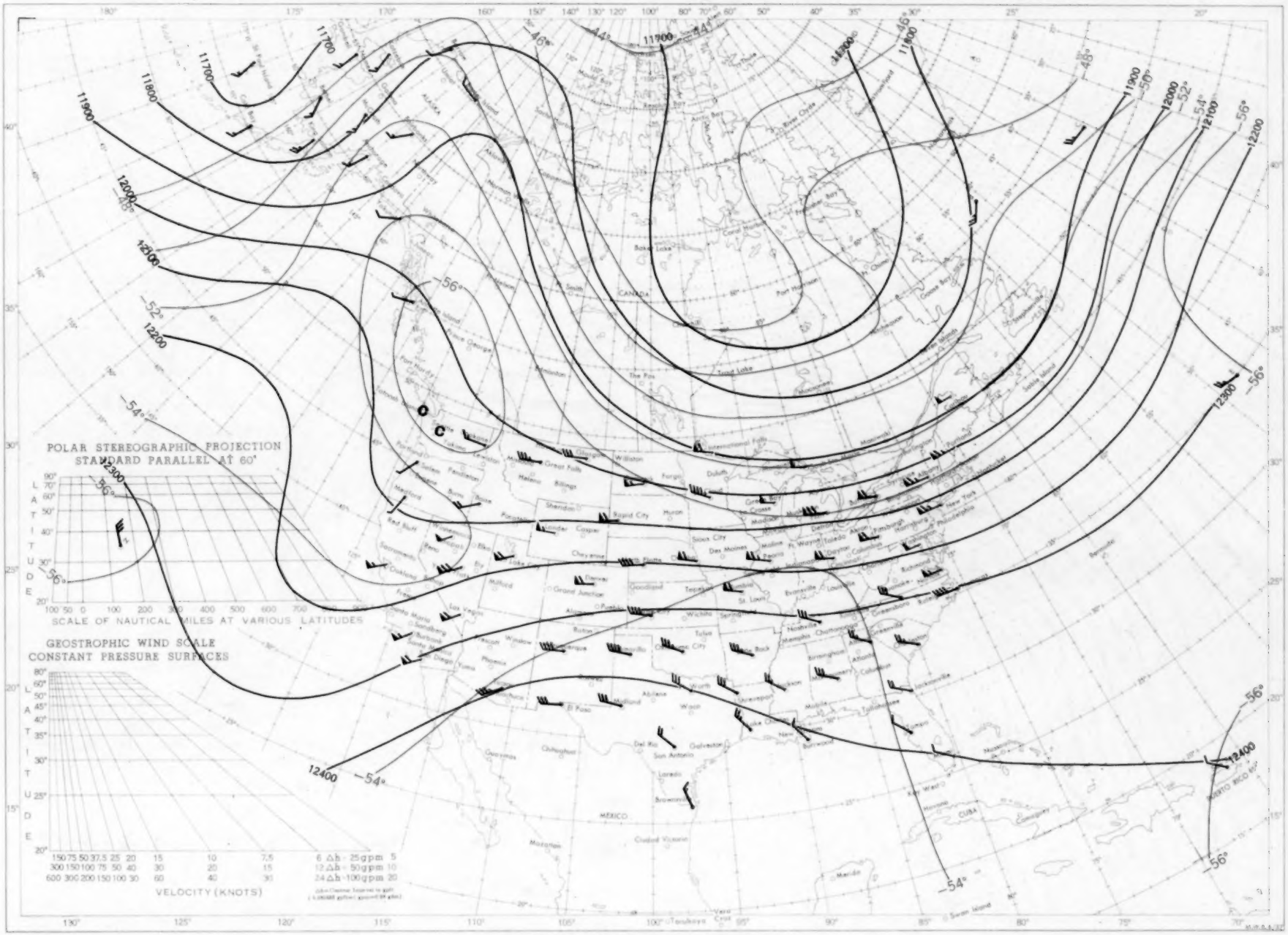

See Chart XII for explanation of map.

Chart XVII. 100-mb. Surface, 1200 GMT, June 1958. Average Height and Temperature, and Resultant Winds.

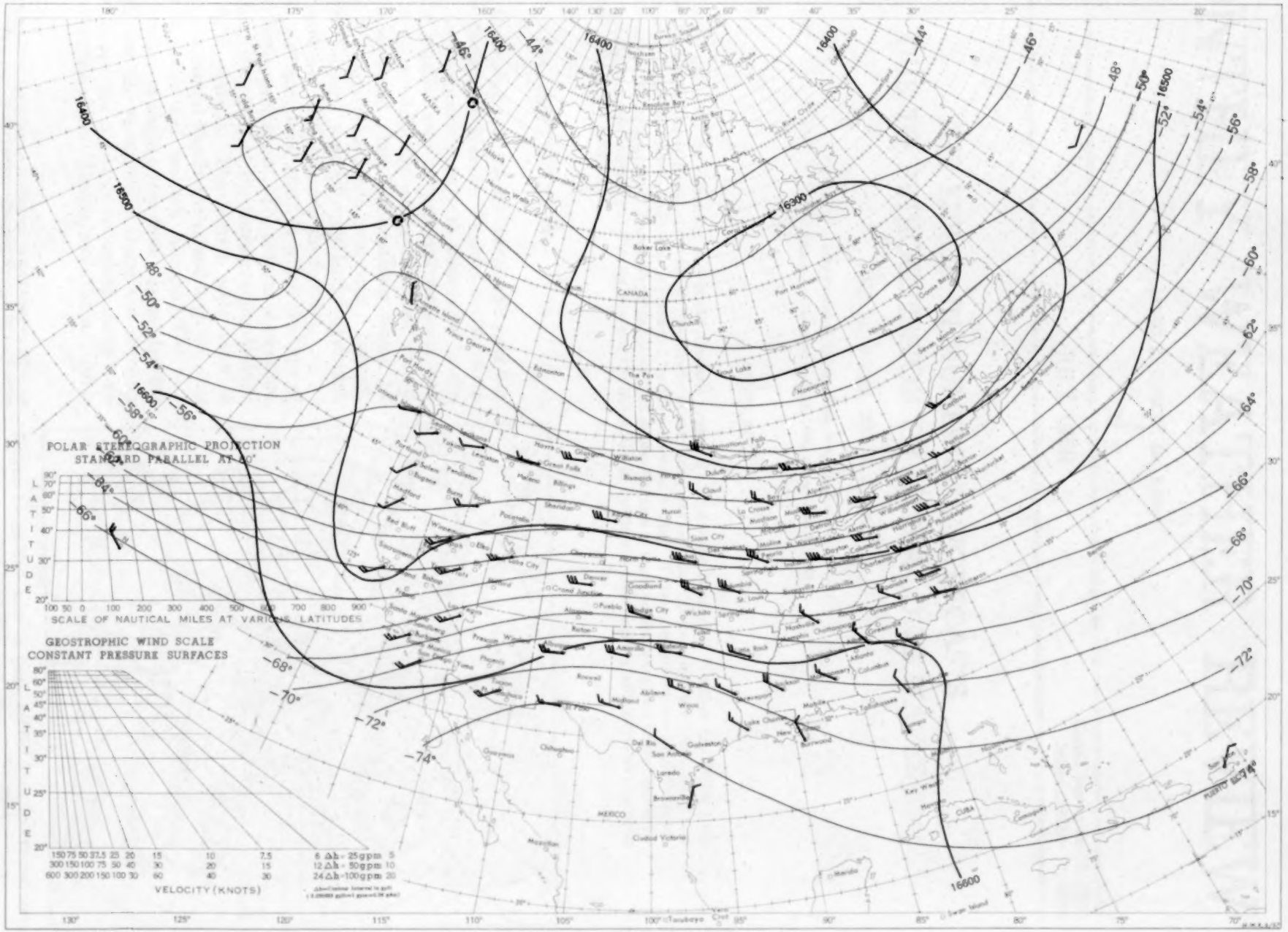

See Chart XII for explanation of map.